UNIVERSIDAD DE CANTABRIA

FACULTAD DE MEDICINA

DEPARTAMENTO DE ANATOMÍA Y BIOLOGÍA CELULAR

TESIS DOCTORAL

"Papel de la Vía Canónica de Wnt en la Función Resortiva del Osteoclasto"

Paula Ruiz Martín

Santander, 2016

UNIVERSIDAD DE CANTABRIA

FACULTAD DE MEDICINA

DEPARTAMENTO DE ANATOMÍA Y BIOLOGÍA CELULAR

"Role of Canonical Wnt Signaling in Osteoclast Bone Resorption"

Tesis Doctoral

presentada por:

PAULA RUIZ MARTÍN

Para optar al Grado de Doctor

Dra. María Ángeles Ros Lasierra, profesora de investigación del Instituto de Biomedicina y Biotecnología de Cantabria (IBBTEC),

Dr. Jesús González Macías, catedrático de Medicina de la Universidad de Cantabria y,

Dra. Marta Martín Millán, profesor asociado de la Universidad de Cantabria

como directores de la Tesis Doctoral titulada "Papel de la Vía Canónica de Wnt en la Función Resortiva del Osteoclasto" "Role of Canonical Wnt Signaling in Osteoclast Bone Resorption"

CERTIFICAN

que dicho trabajo ha sido realizado por Doña **Paula Ruiz Martín** y consideran que se encuentra terminado y reúne los requisitos para su presentación como memoria de doctorado por el interesado, al objeto de poder optar al grado de Doctor por la Universidad de Cantabria.

MªÁngeles Ros Lasierra *Jesús González Macías* *Marta Martín Millán*

Santander, a 28 de Junio de 2016

CONTENTS

ABBREVIATIONS

µCT	Micro-computed tomography
ALP	Alkaline phosphatase
BM	Bone marrow
BMD	Bone mineral density
BMP	Bone morphogenetic protein
BMPRIA	BMP receptor type IA
BMU	Basic multicellular unit
bp	Base pair
Bsp	Bone sialoprotein
BV/TV	Bone volume per total volume
CA II	Carbonic anhydrase II
CC	Chondrocytes
ClC-7	Chloride channels 7
Col1	Collagen type 1
CtsK	Cathepsin K
CtsKCre	*CathepsinK-Cre*
DAP12	DNAX-activating protein 12
DKK	Dickkopf
DSH	Dishevelled
ERα	Estrogen receptor α

FcRγ	Fc receptor common γ subunit
Fz	Frizzled
GOF	Gain-of-function
Grb2	Growth factor receptor bound protein 2
GSK-3β	Glycogen synthase kinase 3β
H-E	Hematoxylin-Eosin
Ihh	Indian hedgehog
ISH	*In situ* hybridization
ITAM	Immunoreceptor tyrosine-based activation motif
JNK	Jun N-terminal kinase
LGR	Leucine-rich repeat-containing G protein-coupled receptor
LOF	Loss-of-function
LRP	Low density lipoprotein-receptor related protein
LysMCre	*LysozymeM-Cre*
MAPKs	Mitogen-activated kinases
MC	Macrophages
M-CSF	Macrophage-colony stimulating factor
MITF	Microphthalmia-associated transcription factors
MMP-9	Matrix Metalloproteinase-9
NB	Newborn

NFATc1	Nuclear factor of activated T cells, cytoplasmic calcineurin-dependent 1
OB	Osteoblasts
OC	Osteoclasts
Oc	Osteocalcin
O/N	Overnight
OPG	Osteoprotegerin
Osx	Osterix
OSCAR	Osteoclast-associated receptor
PCP	Planar cell polarity
PCR	Polymerase chain reaction
qPCR	quantitative PCR
PFA	Paraformaldehyde
PI3K	Phosphoinositide 3-kinase
PIR-A	Paired immunoglobulin-like receptor-A
PKB	Protein kinase B
PLCγ	Phospholipase Cγ
PTHrP	Parathyroid hormone-related protein
R26R	Rosa26 reporter
RANK	Receptor activator of nuclear factor κβ
RANKL	Receptor activator of nuclear factor κβ ligand
ROR2	Receptor tyrosine kinase-like orphan receptor 2

RT	Room temperature
SERMs	Selective estrogen receptor modulators
SIRPβ1	Signal-regulatory protein β1
sFRP	Secreted frizzled related proteins
TGF-β	Transforming growth factor β
TNF	Tumor necrosis factor
TbN	Trabecular number
Tm	Melting temperature
Tph1	Tryptophan hydroxylase 1
TRAF	TNF receptor-associated factor
TRAP	Tartrate resistant alkaline phosphatase
TREM-2	Triggering receptor expressed in myeloid cells-2
TbSp	Trabecular space
TbTh	Trabecular thickness
VEGF	Vascular endothelial growth factor
WIF	Wnt-inhibitory factor

RESUMEN

RESUMEN

El mantenimiento de la integridad esquelética requiere un balance adecuado entre la destrucción y la formación ósea en el proceso de remodelación, en el que están implicados los osteoclastos y los osteoblastos, respectivamente. Los osteoblastos provienen de progenitores mesenquimales de la médula ósea, mientras que los osteoclastos derivan de progenitores hematopoyéticos. Las células osteoclásticas necesitan factores para su proliferación y diferenciación como son el factor estimulante de colonias de macrófagos (M-CSF) y el ligando activador del receptor de NF-kβ (RANKL), ambos producidos por células osteoblásticas. RANKL, actúa uniéndose a su receptor RANK en la superficie de los osteoclastos, favoreciendo la osteoclastogénesis. Además de M-CSF y RANKL, los osteoblastos producen osteoprotegerina (OPG), que actúa uniéndose a RANKL, evitando así que éste pueda unirse a su receptor y por tanto actúa como inhibidor de la diferenciación osteoclástica. Es necesario un ajuste entre éstos y otros múltiples factores, generales y locales, para regular el proceso de remodelación ósea. Un desequilibrio en estos factores puede conducir a una disminución (osteoporosis) o a un aumento (osteosclerosis) de la masa ósea.

La importancia de la señalización Wnt/βcatenina en la regulación de la masa ósea y su homeostasis se ha puesto de manifiesto en los últimos quince años. Varios grupos de investigación han establecido que diversas enfermedades óseas de carácter genético, tales como el síndrome osteoporosis-pseudoglioma (Gong et al. 2001), esclerosteosis (Balemans et al. 2001; Brunkow et al. 2001), el

síndrome de masa ósea alta familiar (Boyden et al. 2002) o la enfermedad de Van Buchem (Balemans et al. 2002; Loots et al. 2005; Staehling-Hampton et al. 2002), guardan relación con alteraciones directas o indirectas en la vía Wnt/βcatenina en los osteoblastos. Estos descubrimientos dieron lugar a numerosos estudios para definir con precisión la función de dicha vía en la biología del hueso, por lo que se realizaron numerosos experimentos de ganancia y pérdida de función del gen de la *βcatenina* mediante modelos experimentales en animales. Dichos estudios determinaron que la βcatenina, en precursores mesenquimales y en las células osteoprogenitoras, juega un papel esencial favoreciendo la diferenciación osteoblástica frente a la condrogénica (Day et al. 2005; Hu et al. 2005; Hill et al. 2005). Además, la señalización de Wnt/βcatenina en osteoblastos y osteocitos provoca un aumento de los niveles de OPG, inhibiendo la formación osteoclástica y la resorción ósea, lo que contribuye al incremento de masa ósea determinado por la acción antes señalada en los precursores mesenquimales y en las células osteoprogenitoras (Wang et al. 2014; Glass et al. 2005; Rodda & McMahon 2006). Por el contrario, una inhibición de dicha señalización da lugar a una disminución de la osteoblastogénesis y a un aumento de la osteoclastogénesis con reducción de la masa ósea (Day et al. 2005; Hu et al. 2005; Hill et al. 2005; Rodda & McMahon 2006; Wang et al. 2014; Glass et al. 2005; Holmen et al. 2005; Kramer et al. 2010).

Los estudios comentados nos han permitido conocer los efectos de la vía canónica de Wnt en las células de linaje osteoblástico. Sin embargo, el hecho de que la vía Wnt/βcatenina sea ubicua, plantea la posibilidad de que actúe también en los osteoclastos, por lo que un

mayor conocimiento de la función de la señalización de Wnt en la biología del hueso, requiere el análisis de su posible papel en estas células. De hecho, resulta sorprendente que apenas se haya considerado la posibilidad de que su alteración en ellas pueda repercutir sobre la masa ósea.

La presencia de la vía de señalización Wnt/βcatenina en los osteoclastos fue descrita en 2010 por Qiang et al. (Qiang et al. 2010), quienes comprobaron la expresión de varios componentes de la vía (Wnt, Frizzled, LRP y TCF) en los osteoclastos, y la acumulación en ellos de βcatenina en respuesta a la proteína WNT3A o al litio. Recientemente, varios estudios han analizado el papel que desarrolla la vía canónica de Wnt en la biología del osteoclasto desarrollando modelos murinos de deleción génica condicional de *βcatenina* en células de este linaje. Por ejemplo, en los modelos en que utilizan la Cre recombinasa bajo el control del promotor de la *Lisozima M* para estudiar su papel en las células precursoras de los osteoclastos, observaron una disminución de la masa ósea con un aumento de la osteoclastogénesis. Los niveles de OPG no estaban alterados, lo que sugiere que la señalización de Wnt/βcatenina en los precursores de osteoclastos tiene un efecto autónomo-celular sobre la masa ósea (Otero et al. 2012; Albers et al. 2013). Por otro lado, Wei et al. han utilizado la línea *PPARγ-tTA TRE-Cre* para estudiar la ganancia y pérdida de función de *βcatenina* en los progenitores de células osteoclásticas, y observaron en ambos casos un llamativo fenotipo osteopetrótico, atribuido en el primer caso a un bloqueo de la proliferación de los precursores osteoclásticos, y en el segundo a un bloqueo de la diferenciación osteoclástica (Wei et al. 2011).

El escaso número de trabajos que se han ocupado de analizar el efecto de la vía Wnt/βcatenina osteoclástica sobre la masa ósea nos ha movido a estudiar el papel de la misma en el osteoclasto maduro. Este es el objetivo de la presente Tesis Doctoral.

Para ello, hemos utilizado como modelo experimental ratones en los que mediante la utilización de la Cre recombinasa, se ha delecionado *βcatenina* de forma condicional en células *CtsK* positivas, ya que ésta es considerada una enzima específica de los osteoclastos en sus últimas etapas de maduración. Además del análisis fenotípico general y esquelético, se examinó en cultivos *in vitro* de osteoclastos el efecto de WNT3A en la supervivencia de los mismos. Los resultados de estos análisis en nuestros animales experimentales (*Ctnnb1*$^{lox(2\text{-}6)/lox(2\text{-}6)}$;*CtsKCre*) pusieron de manifiesto a las 12 semanas de edad una intensa pérdida de hueso, tanto cortical como trabecular, que se desarrolla progresivamente desde las 4 semanas. Además, pusieron de manifiesto que la señalización Wnt/βcatenina favorece la apoptosis de los osteoclastos tanto en cultivos desarrollados a partir de células de la médula ósea de ratones de la línea *LysMCre* como de células procedentes de ratones *CtsKCre*. Pudimos comprobar también, una disminución de la expresión de *Opg* en el hueso de los animales experimentales, lo que sugiere que los osteoclastos, con independencia de la alteración funcional determinada en ellos por la deleción de *βcatenina*, estaban siendo estimulados en su función resorbedora desde el exterior, por células ajenas a ellos. Ello nos llevó a estudiar la expresión de *CtsK* en otras células óseas, encontrando células de estas características en la capa interna del

periostio. Estas células coinciden en expresión con *Colágeno tipo 1*, lo que sugiere que dichas células pertenecen al linaje osteoblástico.

Por lo tanto, nuestros resultados indican que la pérdida ósea observada en los ratones *Ctnnb1*$^{lox(2-6)/lox(2-6)}$;*CtsKCre* se debe tanto a un mecanismo autónomo-celular de los propios osteoclastos, como a un efecto indirecto mediado por células de estirpe osteoblástica.

1. INTRODUCTION

1) INTRODUCTION

Bone is the main component of the adult skeleton providing scaffolding support for the body, houses hematopoiesis and serves as a mineral reservoir. It also provides attachment to muscles, ligaments and tendons allowing movement and locomotion of the body and protection to internal organs. Bone is a connective tissue formed by mineralized extracellular matrix and specialized cells (osteoblasts, osteoclasts and osteocytes). 90% of the organic component in the matrix is type 1 collagen, and the remaining 10%, is composed by osteocalcin, osteonectin, some phosphoproteins, sialoproteins, growth factors and serum proteins. The inorganic phase is composed by hydroxyapatite crystals [$Ca_{10}(PO_4)_6(OH)_2$]. Collagen and hydroxyapatite crystals together provide the appropriate characteristics of rigidity, flexibility and endurance. Skeletal bones show different sizes and shapes which match with structural demands, but all of them have a common structure: a compact or cortical bone cortex (80% of the total volume of bone) and a cancellous or trabecular bone (20% of total volume of bone). Compact bone predominates in the appendicular skeleton and is suitable to resist bending, torsion and compression. It has an outer periosteal surface and inner endosteal surface. The periosteum is a thick layer that covers the outer surface of bones and is composed by two distinct layers: an outer fibrous layer that lends structural integrity and an inner layer, which has osteogenic potential. The fibrous layer is a relatively cell poor layer, primarily composed of fibroblasts, collagen, and elastin while inner layer, also called cambium layer, is a cell rich layer formed by bone cells progenitors such as mesenchymal progenitors and osteoblasts (Dwek 2010; Roberts et al. 2015). The

cambium layer is known to be thicker during childhood, and progressively becomes thinner with age (O'Driscoll et al. 2001). The endosteum is a membranous structure covering the inner surface of cortical and cancellous bone. In humans, cortical bone is made of a system of functional units called osteons (or Haversian system), each formed by concentric lamellae of compact bone surrounding the Haversian canal, in which blood vessels and nerves are contained. In between the lamellae, osteocytes are laid down, the most abundant cells found in compact bone. Each osteon is in direct contact with the periosteum, the bone marrow (BM) and other osteons through the Volkmann's canals.

On the other hand, trabecular bone is composed of a network of trabeculae which are oriented parallel to the lines of forces and predominate in the axial skeleton where it is suitable to hold the forces of compression and tension generated in this region.

1.1 Bone Ossification

Bone development can occur through one of these two processes: intramembranous or endochondral ossification. Intramembranous ossification is restricted to the skull and part of the clavicle. In this type of ossification, mesenchymal cells condensate and differentiate directly to bone cells. By contrast, in endochondral ossification, mesenchymal cells differentiate into cartilage that is later replaced by bone. Most bones are formed through endochondral ossification including the spine and long bones of the limbs.

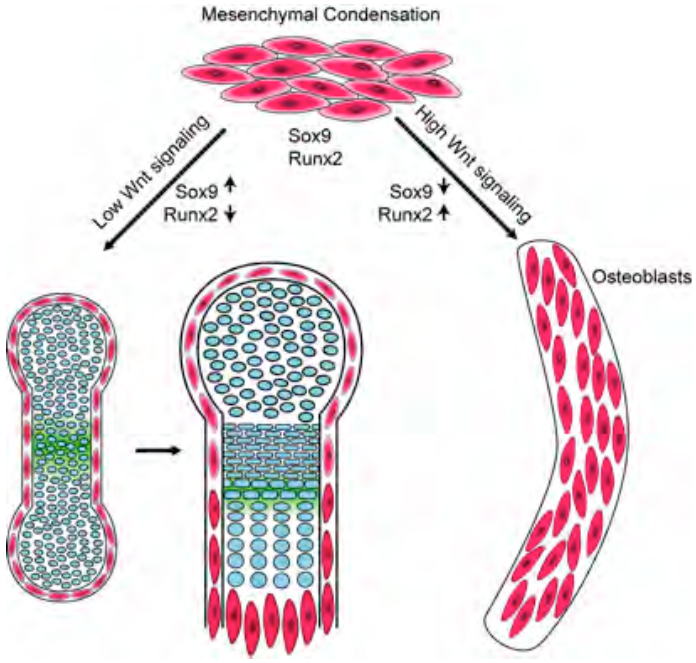

Figure 1. Differentiation of mesenchymal cells is regulated by Wnt/βcatenin and Indian hedgehog (Ihh) signaling. Canonical Wnt signaling controls the differentiation of chondrocytes or osteoblasts from mesenchymal progenitor cells in the mesenchymal condensations. Low Wnt signaling results in cartilage differentiation (endochondral ossification), while high Wnt signaling leads to osteoblast differentiation (intramembranous ossification). *Ihh* expression in the prehypertrophic chondrocytes (green shade) signals the perichondrium to regulate osteoblast differentiation of mesenchymal progenitor cells (taken from Day & Yang, 2008).

During embryonic development the Wnt/βcatenin signaling pathway plays a crucial role in directing the differentiation of mesenchymal cells. In the presence of high Wnt signaling, mesenchymal cells

differentiate to osteoblasts while in absence of Wnt signaling they differentiate to cartilage cells (Fig. 1).

1.1.1 Endochondral ossification

This type of ossification begins with the formation of condensations by the accumulation of mesenchymal cells. Through expression of *Sox9* and a decrease in canonical Wnt signaling, cells in these condensations differentiate into chondroblasts that form a cartilage hyaline template of the future bone. Chondroblasts secrete the cartilage matrix and become chondrocytes. The cartilage element grows by proliferation of the chondrocytes and by the deposition of abundant extracellular matrix typical of cartilage rich in type II collagen and in the proteoglycan aggrecan. In the center of the element, the chondrocytes mature and become hypertrophic. At this stage they start to synthesize type X collagen and secrete factors that decrease the pH and calcify the matrix leading to hypoxic conditions and eventually to the death of the cells. The hypoxic conditions attract blood vessels through production of vascular endothelial growth factor (VEGF) that penetrate the cartilage. With the blood vessels, osteoblasts and osteoclasts enter into the cartilage scaffold and begin to replace it by bone. The cells forming the external layer of the condensation remain flat and form the perichondrium, which surrounds the cartilage of the developing bone. This layer plays an important role as source of signals regulating the growth and differentiation of the cartilage (Fig. 2).

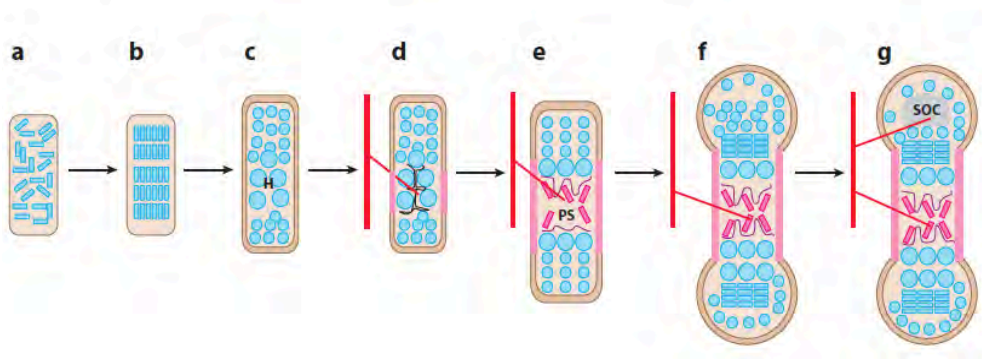

Figure 2. Endochondral ossification. Under low Wnt signaling, mesenchymal cells condense, differentiate in chondrocytes and make a template of the future bone (a-b). During maturation, chondrocytes go through the proliferative, prehypertrophic and hypertrophic stages starting in the central part of the template (c-d). Eventually cartilage cells die and are replaced by bone cells (e-g) (taken from Karsenty, Kronenberg, & Settembre, 2009).

In long bones, the ossification starts in the center of the element forming the primary ossification center and later, at each end, the secondary ossifications centers are formed, starting with a cartilage template that is replaced by bone from the center of the template to the edges, as explained above. A layer of cartilage called the growth plate remains allowing the longitudinal growth of the element. The differentiation of the cartilage is highly ordered to permit longitudinal growth. Several layers of chondrocytes in different phases of differentiation are clearly distinguished. Initially the chondrocytes are small, display a round shape and are called resting chondrocytes. Then, they proliferate faster and have a flat shape forming columns. After this stage, chondrocytes leave the cell cycle to become prehypertrophic and then, hypertrophic chondrocytes (Fig. 3).

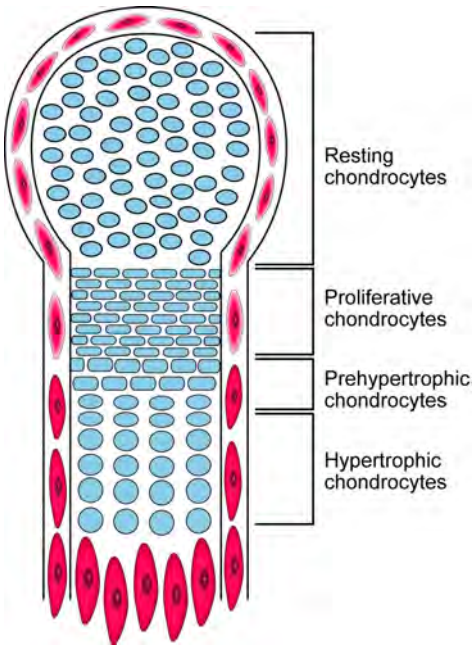

Figure 3. Cartilage development. Resting chondrocytes start to proliferate forming the proliferative or columnar zone. These chondrocytes, become pre- and hypertrophic chondrocytes which secrete factors required for bone development (taken from Day & Yang, 2008).

Several signaling pathways, in addition to canonical Wnt pathway, control the transition steps during bone formation, such as the Indian hedgehog (Ihh)/parathyroid hormone-related protein (PTHrP) signaling pathway (Fig. 4). PTHrP is produced by chondrocytes and perichondrial cells at the bone ends. PTHrP prevents resting chondrocytes from entering the proliferative stage. Ihh, synthesized by early hypertrophic chondrocytes, favors chondrocyte proliferation and stimulates PTHrP production (Vortkamp et al. 1996) establishing a negative-feedback loop that controls the pace of chondrocyte maturation.

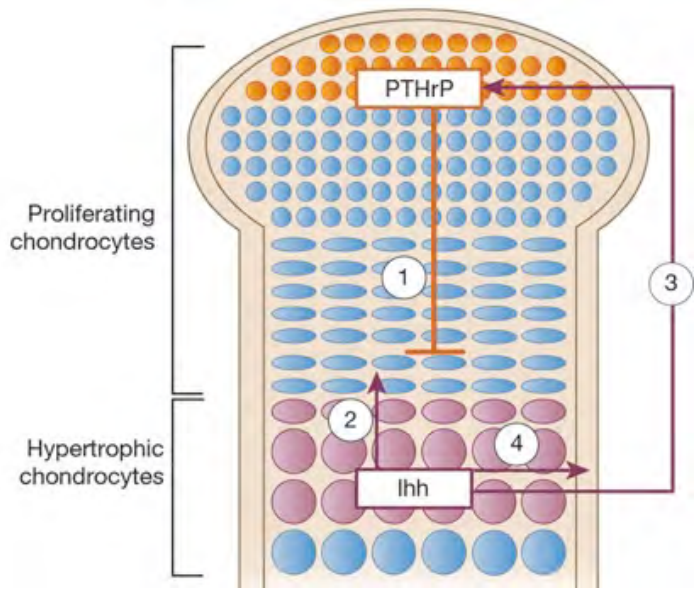

Figure 4. Indian hedgehog (Ihh)/parathyroid hormone-related protein (PTHrP) negative-feedback loop. PTHrP is secreted from perichondrial cells and chondrocytes at the ends of long bones. PTHrP maintains proliferating chondrocytes and therefore, delays the production of Ihh (1). When the cells are sufficiently distant from PTHrP production, they start to produce Ihh. Ihh increases proliferation (2) and, stimulates the production of PTHrP at the ends of the bone (3). Ihh also acts on perichondrial cells to convert these cells into the osteoblasts of the bone collar (4) (taken from Kronenberg, 2003).

The bone morphogenetic protein (BMP) signaling is also an important pathway during bone development because of its widely known osteogenic role. Osteoblasts are the bone cells in charge of synthesis and secretion of new bone. BMP induces osteoblast differentiation markers such as alkaline phosphatase (ALP) and osteocalcin (Oc) (Yamaguchi et al. 2010) favoring bone formation. Moreover,

conditional deletion of both *Bmp2* and *Bmp4* using *Prx1-Cre* line, caused defects in osteoblast differentiation (Bandyopadhyay et al. 2006). Furthermore, disruption of BMP receptor type IA (BMPRIA) showed increased bone mass due to a reduction of the osteoclast numbers through increasing osteoprotegerin levels (an anti-osteoclastogenic factor explained later with detail) (Kamiya et al. 2008).

1.2 Bone cells

Bone mainly exhibits four types of cells (Fig. 5): the osteoblasts (in charge of forming new bone), the osteocytes (differentiated from osteoblasts that are embedded in bone matrix), the bone linning cells (which protect bone surface) and the osteoclasts (cells that resorb bone).

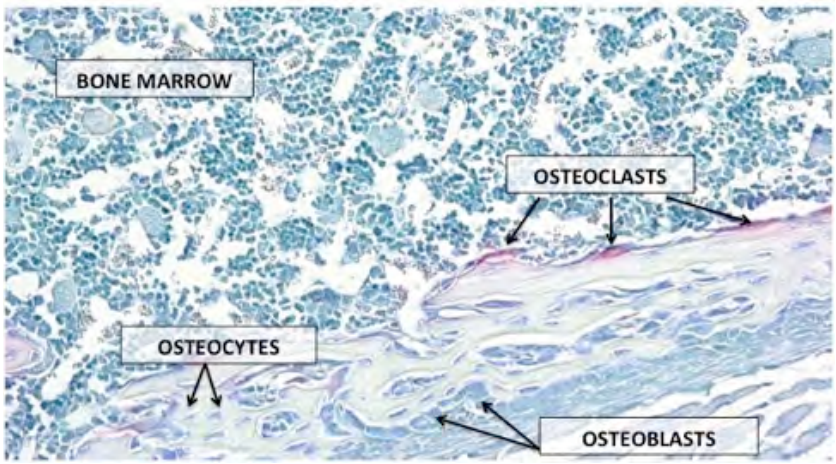

Figure 5. Bone cells. The osteoclasts stained in red with tartrate resistant alkaline phosphatase (TRAP) staining, are in charge of resorbing bone, the osteoblasts stained in blue are the bone-forming cells and the osteocytes are embedded in the bone matrix.

1.2.1 Osteoblasts and osteocytes

Osteoblasts, the bone-forming cells, are responsible for matrix deposition and contribute to its mineralization. Osteoblasts derive from mesenchymal stem cells that are also the common progenitors of myoblasts, fibroblasts, adipocytes and chondrocytes. The cell fate of mesenchymal stem cells is determined by several growth factors, cytokines, hormones and signaling pathways (Fig. 6). As previously mentioned, an important regulation pathway is Wnt/βcatenin that induces the mesenchymal progenitors to differentiate to the osteoblast lineage and blocks the chondrogenic or adipogenic fate. A key factor of osteoblast differentiation and function during intramembranous and endochondral bone formation is RUNX2 (also called CBFA1), a transcription factor expressed in the mesenchymal condensations and chondrocytes in addition to osteoblasts. The promoters of osteoblast-specific markers such as *Type 1 collagen* (*Col1*), *Osteocalcin* (*Oc*), *Bone sialoprotein* (*Bsp*) and *Osteopontin*, present RUNX2 binding sites. *Runx2* inactivating mutations present absence of osteoblasts and lack of ossification although cartilage formation was mostly unaffected indicating that its activity is not essential for chondrogenesis (Otto et al. 1997; Ducy et al. 1997).

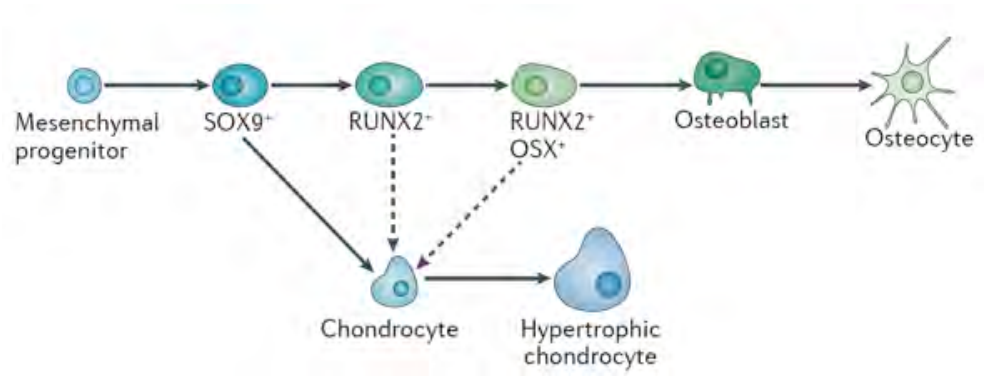

Figure 6. Osteoblast differentiation. Mesenchymal progenitors that give rise to osteoblasts and chondrocytes are initially marked by the expression of the transcription factor *Sox9*. This is followed by the expression of *Runx2* and then *Osx*, ultimately leading to the development of osteoblasts. A subset of osteoblasts can become osteocytes upon being trapped in the bone matrix. *Sox9*$^{+}$ and *Osx*$^{+}$ cells are bipotential and can also differentiate into chondrocytes (taken from Long, 2011).

Another transcription factor downstream of *Runx2* required for osteoblast differentiation is OSTERIX (Osx). It is needed for directing precursor cells from the chondrocyte to the osteoblast lineage. *Osx*$^{-/-}$ mice show absence of cortical and trabecular bone and lack bone matrix (Nakashima et al. 2002).

In cranial neural crest cells, deletion of *Osx* causes *Runx2*$^{+}$ cells to undergo chondrocyte differentiation. Moreover, deletion of the gene encoding *βcatenin* at different developmental stages can cause either *Runx2*$^{+}$ or *Runx2*$^{+}$*Osx*$^{+}$ cells to become chondrocytes, indicating that these cells may be able to switch fates under these conditions (dashed arrows in Fig 6).

Ultimately some osteoblasts are embedded in their bone matrix and become osteocytes, the most abundant cells in bone, resting in small pits in the matrix called lacuna. They communicate one to each other by means of their extensions of plasma membrane through small canals, named canaliculus. Osteocytes can also communicate with other bone cell type populations such as osteoblasts and osteoclasts, even in the bone surface, to regulate bone metabolism through expression of several molecules and cytokines. Osteocytes control the mechanical bone response too, acting as mechanoreceptors. Moreover, some osteoblasts can differentiate to bone linning cells which cover the surface of inactive bone that is not under remodeling, acting as protectors of bone surface.

1.2.2 Osteoclasts

Osteoclasts are large multinucleated bone cells of hematopoietic lineage. Their main function is to degrade the bone matrix. The osteoclast precursors are attracted to sites on the bone surface destined for resorption and fuse with one another to form the multinucleated cells that resorb calcified matrix. The resorbing osteoclasts present different membrane domains due to cytoskeletal reorganization and cellular polarization (Bruzzaniti & Baron 2006; Vaananen 2004). The membrane domain which faces with bone surface is called ruffled border. Osteoclasts adhere tightly to bone through the sealing zone, an actin rich area surrounding the ruffled border. In this area, the cell membrane closely interacts with bone matrix via αvβ3 integrins, which bind to matrix proteins. The sealed compartment formed between the osteoclast and bone surface, called

lacuna, is acidified by the V-ATPase proton pump that actively transports H^+ produced by carbonic anhydrase (CAII) in the cell to maintain the ion equilibrium. The chloride channels (ClC-7) maintain the electrical balance within the cell, moving Cl^- into the resorption lacuna. The proton secretion is necessary for bone mineral solubilization, releasing calcium ions, phosphate ions, and water in solution. Key enzymes involved in the acidification process are very important for normal bone resorption. Mutations in H^+ ATPase pump, ClC-7 chloride channel or CAII can lead to osteopetrosis in mice and humans (Bruzzaniti & Baron 2006; Kornak et al. 2001).

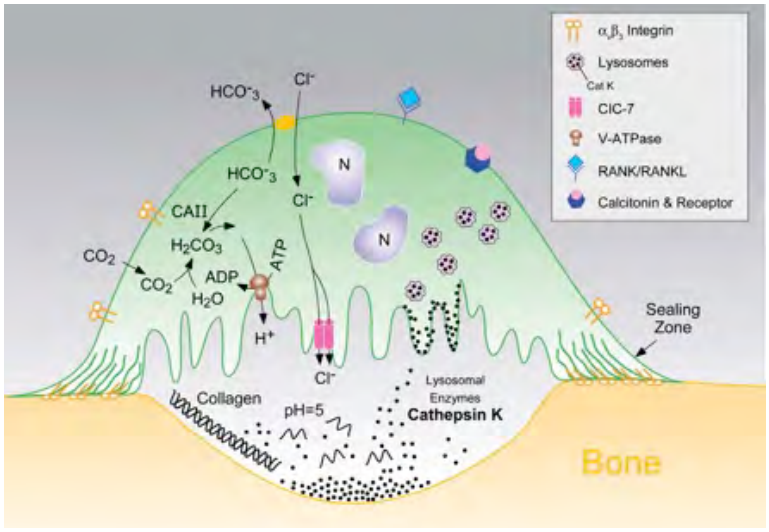

Figure 7. Representation of a resorbing osteoclast lacuna. The osteoclast acidifies the resorption lacuna by secreting H^+ for demineralization, and proteases such as cathepsin K for degradation of the organic components of the bone matrix (taken from Rodan & Duong, 2008).

On the other hand, metalloproteinases and cysteine proteases such as cathepsin K (CtsK), a protease considered the major enzyme

responsible for degradation of the organic bone matrix, are transported from the endoplasmic reticulum within lysosomes and other secretory vesicles which are secreted from the ruffled border to the resorption lacuna, where they degrade the bone matrix (Fig. 7).

CtsK expression is stimulated by several agents and cytokines, such as RANKL (receptor activator of nuclear factor kβ ligand), MITF (microphthalmia-associated transcription factors), and other factors like retinoic acid and tumor necrosis factor (TNF). Some CtsK inhibitors are estrogen and osteoprotegerin (OPG) (Troen 2004). Mutations in *CtsK* cause a rare autosomal recessive bone disorder called pycnodysostosis. Affected individuals are typically short in stature and, in spite of having high bone mass, suffer from an increase in the incidence of fractures. These patients also have an accumulation of undigested collagen fibrils, delayed closure of cranial fontanelles and aplasia of the terminal phalanges (Rodan & Duong 2008; Everts et al. 2003).

Other important enzymes for degrading organic matrix are matrix metalloproteinase-9 (MMP-9), and tartrate resistant alkaline phosphatase (TRAP). Inactivating mutations of these two proteolitic enzymes in genetic studies in mice, caused defects in bone development of endochondral bones and displayed osteopetrotic phenotypes (Page-McCaw et al. 2007; Chaoyang et al. 2004; Hayman & Cox 2003).

The release and elimination of the degraded organic and inorganic products occur by transcytosis through the cell in vesicles until

osteoclast apical surface, where the degraded products are secreted to the extracellular space. The transcytosis mechanism can mobilize calcium, collagen and degraded bone components but also other factors such as transforming growth factor beta (TGF-β) latent in bone matrix. TGF-β is stored in a latent form bound to bone matrix, until it is released during osteoclastic bone resorption (Fig. 8).

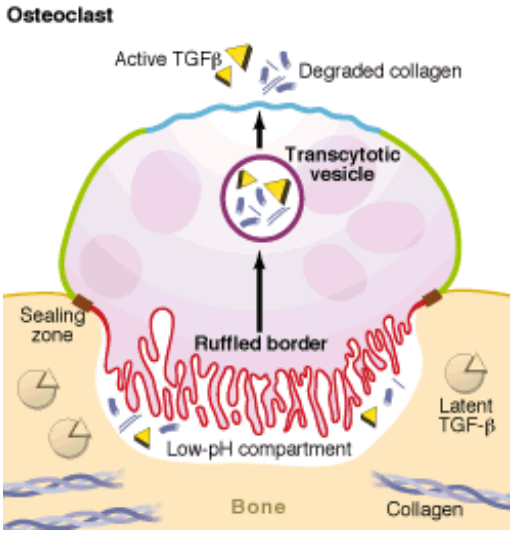

Figure 8. Osteoclast transcytosis. The degraded products of bone resorption are release to the extracellular space through transcytotic vesicles secreted by the apical surface of osteoclasts (taken from Mostov and Werb, 1997).

Despite the low pH of the lacuna, latent TGF-β from the bone matrix can be activated and once it is released, can acts on other cells, such as other osteoclasts and osteoblasts, promoting the coupling of bone degradation with the deposition of new bone (Salo et al. 1997; Pfeilschifter & Mundy 1987; Cohen, Jr 2006).

Analysis of mutant mice with impaired bone formation has provided insights into signaling pathways involved in osteoclast development. Among them, two molecules expressed by osteoblastic cells in the bone marrow are necessary and sufficient for osteoclast formation: the macrophage colony-stimulating factor (M-CSF) and the receptor activator of nuclear factor κβ ligand (RANKL). Hematopoietic mononuclear cells respond to M-CSF produced by nearby stromal cells, through M-CSF binding to c-fms (the receptor tyrosine kinase for M-CSF). M-CSF signaling regulates the proliferation and survival of the osteoclast precursor cells. Its binding results in the dimerization and the auto-phosphorylation of c-fms on selected tyrosine residues. This triggers a high number of downstream signals. Among them, one key interaction is between the receptor and c-SRC family kinases, which then phosphorylates the protein c-CBL. C-CBL recruits a multiprotein complex (which also interacts simultaneously with c-fms) containing growth-factor-receptor-bound protein 2 (GRB2) and phosphoinositide 3-kinase (PI3K). The former binds to SOS protein and activates Raf/MEK/ERK cascade. And the PI3K activates the protein kinase B (PKB) or serine/threonine kinase AKT cascades, both acting as downstream effectors for finally inducing proliferation and survival of monocyte/macrophage lineage cells (Ross, 2006 and Fig. 9). The pivotal role of M-CSF in osteoclast development was known when mice lacking *M-csf* show deficient mature macrophages and do not present osteoclasts (Yoshida et al. 1990) leading to an osteopetrotic phenotype.

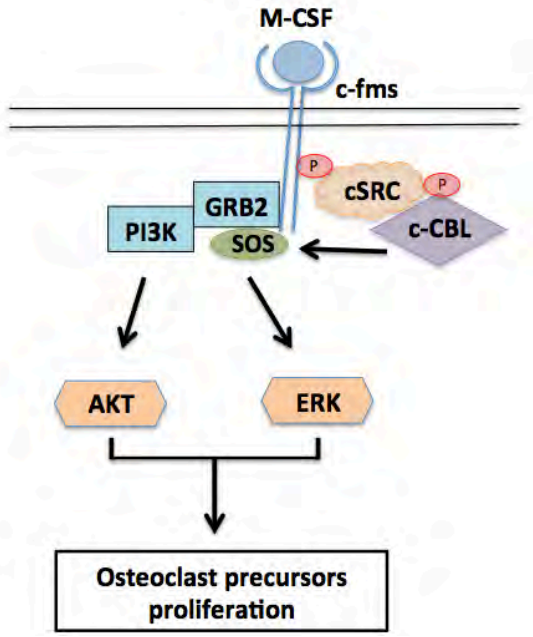

Figure 9. Osteoclastic M-CSF signaling. M-CSF binds to its receptor c-fms, leading to its dimerization and auto-phosphorylation. Once the receptor is activated, SRC kinases bind to it and phosphorylate c-CBL, which recruits a protein complex formed by GRB2, SOS and PI3K. GRB2 and SOS trigger Raf/MEK/ERK signaling cascade and PI3K, the AKT signaling.

The other molecule, RANKL, is also produced by stromal cells and facilitates association of co-activators of transcription factors recruited by initial stimulation of M-CSF. RANKL, in response to activation of its receptor RANK, induces the polarization of the osteoclast cell body that undergoes internal structural changes that prepare it to resorb bone, such as the rearrangements of the actin cytoskeleton and formation of a tight junction between the bone surface and basal membrane to form the sealed compartment (Dougall et al. 1999; Boyce & Xing 2007). *Rankl*$^{-/-}$ mice display severe osteopetrosis,

impaired growth, and defective tooth eruption resulting from block of osteoclast differentiation (Kohli & Kohli 2011; Pettit et al. 2001).

RANK signaling is transduced by recruiting adaptor molecules such as the TNF receptor-associated factor (TRAF) family proteins composed by seven members (TRAF 1, 2, 3, 4, 5, 6 and 7). The cytoplasmic tail of RANK contains three TRAF6 binding sites and two sites for the binding of other TRAF family members including TRAF2, TRAF3 and TRAF5. Mice lacking TRAF6 (*Traf6*$^{-/-}$) present severe osteopetrosis due to impaired bone resorption, indicating the important role of the adaptor proteins TRAF (Lomaga et al. 1999).

Activation of the receptor RANK through binding to TRAF6, induces osteoclast precursors to further differentiate to mononuclear osteoclasts by means of the trimerization and activation of TRAF6, leading to the activation of NF-κβ, mitogen-activated kinases (MAPKs) including Jun N-terminal kinase (JNK) and p38 and the calcium/calmodulin signaling. The activation of these signaling pathways induces transcription factors such as c-FOS and triggers NFATc1 translocation to the nucleus and further up-regulation of its expression. These activations lead to promote the transcription of osteoclast-related genes such as those encoding *Trap* and *CtsK* (Fig. 10) required for osteoclast formation and differentiation. Mononuclear osteoclasts then fuse to form multinuclear osteoclasts and function as polarized bone resorbing cells. This signaling also activates the resorption by mature osteoclasts and its survival and participation in new rounds of bone degradation (Fleischmann et al. 2000; Takayanagi et al. 2002).

The essential role of NFATc1 in osteoclast differentiation has been well established by several studies performed on genetically modified mutant mice and cells. Osteoclast-specific conditional *Nfatc1* deficient mice develop osteopetrosis owing to impaired osteoclastogenesis and up-regulation of the expression of *Opg*. Lack of *Nfatc1* also leads to precursor cells fail to differentiate into mature osteoclasts (Takayanagi et al. 2002; Aliprantis et al. 2008; Winslow et al. 2006).

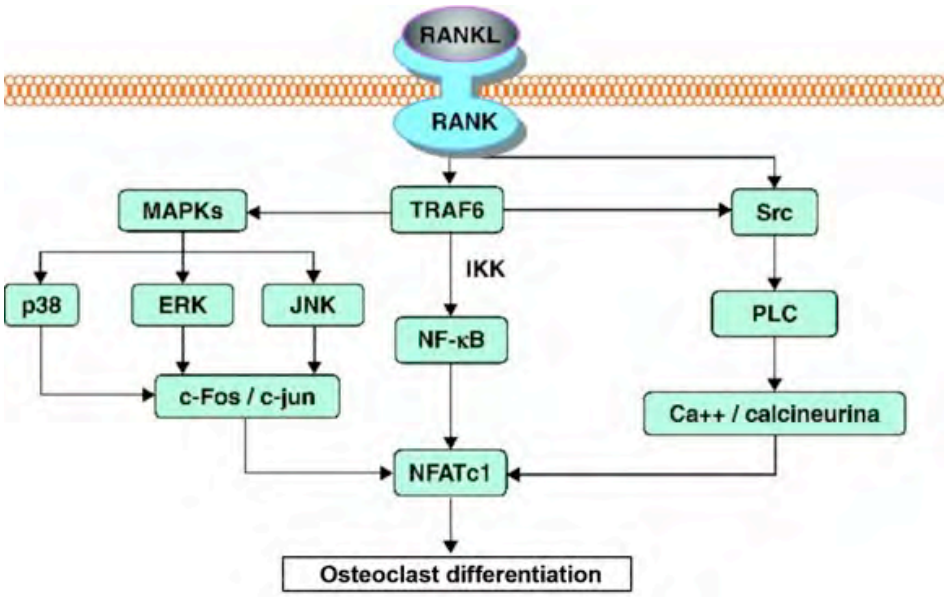

Figure 10. Osteoclastic NF-kβ signaling. RANKL produced by osteoblasts binds to RANK on the surface of osteoclast precursors and recruits the adaptor protein TRAF6, leading to NF-kβ activation and translocation to the nucleus. NF-kβ and c-Fos interact with *Nfatc1* to trigger the transcription of osteoclastogenic genes. Calcium signaling also contributes to up-regulation of *Nfatc1* (modified from Riancho & Delgado-Calle, 2011).

RANK signaling presents a co-stimulatory signals mediated by several receptors, such as OSCAR (osteoclast-associate receptor), TREM-2 (triggering receptor expressed in myeloid cells-2), PIR-A (paired immunoglobulin-like receptor-A), and SIRPβ1 (signal-regulatory protein β1) in osteoclasts, involved in stimulation of calcium signaling (Fig. 11).

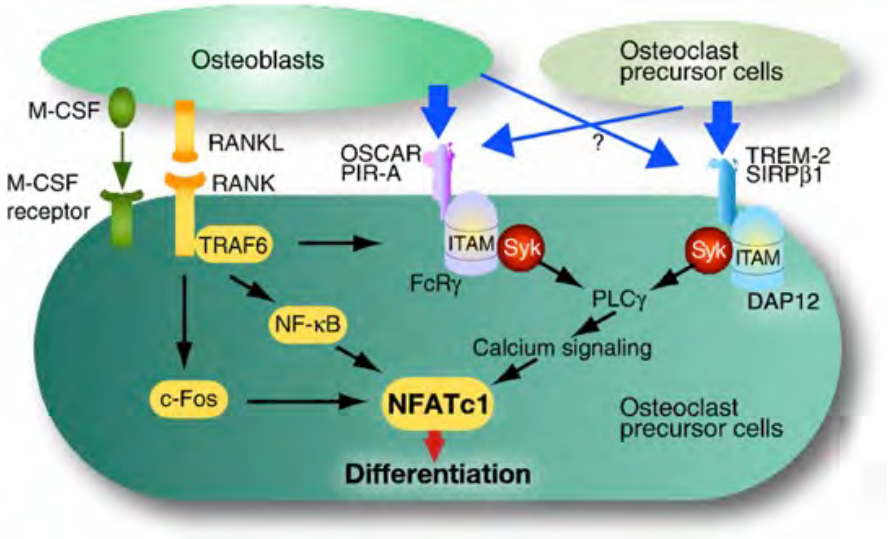

Figure 11. Co-stimulatory ITAM signals for RANK signaling. The ITAM-harboring adaptors FcRγ and DAP 12 associate with immunoglobulin-like receptors such as OSCAR and TREM-2. Then, the Syk kinase is recruited to the phosphorylated tyrosine residues of ITAM adaptors via its SH2 domain. This leads to the activation of phospholipase Cγ (PLCγ) and calcium signaling, which is critical for NFATc1 induction and activation (taken from Asagiri & Takayanagi, 2007).

These receptors associate with an adaptor molecule, such as FcRγ (Fc receptor common γ subunit) and DAP12 (DNAX-activating protein 12) which harbor an immunoreceptor tyrosine-based activation motif (ITAM) observed in osteoclast precursor cells. OSCAR and PIR-A are associated with the ITAM-harboring adaptor FcRγ and TREM-2 and SIRPβ1 are associated with the ITAM-harboring adaptor DAP12 (Kim & Kim 2014; Kaifu et al. 2003; Koga et al. 2004).

Mutant *Trem2*$^{-/-}$ mice display an osteopenic phenotype due to an increase of osteoclast specific genes such *as CtsK* and *Nfatc1* leading to an increase of osteoclast numbers (Otero et al. 2012). ITAM-mediated signals cooperate with RANK to stimulate calcium signaling through up-regulation of ITAM phosphorylation signaling and the resulting activation of Syk and PLCγ (phospholipase Cγ) that finally induce *Nfatc1* expression (Mócsai et al. 2004). Moreover, RANKL stimulation results in an increased expression of immune-receptors such as OSCAR and thereby increasing the ITAM signal (Kim & Kim 2014; Kim et al. 2005; Koga et al. 2004).

There are important transcription factors involved in osteoclastogenesis (Fig. 12) downstream of *M-csf* and *Rankl* such as MITF (microphthalmia-associated transcription factor), PU.1, c-FOS, NF-kβ (nuclear factor kβ) and NFATc1 (nuclear factor of activated T cells, cytoplasmic calcineurin-dependent 1) (Sharma et al. 2007). MITF has been shown to regulate three osteoclast target genes, *tartrate resistant acid phosphatase* (*Trap*) (Luchin et al. 2000), *Ctsk* (Motyckova et al. 2001), and alone or in combination with PU.1 activates *Oscar* (So et al. 2003). PU.1 transcription factor is involved

in the earliest event of osteoclastogenesis. PU.1 deficient mice show an osteopetrotic phenotype caused by development arrest of both macrophages and osteoclasts, suggesting its involvement in the initial stages of myeloid differentiation (Tondravi et al. 1997).

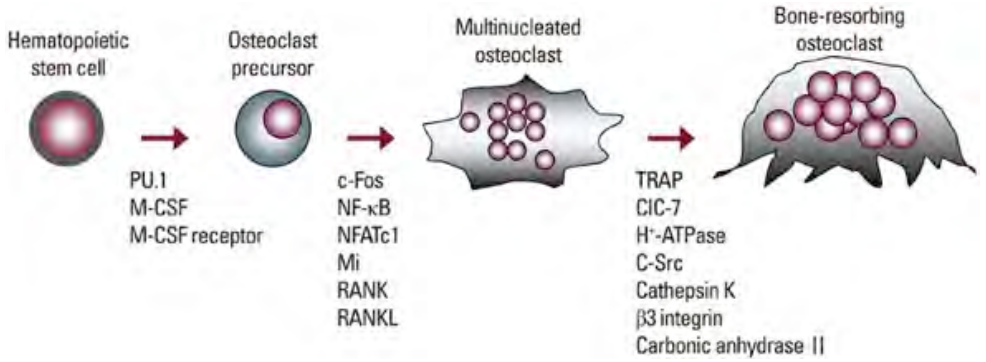

Figure 12. Osteoclast differentiation. Osteoclasts are derived from hematopoietic precursors. M-CSF induces myeloid precursors to differentiate to osteoclast precursors, which become mature multinucleated osteoclasts though induction of RANKL signal which leads to the expression of osteoclastogenesis-specific transcription factors such as *Trap* and *CtsK* (Lee 2010).

1.3 The RANK/RANKL/OPG system

To maintain and regulate bone mass, osteoblasts and osteoclasts are in constant communication through the RANK/RANKL/OPG system. Osteoblasts express the two cytokines M-CSF and RANKL essential for osteoclast development and OPG (osteoprotegerin), a RANKL decoy receptor that prevents its binding to its RANK receptor (Fig. 13). Thus, RANKL, by binding to its receptor in the surface of osteoclasts

(RANK), promotes the differentiation and maturation of osteoclasts and increased bone resorption. In contrast, increased OPG levels, by sequestering RANKL, prevent ligand-receptor binding favoring bone formation. Once RANKL binds to RANK, NF-kβ signaling pathway is activated and induces expression of osteoclast differentiation genes such as *c-fos* and *Nfatc1* as previously mentioned (Fig. 10). The RANK/RANKL/OPG system is one of the most important crosstalk between bone cells and is controlled by the Wnt/βcatenin pathway, being *Opg* a target gene of βcatenin in osteoblasts (Kieslinger et al. 2005; Glass et al. 2005).

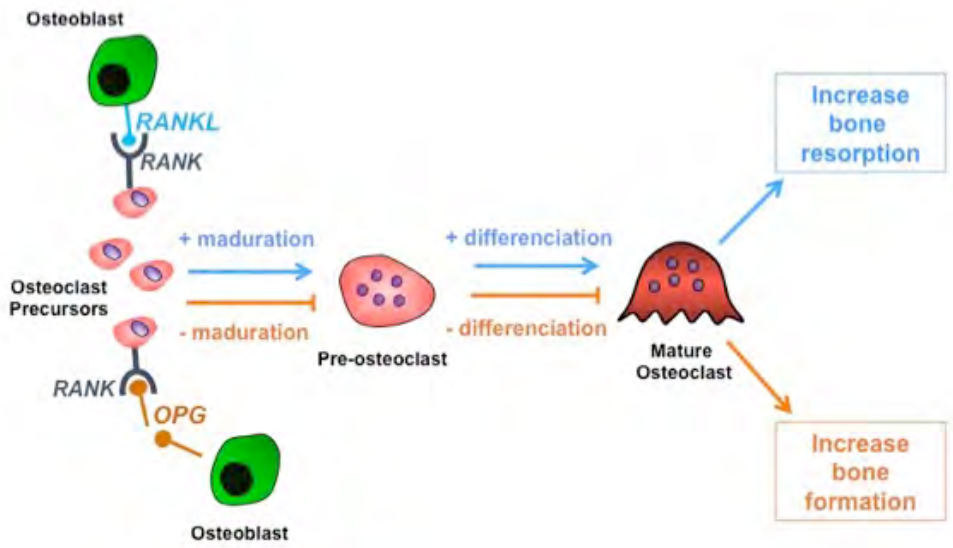

Figure 13. RANK/RANKL/OPG system. The balance among the system components RANK, RANKL and OPG maintains physiologic bone remodeling.

1.4 Bone remodeling

Although bone can appear a static organ, it is continually being remodeled, this is constantly being resorbed and formed. Bone remodeling is crucial for the maintenance of the skeleton as it permits the repair of micro-fractures caused by everyday stress. It also permits the homeostasis of calcium and phosphate. The remodeling cycle takes place in certain functional areas called basic multicellular unit (BMU) and it is triggered with local and systemic signals induced by mechanical loading, microdamage, hormonal changes, interleukins, etc (Manolagas 1999). The cycle presents three consecutive phases in which osteoblasts and osteoclasts are involved: resorption, reversal and formation (Fig. 14).

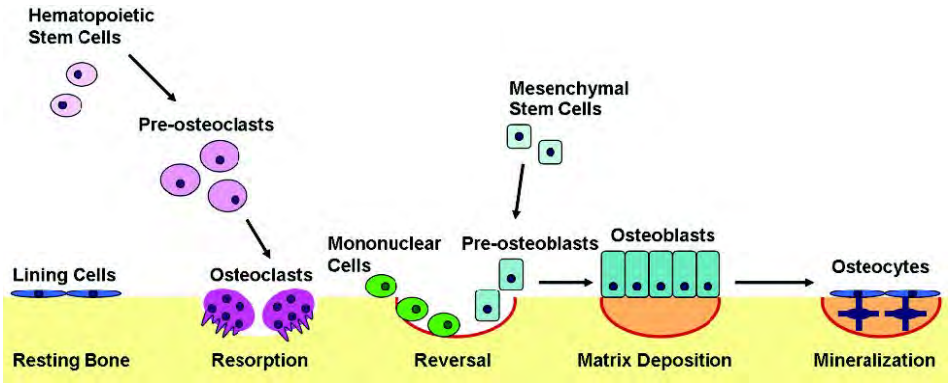

Figure 14. Bone remodeling. Osteoclasts resorb bone mineral and matrix. Mononuclear cells prepare the resorbed surface for osteoblasts, which generate newly synthesized matrix. Finally some osteoblasts are embedded in the bone matrix and become osteocytes (Kapinas & Delany 2011).

The resorption phase initiates with the recruitment of osteoclast precursors to the BMU where they differentiate to mature osteoclasts. The osteoclasts degrade the bone matrix secreting collagenases and other proteolytic enzymes such as CtsK and phosphatases like TRAP as previously explained (Goto et al. 2003). These events last for three weeks and finish with osteoclasts apoptosis (Parfitt 2002). After osteoclast activity, there is a reversal phase during 1-2 weeks, in which mononuclear cells cover the bone surface and prepare it for the arrival of osteoblasts. The formation phase take place in 3 months where the osteoblasts proliferate and secrete extracellular matrix rich in type 1 collagen and facilitate its mineralization. Finally some osteoblasts undergo apoptosis and the rest become lining cells or osteocytes (Kapinas & Delany 2011; Hadjidakis & Androulakis 2006).

During the youth, bone mass remains stable since the remodeling presents balance zero, i.e. the osteoblasts are able to synthesize bone matrix such as is destroyed by osteoclasts. However, because of age, menopause or bone diseases, this balance is deregulated and osteoblasts are not able to synthesize the bone that osteoclasts have previously degraded leading to the resorption predominates on formation. This negative balance causes bone thinning and osteoporosis. Nevertheless, under certain conditions as diseases and mutations explained later, the balance between bone formation and resorption can be positive causing high bone mass and diseases such as osteosclerosis (Fig. 15).

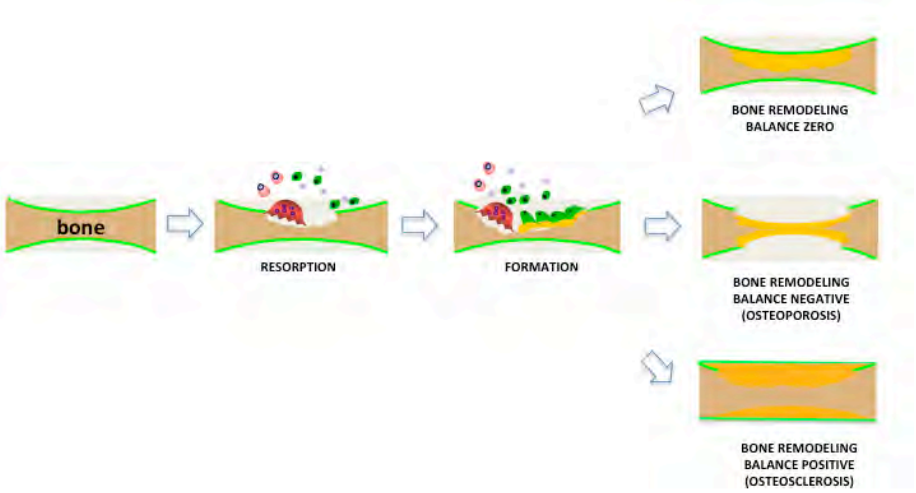

Figure 15. Bone Balance. During remodeling, the balance between bone formation and bone destruction changes with age or under certain conditions. If destruction is equal to formation the balance is zero and no changes in bone mass occur, but if destruction is lower or higher than formation the bone balance is negative or positive leading to osteoporosis or osteosclerosis respectively.

Alterations in bone remodeling cause bone disorders such as Paget's disease, where remodeling is disturbed and not synchronized obtaining fragile and misshapen bones. The pathologic abnormality in patients with Paget's disease mainly involves an increase in the osteoclast numbers leading to increased bone resorption which recruits osteoblasts to bone formation. However, new bone is formed at such a rapid rate that bone is formed in a sporadic and haphazard way, obtaining bones expanded in size, structurally disorganized, and mechanically weak, leading to bone deformity, pathological fracture, and various other complications. The origin of Paget's disease remains unknown though it has been associated with genetic causes

or viral infection because of the presence of viral-like nuclear inclusions in the pagetic osteoclasts (Roodman et al. 1990; Reddy et al. 1999; Reddy 2004).

Most bone diseases are due to excessive bone resorption, where osteoclasts are the primary therapeutic targets. Inhibition of bone resorption can come from reduction of osteoclast formation or osteoclast activity. In the fifth decade of life, both men and women develop a loss of bone mass and strength, which is accompanied with other factors such as major tendency to fall. This increases their propensity to fractures. In the case of the women, the reduction of bone mass is more marked because of menopause, when the production of estrogens is decreased. One of the best-known treatment against bone loss in women is the estrogen administration or selective estrogen receptor modulators (SERMs). Treatment with estrogens clearly inhibits osteoclast formation by decreasing factors and cytokines that rise osteoclast numbers and activity (IL-1, M-CSF, TNFα, RANKL, and prostaglandin E). The result is the prevention in bone loss. The decrease in some of these factors (IL-1, IL-6, TNF) comes in part from indirect mechanisms, through inhibition of cytokines production by lymphocytic cells (Girasole et al. 1992). Moreover, estrogens prevent bone loss by increasing OPG and inhibiting RANKL production in cells of osteoblastic lineage (Shevde et al. 2000; Krum et al. 2008; Gallagher & Tella 2014). Furthermore, they can promote osteoclast apoptosis (Kameda et al. 1997; Almeida et al. 2013). It has been stated, in addition, that estrogens can directly induce bone formation by promoting osteoblast development (Okazaki et al. 2002; Dang et al. 2002; Jilka et al. 1998). But they also cause

undesirable effects in other organs like breast and uterus, increasing the risk of cancer in these tissues. To avoid these undesirable effects while maintaining those which are beneficial, new drugs, called SERMs, were developed. They bind to estrogen receptors (ER) acting as agonists in some tissues and antagonists in others, due to their unique structural features that trigger the recruitment of certain co-activator proteins. For instance, raloxifene acts as an estrogen agonist in bone but as an antagonist in breast and uterus (Rodan 2000; Stepan et al. 2003).

Other treatments against bone loss are the bisphosphonates and calcitonin. Bisphosphonates are well established for the treatment of osteoporosis and other bone diseases associated with excessive bone resorption because of their high binding affinity for bone mineral and their inhibitory effects on osteoclast activity. Moreover, bisphosphonates also act through intracellular mechanisms. They are taken up by osteoclasts during bone resorption and inhibit certain intracellular metabolic pathways which are essential for osteoclast resorption. In particular, nitrogen-containing bisphosphonates inhibit the enzyme farnesyl pyrophosphate synthase, which is in charge of generating lipids required to post-translational modification of small GTP-containing proteins, like Rho, Rac, cdc42, and Rab needed for osteoclast activity and survival (Rodan 2000; Russell et al. 2007). In addition, bisphosphonates inhibit the precipitation of calcium phosphate, the aggregation of hydroxyapatite crystals and its dissolution.

Calcitonin is a polypeptide hormone in charge of blocking osteoclast activity and therefore, bone resorption. The physiological role of calcitonin is the regulation of extracellular calcium homeostasis confined to times of calcium stress, such as growth, pregnancy, lactation and high calcium intake. It is approved for the treatment of postmenopausal Paget's disease. Previously, it was also indicated for the treatment of osteoporosis, although, due to secondary effects, this indication has been canceled. The inhibition of bone resorption by calcitonin is mediated by its binding to the calcitonin receptors present in the osteoclast membrane. This leads to a loss of the ruffled border, cessation of motility, pseudopodial retraction and inhibition of osteoclast secretion of the proton pump and proteolytic enzymes (Zaidi et al. 2002; Stepan et al. 2003; Chesnut et al. 2008).

More recently, the new antiresoptive therapies include CtsK inhibitors, mostly used in postmenopausal osteoporosis treatment. CtsK reduction results in a decrease of proteolysis of matrix proteins, reducing bone resorption (Eisman et al. 2011). Some drugs of this family induce severe dermatological reactions and therefore their study has been stopped. Others such as odanacatib, however do not show relevant skin problems, and will probably be marketed soon.

1.5 The Wnt signaling pathways

Wnt proteins are a family of highly conserved molecules that regulate different interactions during embryogenesis including cell differentiation and proliferation of different organs like the lung, gastrointestinal tract, skin and bone. To regulate all those functions Wnt ligands signal through several pathways, the best studied of them

is the Wnt/βcatenin pathway, also known as Wnt canonical pathway. Other Wnt pathways are globally known as non-canonical pathways, the planar cell polarity (PCP) pathway and the Wnt/calcium (Wnt/Ca^{2+}) pathway. Mutations in Wnt genes or other components of these Wnt signaling pathways can cause developmental defects or diseases, even cancer.

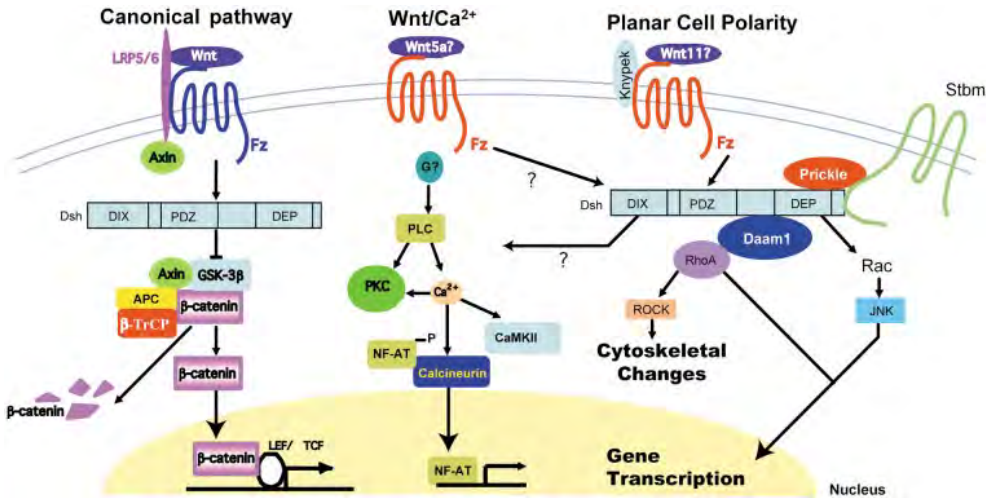

Figure 16. Canonical and non-canonical Wnt pathways. The canonical pathway acts through βcatenin. The non-canonical pathways regulate Ca^{2+} flux and JNK pathway (Yang 2003).

The human and mouse genomes contain nineteen Wnt genes. In the canonical Wnt pathway, its activation occurs upon binding of Wnt proteins to a receptor complex, consisting of one of the seven-helix-receptors of the Frizzled family and one of two co-receptors of the LRP (low density lipoprotein-receptor related protein) family, either LRP5 or LRP6. This binding leads to the activation of dishevelled

(DSH) protein. In that case, AXIN2 is phosphorylated and recruited by LRP5/6. The protein complex formed by AXIN2, APC and GSK3-β (glycogen synthase kinase 3-β) that sequester βcatenin is subsequent destabilized and βcatenin cannot be phosphorylated, accumulates in the cytoplasm and translocates to the nucleus where it binds to transcription factors like TCF and LEF, activating the transcription of Wnt target genes (Fig. 16).

In the absence of Wnt proteins, Frizzled and LRP5/6 are inactive and, therefore, they cannot activate the DSH protein and the cytoplasmic protein complex is stabilized. This complex promotes the phosphorylation of βcatenin by GSK3-β. The phosphorylation labels βcatenin to proteosomal degradation and Wnt target genes are not transcribed.

Wnt signaling can be enhanced by other proteins like R-spondins and Norrin. The first one, acts through LGR (leucine-rich repeat-containing G protein-coupled receptor) family receptors. Co-stimulation with the R-spondins and Wnt ligands leads to interaction of LGR with the Wnt co-receptors LRP and Frizzled in their extracellular domains forming a super complex which is rapidly internalized enhancing the canonical Wnt pathway and then degraded (Fig. 17) (Carmon et al. 2012).

Other protein is Norrin, that binds with high affinity to the receptor Frizzled-4 and requires LRP5/6 as co-receptor to form the ternary complex inducing activation of the canonical Wnt signaling pathway (Ke et al. 2013).

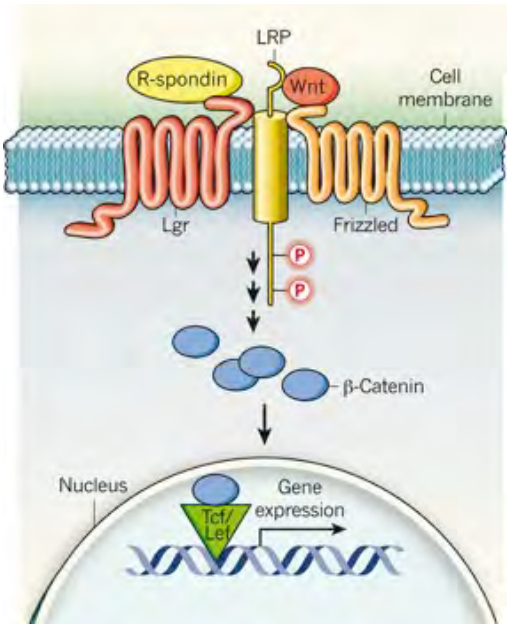

Figure 17. Canonical Wnt signaling is reinforced with R-spondins proteins. R-spondins activate LGR membrane proteins, to form the LGR-LRP–Frizzled receptor complex, that reinforces Wnt signaling (taken from Birchmeier, 2011).

In addition to the cytoplasmic βcatenin, there is a stable membrane-associated pool of βcatenin involved in the formation of *adherens* junctions through interactions with specialized cell-surface proteins such as E-cadherin. *βcatenin*$^{-/-}$ embryos have intact *adherens* junction, since plakoglobin (a member of the catenin protein family and homologous to βcatenin) replaces the role of βcatenin in cell adhesion (at early stages because *βcatenin*$^{-/-}$ embryos die in uterus) (Hu et al. 2005; Huelsken et al. 2000).

βcatenin is composed of an N-terminal domain, armadillo repeats domain and the C-teminal domain. The armadillo domain presents several binding sites for partners which are components of the Wnt/βcatenin pathway that regulate βcatenin activity and localization (Fig. 18) (Shapiro 2001; Graham et al. 2000).

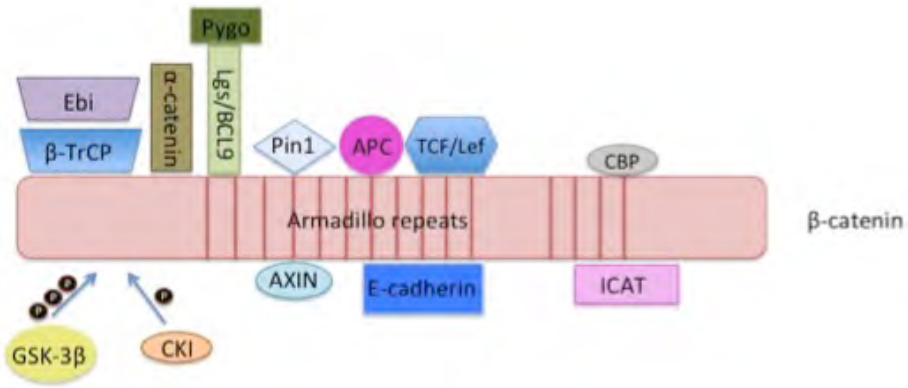

Figure 18. βcatenin and its binding partners. βcatenin activity is regulated by several binding partners that determine its stability and localization.

As previously mentioned, there are other non-canonical pathways. The two best studied are the Wnt/Ca^{2+} and the PCP pathways (Fig. 16). The non-canonical Wnt pathways are also involved in developmental processes, such as gastrulation movements, cell morphology, etc. Intracellularly, these pathways have been shown to activate JNK, Ca^{2+} flux and small trimeric G proteins (Topczewski et al. 2001). The non-canonical Wnt pathways also signals through receptors of the Frizzled family but several co-receptors are involved instead of LRP family, such as ROR2 (receptor tyrosine kinase-like

orphan receptor 2), which is a member of ROR family that plays a role in the planar cell polarity pathway.

DSH protein is also involved in these non-canonical pathways but it appears that the function of DSH differs between the canonical and non-canonical Wnt pathways. DSH mainly has three domains DIX, PDZ and DEP. The first two are clearly used for canonical Wnt signaling, and some contribution may also be made by the DEP domain. In the PCP signaling pathway, the PDZ and DEP domains are required. For WNT/Ca^{2+} signaling, the PDZ and DEP domains, but not the DIX domain, are essential (Fig. 19; Axelrod, Miller, Shulman, Moon, & Perrimon, 1998; Boutros, Paricio, Strutt, & Mlodzik, 1998; Heisenberg et al., 2000; L. Li et al., 1999; Tada & Smith, 2000).

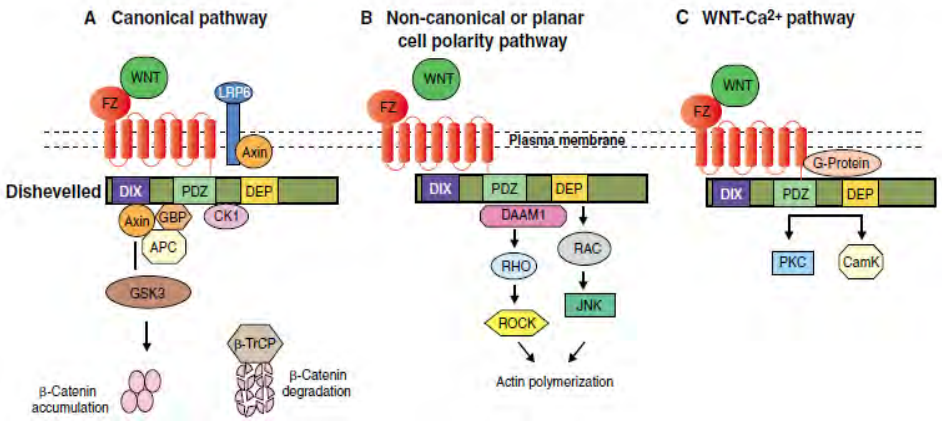

Figure 19. Dishevelled protein domains. DSH is involved in the canonical and non-canonical Wnt pathways, but each pathway requires different domains (Wallingford & Habas 2005).

Wnt signaling pathways also have some antagonists (Fig. 20), like sFRP (secreted frizzled related proteins) or WIF (Wnt-inhibitory factor) which directly bind to Wnt ligands and thus, inhibit the binding to its receptors. Others Wnt antagonists are dickkopf (DKK) or sclerostin (*Sost* gene product) which bind to LRP5/6 co-receptor diminishing the number of Wnt co-receptors available for signaling (Mao et al. 2002).

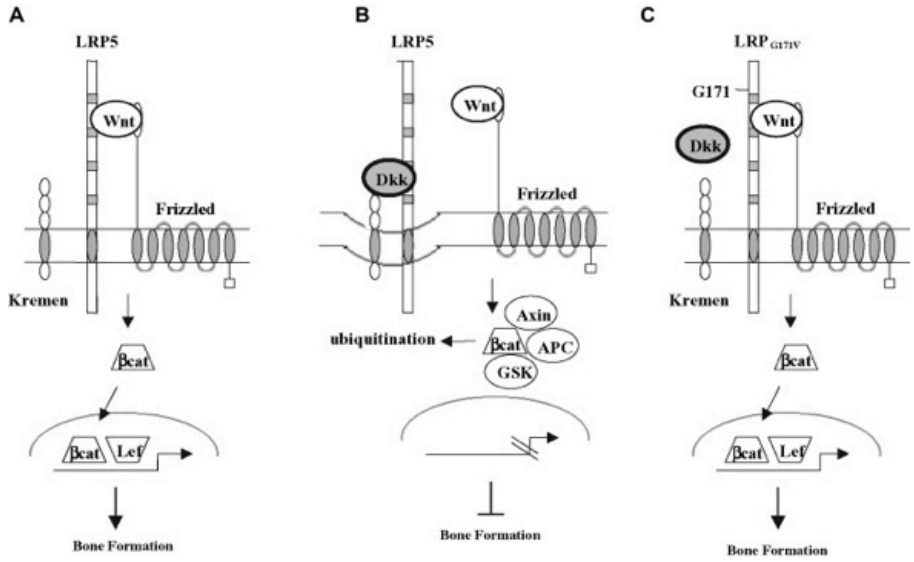

Figure 20. Wnt signaling antagonists. In normal conditions Wnt binds to its receptor Frizzled and co-receptor LRP5 activating the Wnt/βcatenin pathway (A). Wnt antagonists such as DKK can lead to the inactivation of Wnt pathway. DKK binds to its Kremen receptor and LRP5 inhibiting the binding between Wnt ligands and LRP5. This inhibition prevents the transcription of genes involved in bone development, resulting in osteoporosis (B). However, gain-of-function mutations (G171V) of *Lrp5* increase its affinity for Wnt ligands preventing DKK from binding to LRP5 and the pathway is more active leading to high bone mass formation or osteopetrosis (C) (Levasseur et al. 2005).

1.6 The canonical Wnt pathway in bone development and homeostasis.

The maintenance of the skeleton under normal conditions requires the existence of a balance between bone resorption and bone formation. This balance is closely related to the canonical Wnt pathway as evidenced in several bone diseases in which this pathway is altered, indicating that it plays a crucial role during bone development.

This importance of Wnt signaling in bone formation was unraveled when it was discovered that mutations in the Wnt co-receptor LRP5 resulted in changes of bone mass. It was shown that the Osteoporosis Pseudoglioma Syndrome (OPPG) (Gong et al. 2001), a rare autosomal recessive disorder consisting of ocular abnormalities and osteoporosis, was caused by an inactivating mutation in the gene encoding the *Lrp5*. On the other hand, the High Bone Mass Syndrome (HBM) (Boyden et al. 2002) was due to gain-of-function of *Lrp5*. Cell specific targeted loss- and gain-of-function mutations in the mouse, confirmed the implication of the Wnt/βcatenin signaling pathway in the genesis of these two syndromes. For example, *Lrp5* KO mice develop postnatal osteoporosis (Kato et al. 2002). In addition, some patients with juvenile idiopathic osteoporosis have been reported to harbor heterozygous mutations in the *Lrp5* gene (Hartikka et al. 2005). Also, it has been shown that common variants of *Lrp5* contribute to variability in bone mineral density (BMD) in the normal population (Riancho et al. 2011).

Other two Wnt pathway related diseases are sclerosteosis and Van Buchem disease, characterized by an increase in bone formation and

caused by alteration of sclerostin. Sclerostin inhibits the Wnt/βcatenin signaling by blocking the binding of Wnt proteins to LRP5. Though this binding to LRP5 does not seem to compete with Wnt proteins, it is thought that it inhibits their action by facilitating the internalization of LRP5 and thereby reducing their availability (Li, Zhang, et al. 2005; Semënov et al. 2005). The genetic defect responsible for sclerosteosis is a loss-of-function mutation of the *Sost* gene (Balemans et al. 2001; Brunkow et al. 2001), while Van Buchem disease is due to a deletion in a region containing transcription regulatory elements (Balemans et al. 2002; Staehling-Hampton et al. 2002; Loots et al. 2005). *Sost* KO mice have increased bone mass, and studies in animals and humans show that, likewise, administering antibodies antisclerostin increases bone mass (Li et al. 2009; Li et al. 2010; Ominsky et al. 2010; Padhi et al. 2011).

Additionally, mutations in Wnt proteins have been identified in human diseases. For instance, *Wnt1* or *Wnt16* mutations have been related with some forms of osteoporosis and osteogenesis imperfecta (Keupp et al. 2013; Laine et al. 2013; Pyott et al. 2013; Zheng et al. 2012). Also non-sense mutations in LGR family have been found to be related with low bone mineral density (Styrkarsdottir et al. 2013).

Because of the importance of these discoveries, the function of Wnt signaling at different stages of skeletogenesis has been extensively investigated. This investigation included the study of the expression patterns of many Wnt pathway members and the use of Wnt reporters in mice (Day & Yang 2008; Day et al. 2005; Hill et al. 2005; Hu et al. 2005; Hens et al. 2005; Parr et al. 1993). Moreover, as previously

mentioned, the canonical Wnt pathway has been genetically modified in many of its components to explore its function in bone development, such as *Axin2*, a negative regulator and the best reporter of canonical Wnt pathway and *Dickkopf-1* (*Dkk1)*, a well-known antagonist of Wnt signaling. *Axin2* null mice show a runt phenotype due to shortening of columnar and hypertrophic zones, while heterozygous have no differences with wild-type mice (Dao et al. 2010). DKK1 has been identified as an inhibitor of the canonical Wnt pathway in early vertebrate embryonic patterning. *Dkk1*$^{-/-}$ knockout mice show defects in head development, polydactyly, vertebral fusions and it is lethal few days after birth. Another *Dkk1* mutant caused by a distant transgenic insertion shows reduced *Dkk1* expression in the double ridge mouse (*Dkk1*^{d}). The residual *Dkk1* expression in *Dkk1*$^{d/d}$ or *Dkk1*$^{d/-}$ mice is sufficient for head development and survival of the mice (Macdonald et al. 2007). Moreover, *Dkk1* is also predominantly expressed in adult bone tissues in addition to its widely and dynamically pattern of expression during embryonic development to modulate the canonical Wnt pathway. It is present in the mature osteoblasts and osteocytes, suggesting that *Dkk1* may regulate bone homeostasis. Mice deficient for *Dkk2* are osteopenic due to a failure in osteoblast maturation and mineralized matrix formation (Li, Liu, et al. 2005).

Due to the complexity of the canonical Wnt pathway and since it converges in βcatenin, the main and nonredundant component of the pathway, a huge effort has been directed to analyze the effect in bone formation and homeostasis of gain- and loss-of-function mutations of *βcatenin* in specific cell types and stages as shown in Tables 1-4.

βcatenin loss-of-function mutations were introduced into osteo-chondrogenic progenitor cells using *Prx1* and *Dermo1-cre* deleter lines and resulted in early osteoblast differentiation arrest, impaired chondrocyte hypertrophy, and ectopic cartilage formation (Table 1) (Day et al. 2005; Hill et al. 2005; Hu et al. 2005).

Cre line	*Cre expression*	*Bone mass*	*Phenotype*	*Bibliography*
Dermo1-cre	Osteo-chondro progenitors	↓	Ectopic cartilage at expense of OB differentiation	Day et al., 2005
Dermo1-cre	Osteo-chondro progenitors	↓	Disrupted OB differentiation and impaired CC maturation and proliferation	Hu et al., 2005
Prx1-cre	Osteo-chondro progenitors	↓	Osteoblastogenesis arrest and precursors change its cell fate to chondrocytes	Hill et al., 2005
Col2a1-cre	Chondrocytes	↓	Perinatal lethal, impaired CC proliferation and maturation. Only endochondral bone is altered	Akiyama et al., 2004
Col2α1-cre3	Chondrocytes	↓	Failure to develop differentiated OB and they convert to CC	Rodda and McMahon, 2006

Col2a1-cre	Chondrocytes	↓	Ectopic chondrocyte differentiation and no osteoblast development	Day et al., 2005
Col2- cre ^{ERT2} (tamoxifen into pregnant female mice at E13.5)	Chondrocytes	↓	Delayed chondrocyte maturation, disorganized and small hypertrophic zone	Dao et al., 2012
Col2-CreER (tamoxifen was administered to 2-week-old cKO mice)	Chondrocytes	↓	Increased OC numbers with a decrease in *Opg* expression and increase in *Rankl* levels, methaphyseal bone loss and no changes in the midshaft. Impaired maturation of growth plate CC	Wang et al., 2014
Col2-OPG-transgenic	Chondrocytes	↑	Delayed formation of secondary ossification center. Reduced OC formation	Wang et al., 2014
α1(1)Collagen-cre	Early osteoblasts	↓	Decrease OPG leading to an increase in osteoclast numbers	Glass et al., 2005
Osx-cre (doxycycline treated prenatally until 2 months of age and then sacrificed at 6 months of age)	Early osteoblasts	↓	Increased bone marrow adiposity because of a shift in the cell fate from osteoblastic to adipocyte lineage decreasing osteogenic differentiation	Song et al., 2012

Osx1-GFP::cre	Early osteoblasts	↓	Impaired OB development and show zones of ectopic cartilage	Rodda and McMahon, 2006
Oc-cre	Mature osteoblasts	↓	Lethal within 5 weeks, impaired OB maturation and mineralization. Reduction of *OPG* levels leading to an increase in OC	Holmen et al., 2005
Dmp1-cre	Osteocytes	↓	Decrease OPG in osteocytes and increased OC numbers	Kramer et al., 2010

Table 1. Loss-of-function *βcatenin* mutants in the osteoblastic lineage cells (OB=osteoblasts, OC=osteoclasts, CC=chondrocytes).

Lack of *βcatenin* in early chondrocytes was studied using the *Col2a1-cre*, *Col2-cre*^{ER} (tamoxifen treatment from 2 weeks of age), *Col2-Cre*^{ERT2} (tamoxifen administration to pregnant female mice at E13.5) lines which show a decrease in bone mass phenotype due to fail of osteoblast development, ectopic cartilage formation and an increase in osteoclast numbers. However, Akiyama et al. using the *Col2a1-cre* line found a reduction in bone mass due to an impaired chondrocyte proliferation and differentiation during endochondral bone formation. In contrast *Col2-OPG-tg* mice show osteopetrosis because of a decrease in the number of osteoclasts through *Opg* induction (Day et al. 2005; Rodda & McMahon 2006; Wang et al. 2014; Dao et al. 2012; Akiyama et al. 2004).

Differentiated osteoblasts *βcatenin* mutants were analyzed with *Col1α1*, *Osx1-GFP-cre*, *Oc-cre* and *Dmp1-cre* mice lines. The results show a loss of bone mass owing to a decrease in OPG, an increase in the number of osteoclasts, impaired osteoblasts maturation and ectopic cartilage formation (Glass et al. 2005; Holmen et al. 2005; Rodda & McMahon 2006; Kramer et al. 2010). The experiments performed with *Osx-cre*, show an osteoporotic phenotype and cell fate shift of preosteoblasts from the osteoblast to adipocyte lineage. In this *Osx-cre* mice, the *Cre* expression was suppressed by administration of doxycycline until 2 months of age (Song et al. 2012).

Cre line	***Cre expression***	***Bone mass***	***Phenotype***	***Bibliography***
Prx1-cre	Osteo-chondro progenitors	↓	Suppress mesenchymal cells enter into chondrocyte lineage	Hill et al., 2005
Col2a1-cre	Chondrocytes	↓	Generalized chondrodysplasia. Only endochondral ossification is affected	Akiyama et al., 2004
Col2a1-cre	Chondrocytes	↓	Impaired cartilage formation and reversion of chondrocytes differentiation	Guo et al., 2004
Col2-CreER (tamoxifen was administered to 2-week-old cKO mice)	Chondrocytes	↑	Decreased OC number with an increase of *Opg* expression and reduction of *Rankl*	Wang et al., 2014

Col2- cre^{ERT2} (tamoxifen into pregnant female mice at E13.5)	Chondrocytes	Ø	Advanced chondrocyte maturation. Impaired ossification centers and perichondral bone formation. Enhanced osteogenic differentiation	Dao et al., 2012
Collagen α1(1)-cre	Early osteoblasts	↑	Decrease OC number due to an increase of OPG	Glass et al., 2005
Osx1-GFP::cre	Early osteoblasts	Ø	Premature mineralization and accelerated promotion of osteoblast development	Rodda and McMahon, 2006

Table 2. Gain-of-function *βcatenin* mutants in the osteoblastic lineage cells (OC=osteoclasts).

By contrast, gain-of-function mutations of *βcatenin* in mesenchymal cells through *Prx1-cre* leads to a failure in skeletal development due to inhibition of the differentiation of mesenchymal cells into the chondrocyte lineage (*Runx2*-negative and *Sox9*-positive skeletal precursors) cells and therefore, leads to chondrogenesis arrest (Hill et al. 2005) (Table 2).

To study the effect of the GOF of *βcatenin* in the chondrocyte lineage, the *Col2a1-cre* line was used, resulting in an low-bone-mass phenotype caused by failure in cartilage formation and impaired endochondral ossification (Akiyama et al. 2004; Guo et al. 2004).

Conditional GOF of *βcatenin* postnatally was achieved treating *Col2-Cre^{ER}* mice with tamoxifen. Treatment from 2 weeks of age, led to osteopetrosis due to an increase of *Opg* expression and subsequent decrease in osteoclast numbers (Wang et al. 2014). Conditional stabilization of *βcatenin* at late developmental stages with the *Col2-Cre^{ERT2}* mice and tamoxifen administration to pregnant female mice at E13.5, showed premature chondrocyte maturation and impaired formation of ossification centers and perichondral bone (Dao et al. 2012).

The effect of βcatenin in osteoblastic cells was assessed using *Col1α1-Cre* and *Osx1-GFP::cre*. GOF of *βcatenin* with the *Collagenα1-Cre* line showed an osteopetrotic phenotype caused by decreased number of osteoclasts, due to an increase in *Opg* expression (Glass et al. 2005). In contrast, GOF of *βcatenin* with the *Osx1-GFP::cre* line presented premature mineralization and an increased proliferation of pre-osteoblasts, but osteoblasts were not able to finish their development, showing a lack of *Osteocalcin* expression (Rodda & McMahon 2006).

Together these results indicate that the canonical Wnt pathway in mesenchymal or osteoblastic cells induces osteogenesis and prevents chondrogenesis or adipogenesis of mesenchymal cells, and moreover, that osteoclasts development is regulated in part by mature osteoblasts Wnt signaling.

The role of Wnt signaling in bone development was questioned in 2008, when it was discovered that *Lrp5* regulates bone mass in a Wnt

independent manner mediated by serotonin synthesis in the gut. *Lrp5* is expressed in the gut cells (enterochromaffin cells in the duodenum), where it negatively regulates the enzyme tryptophan hydroxylase 1 (Tph1) required for the biosynthesis of serotonin. Serotonin circulates through the blood to the osteoblasts, where it interacts with its receptor Htr1b to negatively regulate osteoblast proliferation (Fig. 21; Yadav et al., 2008).

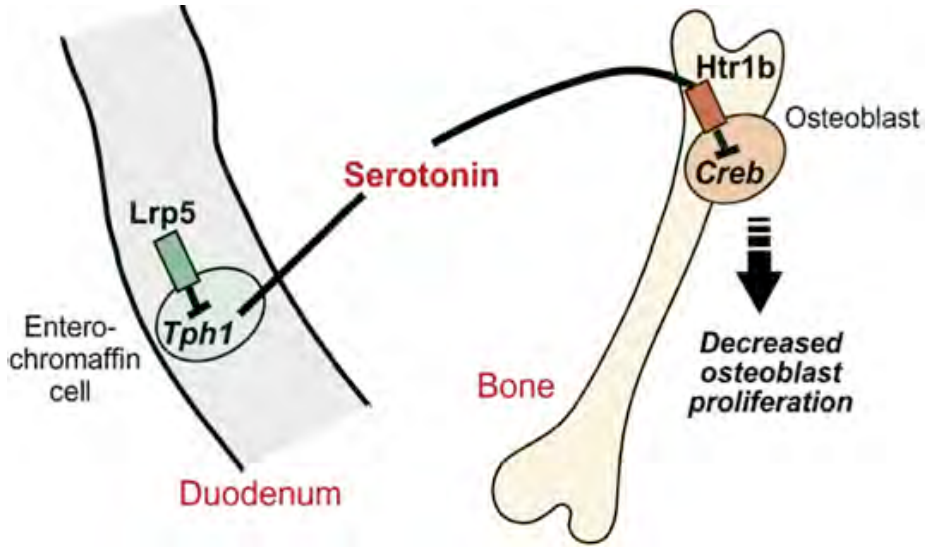

Figure 21. **Bone mass regulation via Lrp5/serotonin.** *Tph1* is negatively regulated by *Lrp5* in enterochromaffin cells. Therefore, LRP5 reduces blood serotonin levels and Htr1b signaling leading to increased osteoblast proliferation (Yadav et al. 2008).

At present, an intense debate remains on whether the role of LRP5 in bone homeostasis is direct or indirect. In any case, the importance of bone LRP5 is well recognized (Cui et al. 2011). It is possible that both mechanisms, the canonical Wnt pathway and the gut serotonin

pathway, regulate bone mass, and further studies are required to clarify this question.

1.7 Canonical Wnt pathway and osteoclasts

The presence of the Wnt/βcatenin signaling pathway components in osteoclasts was reported in a study in patients with myeloma (Qiang et al. 2010). In this study, the expression of genes of various components of the pathway (*Wnt*, *Frizzled*, *Lrp* and *Tcf*), the accumulation of βcatenin in response to WNT3A protein or lithium chloride (GSK3-β inhibitor), the inhibition of this response in the presence of DKK1 or sFRP1 and the induction of transcriptional activity TCF/LEF by WNT3A were reported in osteoclasts.

Modarresi et al. described that ritonavir, a drug used in treating patients with HIV infection and responsible, at least in part, of the bone loss suffered by these patients, suppressed genes involved in the Wnt canonical pathway and blocked the nuclear translocation of βcatenin in osteoclasts. In addition, exposure to lithium chloride and overexpression of *βcatenin* in osteoclast precursors suppressed their differentiation (Modarresi et al. 2009).

These studies provided support for Wnt/βcatenin functioning in osteoclasts and suggested its implication in osteoclast differentiation and function. However, while intense research on the role of the Wnt/βcatenin pathway in osteoblasts has been performed and is currently underway much little has been investigated about its role in osteoclasts.

Cre line	*Cre expression*	*Bone mass*	*Phenotype*	*Bibliography*
Tie2-cre	hemangioblast stem cell	↑	Decreased number of OC and resorption	Wei Wei et al., 2011
Tie2-Het	hemangioblast stem cell	↓	Increase number of OC and resorption	Wei Wei et al., 2011
PPARγ–tTA;TRE-cre	osteoclast progenitors	↑	Blockade osteoclast proliferation	Wei Wei et al., 2011
LysM-cre	macrophage precursors	↓	Increase resorption	Wei Wei et al., 2011
LysM-Het	macrophage precursors	↓	Decrease trabecular bone and increase OC number and resorption	Wei Wei et al., 2011
LysM-Cre	macrophage precursors	↓	Decrease OC progenitors proliferation but accelerated osteoclastogenesis	Otero et al., 2012
LysM-CRE	macrophage precursor	↓	Increased osteoclastogenesis and resorption	Albers et al., 2013
CtsK-cre	preosteoclasts and mature osteoclasts	↓	Increased resorption	Wei Wei et al., 2011
CtsK-Het	preosteoclasts and mature osteoclasts	↓	Intermediate bone loss	Wei Wei et al., 2011

Table 3. Loss-of-function mutations of *βcatenin* in the osteoclastic lineage cells (OC=osteoclasts).

During the carrying out of this thesis, several studies on βcatenin effects in the osteoclast lineage have been reported (Table 3 and 4). Wei et al. established mouse genetic models harboring *βcatenin* loss-of-function mutations leading to a truncated form of the protein in the osteoclast lineage employing several Cre drivers including *Tie2-cre* and *Tie2-Heterozygous*, for hemangioblast stem cell targeting, *LysMCre* for macrophage precursor targeting, and *CtskCre* for pre-osteoclast and mature osteoclast targeting (Table 3). In these studies a decrease in bone mass was found, which was due to an increase in osteoclast numbers and bone resorption, although this analysis was very slight in details. They also used *PPARγ-tTA;TRE-cre* mice to target the osteoclast progenitors. Those mice show osteopetrosis, because of osteoclast proliferation blockade (Table 3). Similarly, Otero et al. observed using *LysMCre* a reduced osteoclast precursor proliferation, but an acceleration in osteoclastogenesis. Moreover, Albers et al., reported a decrease in osteoclastogenesis induced by WNT3A (Wei et al. 2011; Otero et al. 2012; Albers et al. 2013) (Table 3).

Wei-Wei et al. also analyzed the effect of gain-of-function mutations of *βcatenin*, which drive a stabilized form of the protein that cannot be degraded (Table 4). These studies through *PPARγ-tTA;TRE-cre, LysMCre* and *CtsKCre* mice indicated that an increase of canonical Wnt signaling in osteoclast lineage, leads to an increase in bone mass due to a reduction in osteoclast numbers preventing its differentiation and bone resorption. Although, *Tie2-cre* line results in the lethality of the embryo at early embryonic stages (Table 4).

These results indicate that Wnt signaling is needed to induce the proliferation stage of the osteoclast precursors, but this signaling has to be down regulated to switch to their differentiation stage; they also showed that βcatenin effect is dose dependent.

Cre line	*Cre expression*	*Bone mass*	*Phenotype*	*Bibliography*
Tie2-cre	hemangioblast stem cell	lethal	ø	Wei Wei et al., 2011
PPARγ-tTA;TRE-cre	osteoclast progenitors	↑	Decrease number of OC and decrease resorption	Wei Wei et al., 2011
LysM-cre	macrophage precursors	↑	Decrease bone resorption	Wei Wei et al., 2011
CtsK-cre	preosteoclasts and mature osteoclasts	↑	Decrease bone resorption	Wei Wei et al., 2011

Table 4. Gain-of-function mutations of *βcatenin* in the osteoclastic lineage cells (OC=osteoclasts).

These studies evidence the canonical Wnt pathway in osteoclasts and that osteoclast precursor cells also has an effect on the development of osteoclasts and bone resorption.

On the other hand, other recent studies suggest that non-canonical Wnt signaling pathways are also involved in osteoclast development. Deletion of *Ror2* (a non-canonical co-receptor previously mentioned) in osteoclasts leads to a decrease in osteoclast numbers and an increase in bone mass (Witte et al. 2009; Maeda et al. 2013). Moreover, ablation of *Lrp5/6* in osteoclast precursors decreases

osteoclast differentiation through activation of non-canonical cAMP/PKA signaling (Weivoda et al. 2016).

In the Discussion section of this Thesis we will relate the results reported both by these authors and ours, and we will try to provide and update a comprehensive vision of the current state of knowledge.

2. AIM OF THE PRESENT THESIS

2) AIM OF THE PRESENT THESIS

The pivotal role of Wnt/βcatenin signaling in bone development and homeostasis is well established. The majority of previous studies were focused on the manipulation of the pathway in the osteoblast lineage. However, a complete understanding of the role of Wnt signaling in bone biology requires the analysis of its potential role in the other bone cells implicated in bone homeostasis, the osteoclasts. This is the aim of the present Thesis, to elucidate the function of canonical Wnt signaling in the osteoclast biology and its effect in bone homeostasis. Therefore, we have generated mice with *βcatenin* inactivation in the osteoclast lineage using the *Cre;LoxP* technology. *LysozymeM-Cre* line was used to introduce the loss-of-function of *βcatenin* in osteoclast precursors and *CathepsinK-Cre* line was used to target the mature osteoclasts. An in depth characterization of the skeleton (*in vivo* studies) as well as the analysis of osteoclast development and osteoclast cell biology (*in vitro* studies) of *CtsKCre* mutant animals were performed.

3. MATERIALS AND METHODS

3) MATERIALS AND METHODS

3.1 Generation of the mouse model

3.1.1 Mouse strains

The mouse strains used in this study were *Ctnnb1*$^{lox(2-6)}$, *CathepsinKCre* (*CtsKCre)* and *LysozymeMCre (LysMCre)*. All animal procedures were conducted accordingly to the EU regulations and 3R principles and reviewed and approved by the Bioethics Committee of the University of Cantabria. All mice were maintained in a C57BL6 genetic background and genotyped based on previously published reports.

The *Ctnnb1*$^{lox(2-6)}$ allele possesses loxP sites flanking exons 2 to 6 of *βcatenin* gene. In the presence of the Cre recombinase enzyme, the DNA fragment comprising exons 2-6 of the gene is excised, obtaining a disrupted form of the βcatenin protein and resulting in a null allele (Brault et al. 2001).

The *CtsKCre* allele expresses the Cre recombinase under the promotor of *Cathepsin K (CtsK)*, which is expressed by osteoclasts in the final stages of maturation (Nakamura et al. 2007).

The *LysMCre* line expresses the Cre recombinase enzyme under the control of the promoter *Lysozyme M (LysM)*, protein characteristic of cells of monocyte/macrophage lineage, the osteoclast precursors (Clausen B.E et al. 1999).

3.1.2 Mouse mating strategies

To generate a mice cohort of 13 males and 17 females with loss-of-function (LOF) of *βcatenin* in the *CstK*-expressing cells and 21 males and 20 females considered as controls, we have utilized the Cre-loxP technology, using *Ctnnb1*$^{lox(2-6)}$ line and the *CtsKCre* deleter line that express the Cre recombinase.

CtskCre$^{+/-}$	X	*Ctnnb1*$^{lox(2-6)/lox(2-6)}$
(50%) *Ctnnb1*$^{lox(2-6)/+}$*;CtsKCre*		(50%) *Ctnnb1*$^{lox(2-6)/+}$

Ctnnb1$^{lox(2-6)/+}$*;CtsKCre*	X	*Ctnnb1*$^{lox(2-6)/lox(2-6)}$
(25%) *Ctnnb*$^{lox(2-6)/+}$*;CtsKCre*		(25%) *Ctnnb*$^{lox(2-6)/+}$
(25%) *Ctnnb*$^{lox(2-6)/lox(2-6)}$*;CtsKCre*		**(25%) *Ctnnb*$^{lox(2-6)/lox(2-6)}$**

Table 5. *Ctnnb1*$^{lox(2-6)/lox(2-6)}$*;CtsKCre* mouse mating cycles. In the first mating cycle was obtained a double heterozygous mice which in a second crossing is mated with *Ctnnb1*$^{lox(2-6)/lox(2-6)}$ to generate our control (*Ctnnb1*$^{lox(2-6)/lox(2-6)}$) and experimental *(Ctnnb1*$^{lox(2-6)/lox(2-6)}$*;CtsKCre)* mice.

To obtain them, we performed two mating cycles (Table 5). First, animals carrying one *CtsKCre* allele were mated with the animals carrying the *Ctnnb1*$^{lox(2-6)}$ allele in homozygosis to obtain double heterozygous mutant (50% of the progeny). In a second crossing,

double heterozygotes from the first crossing were mated with homozygous *Ctnnb1*$^{lox(2-6)}$ mice. 25% of the animals from the last crossing are homozygous for floxed allele and heterozygous Cre carriers. The latter are the ones we use as experimental animal (*Ctnnb1*$^{lox(2-6)/lox(2-6)}$*;CtsKCre)*.

LysMCre$^{+/-}$	X	*Ctnnb*$^{lox(2-6)/lox(2-6)}$
(50%) *Ctnnb*$^{lox(2-6)/+}$*;LysMCre*		(50%) *Ctnnb*$^{lox(2-6)/+}$

Ctnnb$^{lox(2-6)/+}$*LysMCre*	X	*Ctnnb*$^{lox(2-6)/lox(2-6)}$
(25%) *Ctnnb*$^{lox(2-6)/+}$*;LysMCre*		(25%) *Ctnnb*$^{lox(2-6)/+}$
(25%) *Ctnnb*$^{lox(2-6)/lox(2-6)}$*;LysMCre*		**(25%) *Ctnnb*$^{lox(2-6)/lox(2-6)}$**

Table 6. *Ctnnb1*$^{lox(2-6)/lox(2-6)}$*;LysMCre* mice mating cycles. Double heterozygous mice were obtained in 50% of the first cycle progeny. In the second mating cycle *Ctnnb1*$^{lox(2-6)/lox(2-6)}$ mice were mated with the double heterozygous mutant mice, obtaining the control *Ctnnb1*$^{lox(2-6)/lox(2-6)}$ and the experimental *Ctnnb1*$^{lox(2-6)/lox(2-6)}$*;LysMCre* mice.

Following the same strategy used for *Ctnnb1*$^{lox(2-6)/lox(2-6)}$*;CtsKCre* mice, the *Ctnnb1*$^{lox(2-6)/lox(2-6)}$*;LysMCre* animals were obtained through two mating cycles (Table 6). Animals with the *LysMCre* allele were crossed with animals bearing the *Ctnnb1*$^{lox(2-6)}$ allele in homozygosis obtaining a 50% offspring double heterozygous mutant. In the second cycle double heterozygous mice were mated with homozygous

Ctnnb1$^{lox(2-6)}$ mice getting our experimental genotype in 25% of the progeny (*Ctnnb1*$^{lox(2-6)/lox(2-6)}$*;LysMCre).*

The mice used in this study of *βcatenin* floxed allele (*Ctnnb1*$^{lox(2-6)}$) and *LysMCre* mice were obtained from The Jackson Laboratory. *CtsKCre* mice were provided by Dr. Shigeaki Kato, Institute of Molecular and Cellular Biosciences (University of Tokyo).

3.1.3 Identification and genotyping of animals

Identification of mice was performed coinciding with weaning at 3 weeks of age. At that time, they were pierced the ears for identification and were cut 0.5 cm tail to extract genomic DNA.

3.1.3.1 Extraction of genomic DNA

For *Ctnnb1*$^{lox(2-6)}$, *CtsKCre* and *LysMCre* mice, the DNA extraction was obtained from the tail fragment transferred to an eppendorf tube containing 100µl of lysis buffer (made with 50mM KCl; 10mM Tris pH 8.3; 2 mM $MgCl_2$; 0,1mg/ml gelatin; 0,45% NP-40; 0,45% Tween20) and 1 µl of proteinase K and incubated overnight at 55ºC. Then, the proteinase K was inactivated by heating at 95ºC for 10 min.

3.1.3.2 Genotyping by PCR

Generated mice were genotyped by the polymerase chain reaction (PCR) analysis from DNA obtained from tail biopsies. 1 µl of extracted DNA obtained from tails was used to the PCR reaction.

Mice were genotyped following standard PCR protocols, varying the temperature and time of the annealing stage depending on the melting temperature (Tm) of the primers used. The PCR reaction was performed using ReadyMixTM Taq PCR Reaction Mix with $MgCl_2$ Mastermix (Sigma-Aldrich). The primers were used in a final concentration of 20μM. The PCR amplification product was visualized on an agarose gel 1% dissolved in TAE electrophoresis buffer (1M Tris-acetate and 0.5 NaEDTA pH 8) and containing Red Safe for DNA staining and visualized in the GelDoc under ultraviolet light. The software used was Quantity–One (BioRad). Finally, the molecular weight of the products was determined with the use of MassRuler DNA Ladder (Fermentas). The set of primers used to genotype each mouse strain and PCR conditions were:

- *Ctnnb1*$^{lox(2-6)}$ allele:

oIMR1512 (F) primer: 5'- AAGGTAGAGTGATGAAAGTTGTT -3'

oIMR1513 (R) primer: 5'- CACCATGTCCTCTGTCTATTC -3'

The thermocycler was programmed for 1 cycle of 1.5 minutes at 94ºC and 35 cycles of 30 seconds at 94°C, 30 seconds at 60°C and 30 seconds 72°C. The reaction ended after a cycle of 2 minutes at 72°C. The expected product sizes are: for mutant band is 324 bp and for wild type band 221 bp.

- *CathepsinK Cre* and *LysozymeM Cre* line:

Cre 5' primer: 5'- CCTGGAAAATGCTTCTGTCCGTTTGCC -3'

Cre 3' primer: 5'- GAGTTGATAGCTGGCTGGTGGCAGATG -3'

The thermocycler was programmed for 1 cycle of 3 minutes at 94ºC and 35 cycles of 45 seconds at 94°C, 45 seconds at 55°C and 1 minute at 72°C. The reaction ended after a cycle of 10 minutes at 72°C. The expected Cre product size is 654 bp.

3.2 RNA extraction, reverse transcription and quantitative PCR

Total RNA of macrophages and mature osteoclasts cultures from 3-4 animals per genotype, was extracted with Trizol (TRI Reagent-SIGMA) and solutions of chloroform, isopropanol and 70% ethanol. The precipitate was diluted in DEPC H_2O (RNAse free water) and incubated at room temperature (RT) for 5 minutes before sample concentration were measured at the nanodrop (Nanodrop technologies ND-1000) and stored at -80ºC. For tissues, RNA extraction was performed using the same procedures that cultures but before extraction, they were weighed (100mg) and homogenized with a homogenizer (POLYTRON PT-2500E, Kinematica, AG) grinding in 1ml of Trizol.

To analyze RNA expression levels in quantitative PCR (qPCR), it is needed to obtain the cDNA from the extracted RNA of cells and tissues. Reverse transcription was performed from 1 µg/µl of total RNA dissolved in 10.5µl RNAase free water and heated at 65ºC for 5 minutes. Afterwards, 9.5µl of a second mix containing a mixture of 5X First Strand Buffer, 0.1M DTT, dNTPs, random primers and reverse transcriptase enzyme (m-mlv-RT) from Invitrogen and RNAse inhibitors (Ribolock) from Thermo Scientific. These mixed reagents are added to the first mix of RNA and the RNAase free water. This

reaction was incubated at RT for 10 minutes first, and then, in the thermal cycler to 42°C for 50 minutes and 5 minutes at 99ºC later. Finally samples are stored at -20ºC.

For the analysis of *βcatenin (Ctnnb1)* and *CtsK* expression in macrophages, osteoclasts and other tissues, taqman qPCR was performed from 100ng of cDNA and mixed with the reagent Premix Ex Taq Master Mix (containing thermostable DNA polymerase). Specific primers for *Ctnnb1* (Mm01350385_g1) and *CtsK* (Mm00484039_m1) were obtained from Takara. The reaction was performed in a volume of 20µl and quantified in a thermocycler (7500 Real time PCR System, Applied Biosystems) that detected, in real time, the fluorochromes FAM and VIC. The relative expression of mRNA was normalized to the internal standard gene (house-keeping) *Gapdh* (Mm99999915_g1).

For analysis of *Rankl* and *Opg* expression was performed a SYBR Green qPCR where we used SYBR Green Supermix, sterile distilled water and primers for *Rankl* (F: 5'-AAATTAGCATTCAGGTGTCC-3' and R: 5'-AATGTTCCACGAAATGAGTC-3') and *Opg* (F: 5'-AAAAATGTCCAGATGGGTTC-3' and R: 5'-ACACAGGGTGACATCTATTC-3'). The relative expression of mRNA obtained was normalized to *tubulin*, used as housekeeping (F: 5'-GCAGTGCGGCAACCAGAT-3' and R: 5'-AGTGGGATCAATGCATGCT-3') and analyzed in a thermocycler (Step One Plus Real Time PCR Systems, Applied Biosystems).

The results were analyzed using method $2^{-\Delta(\Delta Ct)}$ (Livak & Schmittgen 2001) that calculates the relative changes in gene expression by correlating the value of the threshold cycle (Ct or cycle at which the fluorescence starts to grow significantly).

$$\textbf{Relative variation} = 2^{-\Delta(\Delta Ct)}$$

$$\Delta Ct = Ct_{sample} - Ct_{housekeeping}$$

$$\Delta(\Delta Ct) = \Delta Ct - \Delta Ct_{negative\ control}$$

All data are reported as the mean ± standard deviation and group mean values were compared by Student's unpaired two-tailed *t* test (*= $P \leq 0.05$).

3.3 Analysis of bone phenotype

3.3.1 X-ray radiographs

Anesthetized mice were examined through X-ray system CCX Digital trophy trex. The radiographs were performed in the right femur and vertebrae of three animals per genotype.

3.3.2 Densitometry

Bone mass densitometry (BMD) was performed in anesthetized animals (10 males and 18 females for each genotype). It was determined by using a DEXA densitometer Lunar MDL PIXI (GE Medical Systems Lunar Division, Madison, WI). The study included

the back-lumbar spine and left femur. The measures were performed blind.

3.3.3 Micro-computed tomography (μCT) analysis

μCT analysis of the fifth lumbar vertebra and femur of 10 control and 10 experimental animals of both sexes, was done after the bones were dissected, cleaned, fixed in ethanol, loaded into 12.3 mm diameter scanning tubes and imaged (μCT40, Scanco Medical, Basserdorf, Switzerland). Scans were integrated into 3-D voxel images (1024 x 1024 pixel matrices for each individual planar stack) and a Gaussian filter (sigma = 0.8, support = 1) was used to reduce signal noise. A threshold of 200 was applied to all analyzed scans. Scans were done at medium resolution (E = 55 kVp, I = 145 μA, integration time = 200ms). The entire vertebral body was scanned with a transverse orientation excluding the pedicles and articular processes. All trabecular measurements were made by manually drawing contours every 10 to 20 slices and using voxel counting for bone volume per tissue volume and sphere filling distance transformation indices without assumptions about the bone shape as a rod or plate for trabecular microarchitecture. Femur cortical thickness was measured at the distal femur and mid-diaphysis. These analyses were performed blind.

3.3.4 Histomorphometry

Three lumbar vertebrae (L2-L4) of 6 animals per genotype, were decalcified in 9% EDTA (pH7.4) and dissected in longitudinal 7-10μm sections. The display of osteoclasts in bone sections was made by

staining with tartrate-resistant acid phosphatase (TRAP) as explained in section 3.4.2. The quantification of the number of osteoclasts per bone perimeter (N.Oc/mm) and bone area relative to the total bone area (BA/TA) was carried out with the ImageJ (Fiji) software.

3.4 Skeletal histology analysis

After harvest the bone samples from a minimum of three animals per genotype, were fixed with 4% paraformaldehyde (PFA), washed in PBS and decalcified only the postnatal bones with 9% EDTA (pH 7,4) for a variable period of time (5-9 days) depending of the stage. Once the bones were decalcified were embedded in paraffin to analyze them in sections. The femurs and vertebrae were rinsed in PBS twice for a progressively dehydration by using changes in rising ethanol concentrations (50%, 70%, 96% and 100% twice) from 1 to 2 hours for each change (depending of the sample stage). The samples were cleared in two changes of xylol (30-45 minutes twice each) and finally transferred to paraffin at 60ºC. 7-10 µm thick sections were performed by a Leica RM2125RT microtome. Paraffin was removed in xylol and Cytoseal was used as mounting medium. Skeletal preparations were observed with the use of an Olympus SZX12 stereoscopic scope and photographs were taken with a Nikon DS-Fi1 camera.

3.4.1 Hematoxylin-Eosin (H-E) staining

To carry out the H-E staining in sections, tissue sections were deparaffined in xylol and rehydrated with changes in decreased concentrations of ethanol. Afterwards, the slides were rinsed in hematoxylin for 1 minute and immediately washed with tap water until

the staining turned to the desirable color. Then, the samples were eosin stained for 3 minutes and washed with distilled water. Finally, they are dehydrated and mounted.

3.4.2 TRAP staining in skeletal sections

To perform TRAP staining in paraffin sections, first, paraffin was removed from the tissue sections by two washes of xylol of 10 min each and routinely rehydrated. The slides are incubated in solution B in a coplin jar at 37ºC for 30 minutes. After this time, the slides are placed in a solution F for 2 minutes at RT and counterstained with toluidine blue. The slides are dehydrated with ethanol and xylol and mounted with Cytoseal medium.

- The solutions that were used for TRAP staining in sections were:

Stock solution A): 0.2M NaK tartrate in distilled H_2O NaAc pH 5; Stock solution B): 10% napthol AS-BI phosphoric acid in the stock solution A; Solution C): 4% pararosaniline in 2M HCl; solution D): 40mg/ml of $NaNO_2$ in distilled H_2O; solution E): 1:1 stock solution C and D; solution F): 7% solution E in the stock solution A.

3.5 RNA probe synthesis

3.5.1 Transformation, amplification and extraction

Specific DNA sequences for RNA probe synthesis are cloned in plasmidic vectors. For plasmid transformation, 1-3µl (1-10 ng DNA) of

the vector containing the target DNA and ampicillin resistant sequence were added to an eppendorf containing 30 µl Dh5α (E. coli) competent bacteria. Transformation was done by heat shock. First, leave for 30 minutes on ice and then, 20 seconds at 37ºC. After this, 2 minutes again on ice. Then, LB medium was added and incubated at 37ºC for one hour before culturing overnight at 37ºC in a Petri dish containing LB and ampicillin (1:1000). The next day, one of the ampicillin resistant individual colonies was selected and transferred to an erlenmeyer containing 10 ml LB and ampicillin and incubated overnight in a rocking platform at 37ºC. The following day, plasmidic DNA extraction was performed using the "High pure plasmid isolation kit for plasmidic DNA extraction" (From Roche).

3.5.2 Plasmid linearization and transcription

To synthesize an anti-sense transcript, a specific restriction endonuclease should be used to linearize the DNA template. Digestion was performed following standard protocols. Probes can be generated by *in vitro* transcription reaction in the presence of the labeled nucleotides, digoxigenin labeled ribouridiltriphosphate nucleotides (Dig-UTP) using the appropriate specific polymerase for each plasmid. Transcription was performed following standard protocols.

To obtain the anti-sense *Collagen 1* riboprobe, the plasmid was linearized using the EcoRI restriction enzyme and the transcription was performed using the T7 polymerase. For *Bone sialoprotein* riboprobe Not I restriction enzyme and Sp6 polymerase was used.

CtsK riboprobe was linearized with PstI and transcribed with Sp6. And for *Sost* riboprobe was used the XhoI enzyme and Sp6 polymerase.

3.5.3 *In situ* hybridization (ISH) in sections

In situ hybridization was done following standard protocols. For a brief description, ISH was done in the tissue sections of the limbs dissected in PBS and fixed in PFA 4% in PBS overnight (O/N). The samples were hydrated in xylol and 100%, 96%, 70% and 50% ethanol. After washing in PBT, they were incubated in proteinase K (Roche) 10µg/ml during 7 minutes and 30 seconds. After proteinase K treatment, they were washed in PBS and fixed in 4% PFA. Afterwards, the slides were rinsed twice in PBS for 5 minutes. PBS washes were followed by an acetylation step (0,1M Triethanolamine, 0,066mM Acetic Anhydride) for 10 minutes to decrease background. Then, the slides were rinsed in PBT for 5 minutes and washed 5 minutes in distilled water (dH_2O) before allowing them to air dry. Once the slides were dried, hybridization buffer (containing the appropriated amount of probe for each experiment) was added and a coverslip was applied over the slides for hybridization in a moist chamber, O/N at 65ºC. The hybridization buffer containing the desired amount of probe was previously heated at 85ºC for 2 min to avoid secondary structures. The following day, covers were removed with 5xSSC at RT (2.5M NaCl, 250mM Sodium Citrate). Then, washes were done at 65°C with 1x SSC/ 50% formamide for 30 minutes (500mM NaCl, 50mM Sodium Citrate and 50% formamide), 2%SSC (1M NaCl, 100mM Sodium Citrate) for 20 minutes and 0.2%SSC (10mM NaCl, 1mM Sodium Citrate) twice, 20 minutes and finally MABT 1X (NaCl 150mM, Maleic Acid 100mM, 0.04% Tween, pH 7.5) at room temperature (twice, 5

minutes). After that, they were kept for 1 hour at RT in a solution 20% sheep serum in MABT 1X. Then, 5% sheep serum solution/MABT 1X with anti-dig-AP antibody (anti-digoxigenin-alkaline phosphatase antibody) was diluted in a ratio 1/2000 and kept O/N at 4°C. Next day washes with MABT were performed at RT. Finally, alkaline phosphatase activity was detected by incubating the samples in a solution with NTM, NBT (3µg/mL) and BCIP (2.3µg/mL). Once obtained the wanted level of signal, the reaction is stopped washing in PBS 1X (5 minutes) and then fixed in 4%PFA for 20 minutes. Slides were washed in PBS for 5 minutes, then in dH_2O others 5 minutes and stained with eosin for 3 minutes for posterior progressive dehydration using changes of 10 minutes in rising ethanol concentrations (50%, 70%, 96%, 100% twice and xylol twice). Cytoseal was used as mounting media. Samples were observed with the Nikon ECLIPSE 80i microscope and photographs were taken with a Nikon DS-Ri1 camera.

3.6 Generation of CtsK antisense probe for ISH by PCR

A 710 bp length *CtsK* specific probe for ISH was generated by PCR, using cDNA samples obtained from wild type 8-week-old liver and skin. Specific primers for PCR amplification of *CtsK* from cDNA samples were designed using on line bioinformatics tools such as Sequence Analysis and BLAST programs, together with the Sequence Manipulation Suite Website (www.bioinformatics.org). Once amplified, the PCR product was run in 1% agarose gel and purify with the use of the Quiaquick gel extraction kit (Quiagen) following manufacturers recommendations and ligated into pGEM-T easy vector. For plasmid transformation, 6µl of the vector were added to an eppendorf

containing 30µl Dh5α (E. coli) competent bacteria and follows as explained in the section 3.5. In addition, recognition sites for the Sp6 polymerase to 5' ends of specific reverse primer used to amplify the gene, enables direct *in vitro* transcription of the antisense probe for ISH directly from the gel purified of PCR products. Primer sequences used are specified below, whereby Sp6 polymerase promoter sequence is in upper case.

CtsK antisense PCR probe primers (5' to 3' orientation):

->CtsK-F: gaccactgccttccaatacg
->CtsK-R: ATTTAGGTGACACTATAGAActgctggaggactccaatgt

3.7 Primary cell cultures of macrophages and osteoclasts

Macrophages and osteoclasts were derived from the red bone marrow (BM) cells of the femur and the tibia of at least, three animals per genotype. Briefly, the bones were dissected and their ends cut off. Then, a 25G needle was inserted into the marrow cavity. The BM cells were flush out with the needle and a loaded syringe with minimum essential medium alpha modified (α-MEM), 10% FBS (Gibco-Life Technologies) and 1% PSG (penicillin, streptomycin and gentamicin). Then, they were seeded and maintained in culture for 16-24 hours.

3.7.1 Macrophages development

The following day, the cells were collected and seeded in α-MEM supplemented with 10% fresh FBS and 1% PSG at a density of $0.1x10^6$/ml with 30µg/ml M-CSF for 4 days.

3.7.2 Osteoclasts development

The following day, the cells were harvested and seeded at a density of $0,1x10^6$/ml with 30µg/ml M-CSF and 30 µg/ml RANKL for 5 days, to displaying osteoclasts.

3.7.3 Analysis of osteoclast cell cultures

The cells obtained directly from the BM were quantified by a counter of nucleated cells (Nucleocounter®, Chemometec), and then were resuspended in α-MEM supplemented with 10% fresh FBS, 1% PSG, 30µg/ml of M-CSF and 30 µg/ml RANKL. Three wells were plated for each individual animal in a 48 well plate with density of 50000 cells. At 5 days of incubation, cells were fixed (4% formaldehyde) and stained with tartrate-resistant acid phosphatase (TRAP). They were quantified by light microscope. Only multinucleated and positive staining cells were quantified as osteoclasts.

RANKL, M-CSF and recombinant mouse WNT3A were from R&D Systems (Minneapolis, MN).

3.8 Staining for tartrate-resistant acid phosphatase (TRAP) in osteoclast cultures

Osteoclasts were fixed with 4% formaldehyde solution for 15 minutes, washed in PBS, distilled water and air dry before proceeding to TRAP staining. Solutions C, D and E were freshly prepared at the day of staining, then cells were covered with solution E for 10 minutes at a temperature of 37 °C.

- The solutions that were used for staining of TRAP were:

Stock solution A: 0.2M NaK tartrate in distilled H_2O NaAc pH 5; Stock solution B: 4% pararosaniline in 2M HCl; Solution C: 40mg/ml of $NaNO_2$ in distilled H_2O; solution D: 1:1 stock solution B and C; Solution E: 7% solution D and 12% napthol AS-BI phosphoric acid in the stock solution A.

3.9 Apoptotic assay in osteoclasts (TUNEL)

Before performing the analysis of apoptosis by TUNEL (terminal deoxy transferase-mediated biotin-dUTP Nick End Labeling), cells isolated from 2 animals per genotype of *Ctnnb1$^{lox(2-6)/lox(2-6)}$;CtsKCre* and *Ctnnb1$^{lox(2-6)/lox(2-6)}$;LysMCre* mice were fixed with 4% formaldehyde. Afterwards, the samples were permeabilized with a 1:100 2mg/ml proteinase K in 10 mM Tris, pH 8 for 5 minutes. Endogenous peroxidases were quenched with a 1:10 30% H_2O_2 in methanol. Labeling of terminal DNA fragments, the cellular apoptosis product, was performed by incubating the sample at 37°C for half an hour in a mixture of 58.4µl biotinylated oligonucleotides and non biotinylated with 1.6µl DNA polymerase I Klenow. Detecting the labeling of the fragments, was performed with 2µl of peroxidase conjugated streptavidin and 98µl of 4% bovine serum albumin (BSA) in PBS for 30 minutes at 37°C, followed by 5 minutes of incubation with 0.7mg of 3,3'Diaminobenzidine (DAB) and 1.6mg H_2O_2/urea diluted in 1ml of tap H_2O. Before performing the counter-staining 0.3% methyl green, the samples were stained with TRAP, as explained above. Finally, they were dehydrated in 100% ethanol and xylene, and then mounted on a slide with Cytoseal media. Osteoclasts were

identified as TRAP positive multinuclear cells (three or more nuclei). Apoptotic cells were detected by the brown insoluble dye, product of the reaction of peroxidase-conjugated streptavidin DAB, localized in the nucleus (FragEL DNA Fragmentation Detection Kit, Colorimetric-Klenow Enzyme, Calbiochem).

4. RESULTS

4) RESULTS

4.1 Generation of mice with conditional excision of Ctnnb1 in mature osteoclasts

To elucidate the role of Wnt signaling in differentiated osteoclasts, *Ctnnb1 (βcatenin*) gene was specifically removed from mature osteoclasts, using the *CathepsinK-Cre* (*CtsKCre*) line because expression of *CtsK* is considered characteristic of the fully developed osteoclasts. The *CtsKCre* line is a knock-in of the *Cre recombinase* in the *CtsK* locus (Nakamura et al. 2007). Mice homozygous for the $Ctnnb1^{lox(2-6)}$ allele ($Ctnnb1^{lox(2-6)/lox(2-6)}$) were mated with *CtsKCre* mice. Double heterozygous mice for the $Ctnnb1^{lox(2-6)}$ and *CtsKCre* alleles, designated here as $Ctnnb1^{lox(2-6)/+}$;*CtsKCre*, were crossed to homozygous $Ctnnb1^{lox(2-6)}$ mice to obtain mice homozygous for $Ctnnb1^{lox(2-6)}$ and heterozygous for *CtsKCre* ($Ctnnb1^{lox(2-6)/lox(2-6)}$;*CtsKCre*). These animals were considered the experimental group while mice homozygous for $Ctnnb1^{lox(2-6)}$ but not carrying the *CtsKCre* allele were used as control group.

In $Ctnnb1^{lox(2-6)/lox(2-6)}$;*CtsKCre* mice, the *Ctnnb1* floxed allele is converted to the null allele in cells that express *Ctsk*, presumably resulting in *Ctnnb1* loss-of-function in mature osteoclasts. To assess the efficiency and specificity of the recombination we analyzed the expression of *βcatenin* by quantitative PCR (qPCR) using a probe specific for the deleted exons of *βcatenin* in macrophages and osteoclast cells derived from the bone marrow (BM) of femur and tibia in cell cultures and in several tissues of experimental and control animals. As described in the *Material and Methods* section, the BM

cells were treated with osteoclast differentiation cytokines, the M-CSF for 4 days to derive macrophages and with M-CSF and RANKL for 5 days to derive osteoclasts. Four animals per genotype were sacrificed and the BM cultures were performed. RNA extraction from cells collected on 4th day of culture for macrophages and 5th day for osteoclasts was realized. As expected, the level of expression of *βcatenin* in macrophages from control and experimental mice was indistinguishable, but the expression of *βcatenin* in mature osteoclasts from *Ctnnb1*$^{lox(2-6)/lox(2-6)}$;*CtsKCre* decreased approximately 64% compared with those obtained from *Ctnnb1*$^{lox(2-6)/lox(2-6)}$ (Fig. 22A-B).

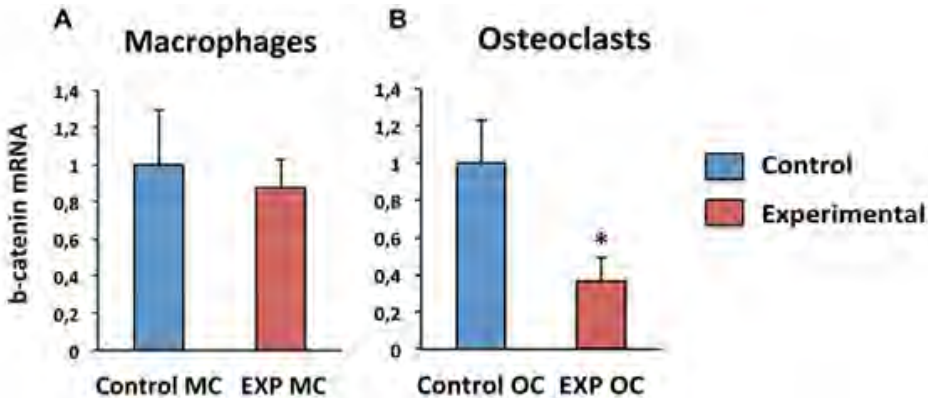

Figure 22. *βcatenin* expression in macrophages and mature osteoclasts. qPCR was performed for *βcatenin* in control and experimental cultures of macrophages and osteoclasts developed in presence of M-CSF and M-CSF and RANKL respectively. Similar expression levels of *βcatenin* were observed in experimental and control macrophages (A) while *βcatenin* expression was significantly reduced in experimental mature osteoclasts compared with control (B). qPCR was normalized with *gapdh* (n=4 per group). *Bars, Mean*± SD, *, P ≤ 0.05. (MC=macrophages, OC= osteoclasts).

We also analyzed *CtsK* expression in macrophages and mature osteoclasts of control animals. As expected, we found no detectable expression in macrophages (Fig. 23) suggesting that activation of *Ctsk* expression is a late event in the process of osteoclast differentiation.

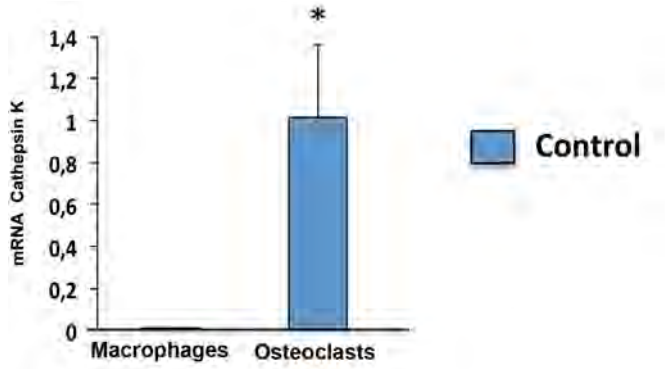

Figure 23. *CtsK* expression in macrophages and mature osteoclasts. qPCR of macrophages and osteoclasts derived from control BM cells, was performed. *CtsK* expression is restricted to mature osteoclasts being undetectable in macrophages. qPCR was normalized with *gapdh* (n=3 per group). *Bars, Mean*± SD, *, P ≤ 0.05.

Deletion of *βcatenin* in tissues other than bone in *Ctnnb1*$^{lox(2\text{-}6)/lox(2\text{-}6)}$;*CtsKCre* mice, was also analyzed through qPCR. Three animals per genotype were sacrificed and biopsies of the kidney, liver, muscle and spleen of 12-week-old mice were obtained. Expression of the *βcatenin* gene in these tissues was evaluated. As expected, the results indicated that there was not deletion of *Ctnnb1* gene in other tissues of experimental animals compared with control samples (Fig. 24).

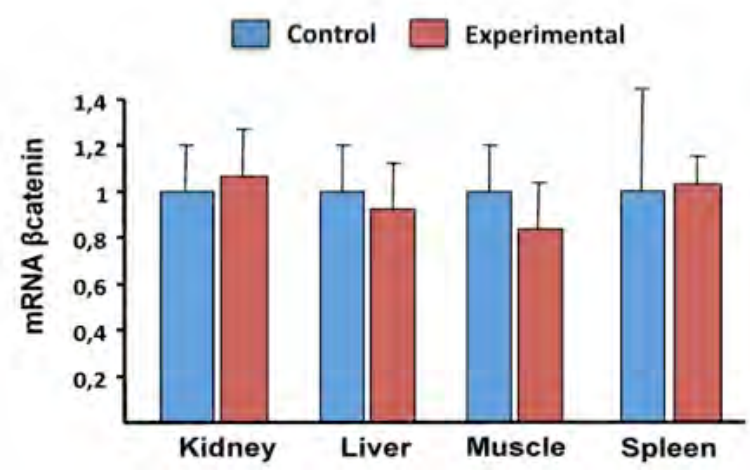

Figure 24. *βcatenin* expression in kidney, liver, muscle and spleen. *βcatenin* expression analysis assessed by qPCR, revealed normal *βcatenin* levels in kidney, liver, muscle and spleen without differences between both experimental and control genotypes. qPCR was normalized with *gapdh* (n=3 per group). *Bars, Mean*± SD, *, P ≤ 0.05.

These results show a specific and significant reduction in the expression of *βcatenin* in mature osteoclasts derived from experimental animals and normal expression levels in tissues other than bone. The partial deletion shown in our experiments was probably due to the presence in the osteoclast culture of non-*Ctsk*-expressing cells such as undeveloped osteoclasts or cells from other different lineages such as the mesenchymal lineage that express normal levels of *βcatenin*.

4.2 Characterization of the phenotype in Ctnnb1$^{lox(2-6)/lox(2-6)}$;CtsKCre mice

To study the effect of *βcatenin* deficiency in *CtsK*-expressing cells in bone mass, we have generated two cohorts (males and females) of mice lacking *βcatenin Ctnnb1$^{lox(2-6)/lox(2-6)}$*;*CtsKCre* mice, and they were compared with the corresponding *Ctnnb1$^{lox(2-6)/lox(2-6)}$* littermate animals, considered as controls.

4.2.1 Macroscopic description of *Ctnnb1$^{lox(2-6)/lox(2-6)}$;CtsKCre* mice

The *Ctnnb1$^{lox(2-6)/lox(2-6)}$*;*CtsKCre* mice were born at the expected Mendelian ratio and appeared normal at birth being their external aspect and size indistinguishable from control mice. However, from 6 weeks of age, the experimental mice presented a discernible phenotype characterized by anomalous hindlimb position and gait, abnormal spine curvature and thin skin with sparse fur (Fig. 25A). These alterations were accentuated over time with the experimental mice eventually dying between 14 and 15 weeks of age, a time when animals looked sick. The ultimate cause of the death remained unknown but it is conceivable that the skeletal defects that will be described later might be playing a role on this observation. At 12 weeks of age, no gross differences in body size were observed. However, there was a tendency to reduced body weight that became statistically significant at 12 weeks of age in males (Fig. 25B).

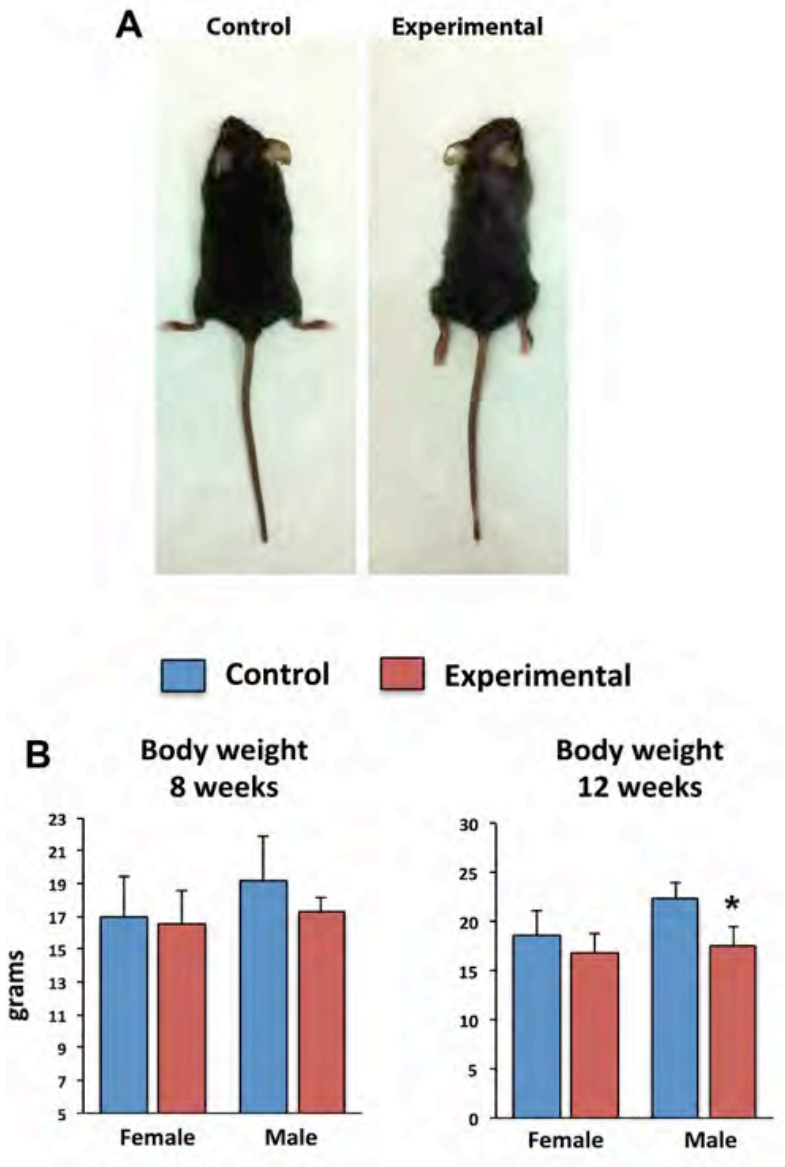

Figure 25. External appearance and body weight of *Ctnnb1*$^{lox(2-6)/lox(2-6)}$ (control) and *Ctnnb1*$^{lox(2-6)/lox(2-6)}$;*CtsKCre* (experimental) mice. Picture of 12-week-old control and experimental animals (A). The analysis of body weight (n=10 for females and n=8 for males of each genotype at 8 and 12-week-old) showed a statistically significant decrease in males 12-week-old (B). ($P \leq 0.05$ versus controls by Student's *t*-test).

4.2.2 Skeletal analysis of experimental mice lacking *βcatenin*

4.2.2.1 Radiographic bone description

The hindlimb malposition and abnormal gait of *Ctnnb1*$^{lox(2\text{-}6)/lox(2\text{-}6)}$;*CtsKCre* mice points to a skeletal defect phenotype. To start characterizing this phenotype, sequential femur and vertebra X-ray examination was performed in 6, 8 and 12-week-old mice. X-ray analysis in hindlimbs at 6 weeks already revealed clear deformities in experimental mice around the knee including radiodensity reduction, cortical thinning and alterations in shape including bone widening of the distal third of the femur and proximal third of the tibia (Fig. 26A). Furthermore, whereas the growth plate and secondary ossification center, distal for the femur and proximal for the tibia, were clearly distinguished in controls, they were markedly misshapen in experimental animals (Fig. 26A). The analysis of the spine at 6 and 12 weeks of age, showed decreased bone density, poor mineralization and ill-defined borders of the vertebrae, being more evident at 12 weeks of age (Fig. 26B).

These results indicate that *βcatenin* gene deficiency in *CtsK*-expressing cells results in a progressive decrease in bone mass in both femur and vertebra of experimental animals.

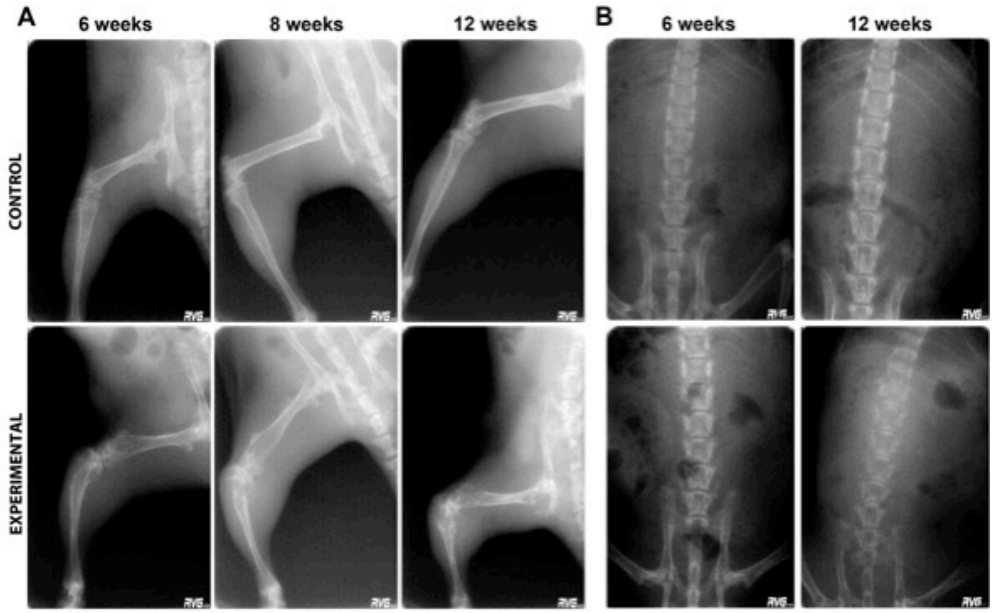

Figure 26. Radiographs of hindlimbs and spine. *Ctnnb1*$^{lox(2\text{-}6)/lox(2\text{-}6)}$;*CtsKCre* lower limbs radiographs at 6, 8 and 12 weeks of age, showed a decrease in bone density in the region surrounding the knee compared with control mice (A). *Ctnnb1*$^{lox(2\text{-}6)/lox(2\text{-}6)}$;*CtsKCre* spine radiographs showed loss of bone density obvious in 12-week-old experimental mice (B).

4.2.2.2 Bone mineral densitometry

For further bone phenotype analysis, we monitored skeletogenesis by measuring bone mineral density (BMD) at 8 and 12-week-old. At 8 weeks of age, a mild but significant bone loss was only detected in the spine of females (Fig. 27A), while at 12 weeks of age a decrease in BMD was significant in femur and spine of both sexes of *Ctnnb1*$^{lox(2\text{-}6)/lox(2\text{-}6)}$;*CtsKCre* mice, as compared to their respective controls (Fig. 27B).

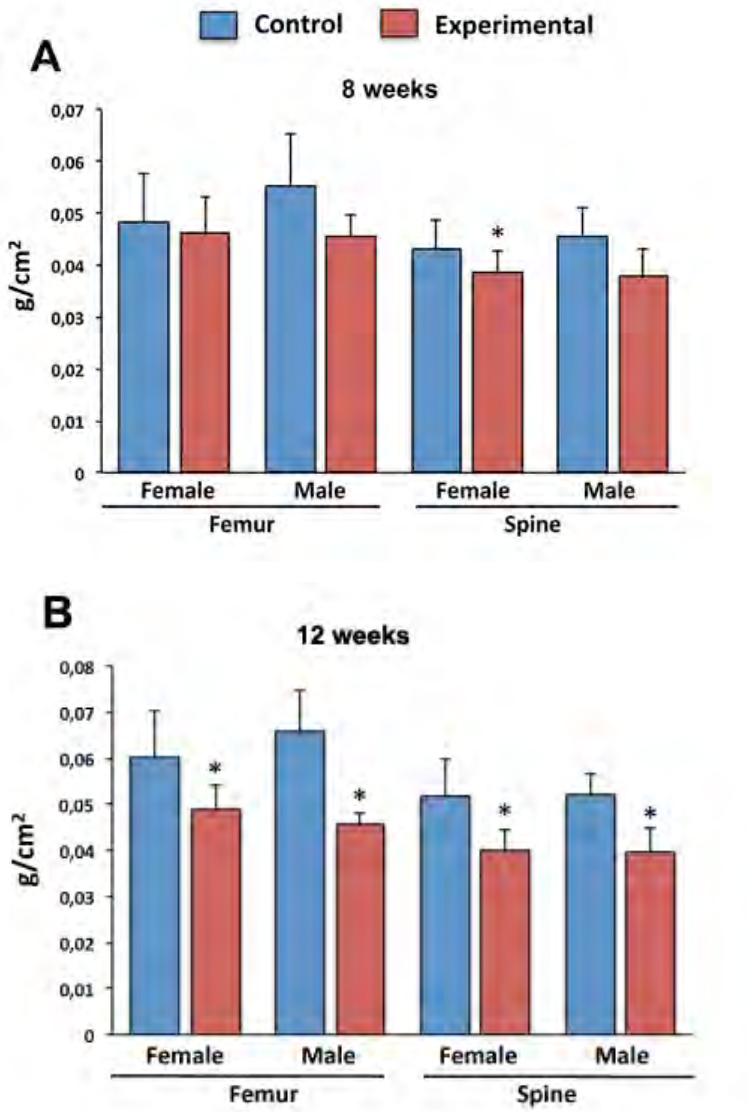

Figure 27. Bone mineral density (BMD) analysis in femur and spine at 8 and 12 weeks of age. BMD in *Ctnnb1*$^{lox(2-6)/lox(2-6)}$;*CtsKCre* mice (n=10 males and n=18 for females) showed no differences at 8 weeks of age except in vertebra of females mice (A), however, 12-week-old experimental mice exhibited a decrease in bone density in femur and vertebra of both genders (n=10 males and n=18 for females) (B). ($P \leq 0.05$ using Student's *t*-test compared with the controls).

4.2.2.3 Tridimensional bone description by micro-computed tomography

To extend our understanding of the skeletal phenotype of the *Ctnnb1$^{lox(2-6)/lox(2-6)}$;CtsKCre* mutant mice, we examine the bone microarchitecture through micro-computed tomography (μCT) at 6 and 12 weeks of age in a cohort of 10 animals per genotype (Fig. 28 and 29).

Tridimensional bone micro-architecture was examined in the fifth lumbar vertebra and the right femur. In line with the X-ray results, this analysis already detected a decrease in bone volume (BV/TV) in experimental femurs at 6 weeks of age, albeit it was not statistically significant despite the bone loss showed in the high resolution scans images of μCT (Fig. 28A). Experimental femurs exhibited a significant reduction in trabecular number (TbN) ($p=0.03$ in females and $p=0.004$ in males) and an increase in trabecular space (TbSp) ($p=0.039$ in females and $p=0.01$ in males) compared with their controls. However, trabecular thickness (TbTh) was only significantly increased ($p=0.02$) in experimental males (Fig. 28B). At 12 weeks of age, three-dimensional surface images from high resolution CT scans of the femur, clearly confirmed a dramatic bone loss in both cortical and trabecular bone (Fig. 28C). At this stage, the analysis revealed that both male and female *Ctnnb1$^{lox(2-6)/lox(2-6)}$;CtsKCre* mice exhibited a significant 50% reduction ($p=0.03$ in females and $p=0.05$ in males) in BV/TV associated with decreased trabecular number ($p=0.1$) and increased trabecular space ($p=0.1$ in females and $p=0.5$ in males) though did not reach the level of significance compared with their

controls. Trabecular thickness was significantly increased (p=0.001) only in females (Fig. 28D).

In stark contrast, despite the enormous damage seen in cortical bone at the distal end, the average cortical thickness (Cortical Th) at the midshaft was unaffected in both male and female *Ctnnb1*$^{lox(2-6)/lox(2-6)}$*;CtsKCre* mice (Fig. 28D).

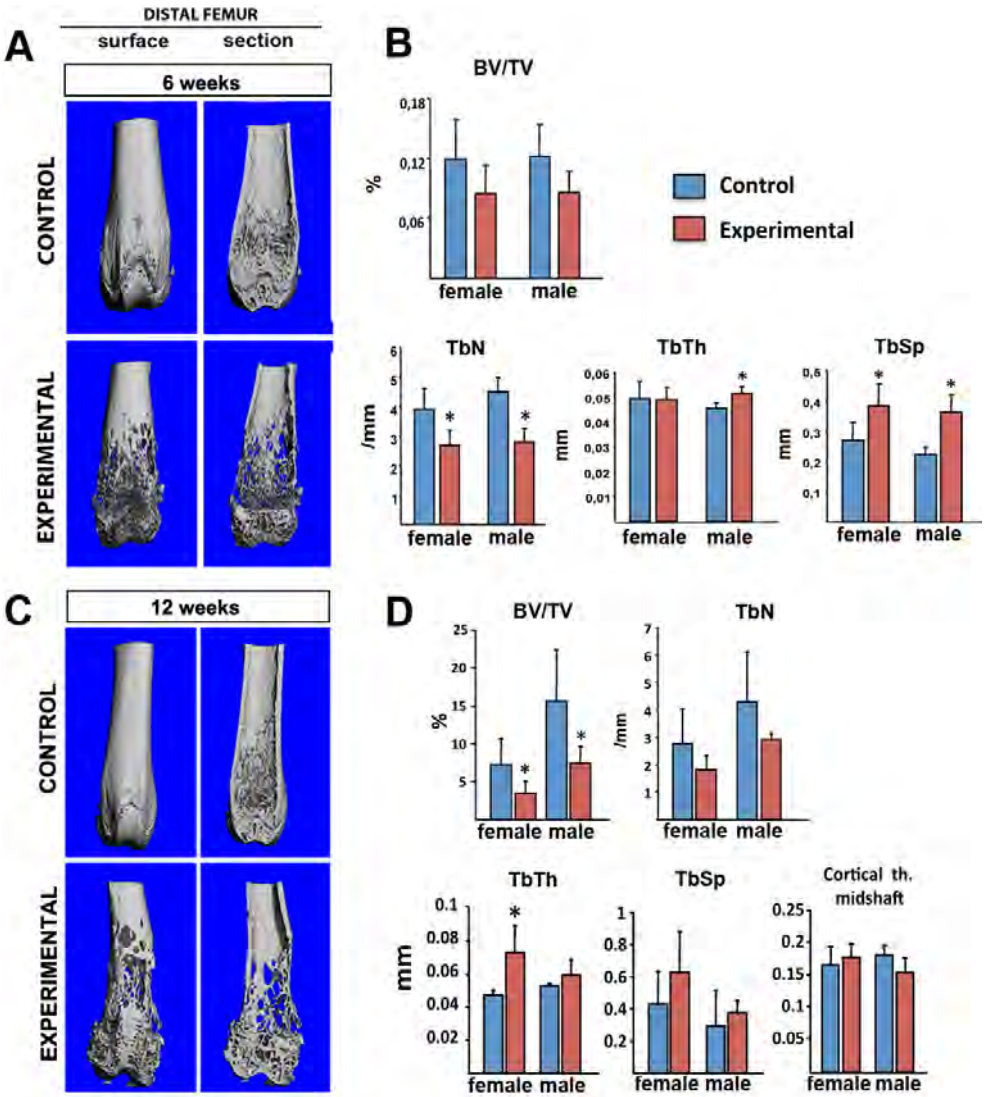

Figure 28. Micro-computed tomography (µCT) analysis and imaging in 6 and 12-week-old femurs. At 6 weeks of age, µCT scan images of the distal femur showed a loss bone phenotype (A). The analysis of the bone parameters indicated a reduction in bone mass that however, is not statistically significant. A decrease in trabecular number (TbN) and an increase in trabecular space (TbSp) reached statistical significance (B). µCT images of 12-week-old distal femur of *Ctnnb1*$^{lox(2\text{-}6)/lox(2\text{-}6)}$;*CtsKCre* and *Ctnnb1*$^{lox(2\text{-}6)/lox(2\text{-}6)}$ revealed a marked decreased in cortical and trabecular bone of experimental distal femur (C). Experimental 12-week-old mice showed a significant reduction in bone volume (BV/TV), although no differences where found in the cortical thickness at midshaft level (D). ($P \leq 0.05$; n=10 per genotype).

Like in femur, µCT images of L5 vertebra of 12-week-old mice also revealed a high bone loss in both cortical and trabecular bone compartments in the experimental group (Fig. 29A). The analysis of the bone parameters showed a significant reduction of BV/TV (p=0.03 in females and p=0.01 in males) and trabecular number (TbN) (p=0.006 in females and p=0.001 in males). The trabecular space is also significantly increased (p=0.001 in females and p=0.006 in males). As in the distal femur, the trabecular thickness is significantly higher only in mutant females (p=0.03) (Fig. 29B).

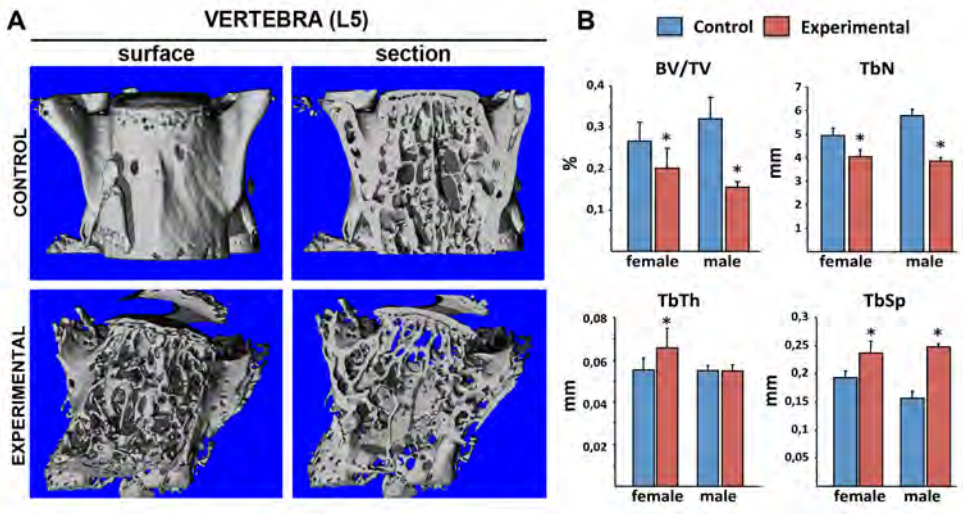

Figure 29. Micro-computed tomography (µCT) analysis and imaging in vertebra. µCT images of L5 vertebra displayed a dramatic bone loss in experimental *Ctnnb1*$^{lox(2\text{-}6)/lox(2\text{-}6)}$*;CtsKCre* mice (A). The quantification analysis showed statistically significant decrease in bone volume (BV/TV) and trabecular number (TbN) and an increase in trabecular space (TbSp) in both males and females. However, trabecular thickness (TbTh) is only significantly increased in females (B). (P ≤ 0.05; n=10 per genotype).

Together, the radiological, densitometry and µCT analysis indicated a low-bone-mass phenotype of progressive loss of both cortical and trabecular bone that started after the first month of postnatal life and worsen progressively in femurs and vertebrae.

4.3 Histological analysis of bone tissue in Ctnnb1$^{lox(2-6)/lox(2-6)}$;CtsKCre mice

4.3.1 Bone analysis of the femurs and vertebrae in *Ctnnb1$^{lox(2-6)/lox(2-6)}$;CtsKCre* mice

Having shown that *Ctnnb1$^{lox(2-6)/lox(2-6)}$;CtsKCre* mice exhibit a striking bone loss phenotype that is first detected around 6 weeks of age, we tried to elucidate the onset of the phenotype and the bone structure of experimental animals by performing a histological sequential analysis. To this end, the distal part of the femurs and lumbar vertebrae from newborn (NB) to 12-week-old experimental (*Ctnnb1$^{lox(2-6)/lox(2-6)}$;CtsKCre)* and control (*Ctnnb1$^{lox(2-6)/lox(2-6)}$*) mice were embedded in paraffin, sectioned and stained with hematoxylin-eosin (H-E). Before 4 weeks of postnatal development, no differences between mutants and control mice were detected in the femur, indicating that prenatal and early postnatal development was not affected (Fig. 30A). In 4-week-old experimental animals, the cortical bone in the distal femur started to be thinner than in controls (Fig. 30B). At 8 weeks of age, the cortical bone of the distal femur was partially absent and the number of trabeculae, strikingly reduced. At 12 weeks of age the cortical and trabecular bone of the distal femur was obviously absent in wide regions (Fig. 30B arrows).

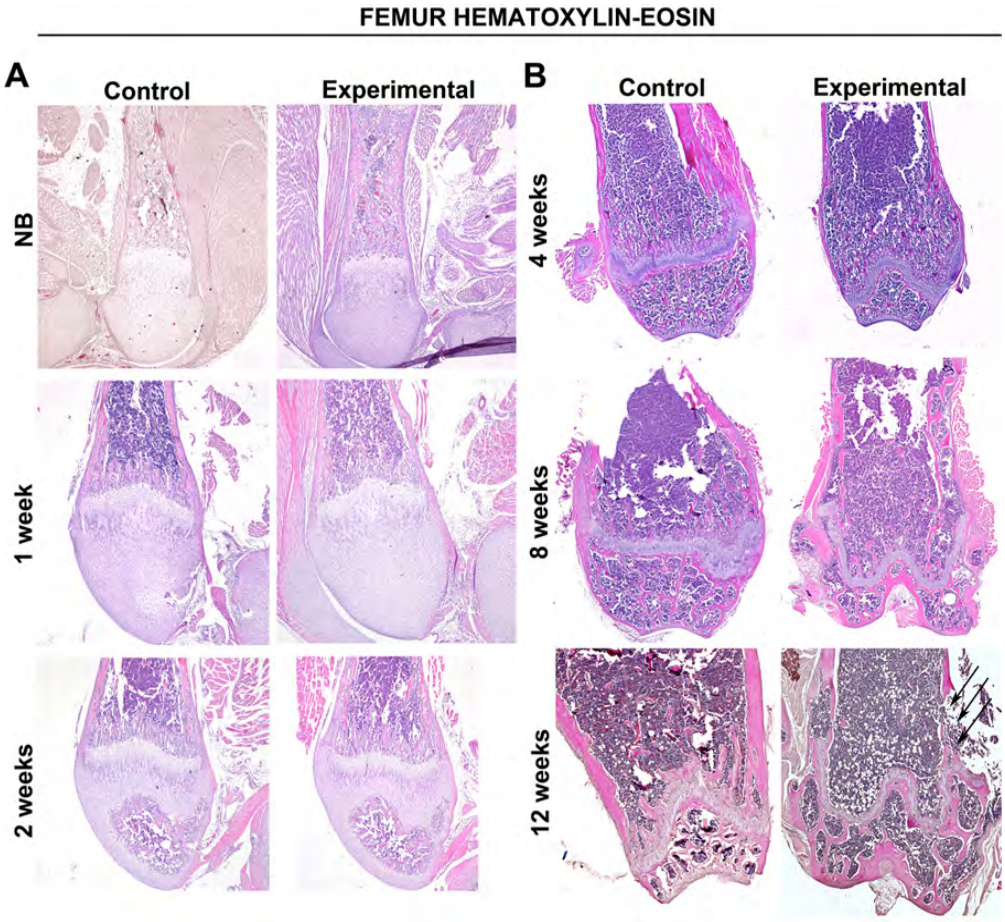

Figure 30. Histological sections of the femur stained with hematoxylin-eosin from NB to 12 weeks of age. Up to 4 weeks of age no differences were found between genotypes (A). Starting in 4-week-old *Ctnnb1*$^{lox(2\text{-}6)/lox(2\text{-}6)}$;*CtsKCre* mice, the cortical and trabecular bone in the distal region becomes thinner compared with their controls. At 12 weeks of age the cortical and trabecular bone is completely absent in some areas (B).

The bone loss phenotype can be clearly appreciated in the images of the fresh bone of the distal femur (Fig. 31A). Interestingly, this

phenotype was accompanied by an extensive increase of adipocytes in the bone marrow of the distal femur (Fig. 31B).

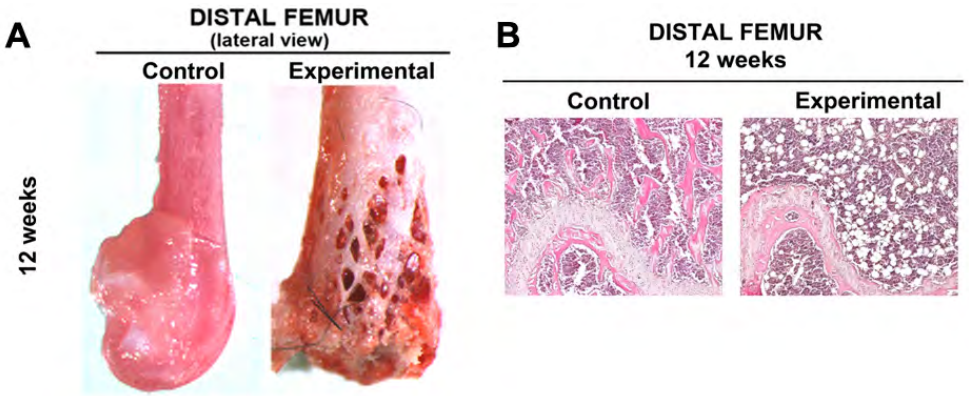

Figure 31. 12-week-old fresh femur images and bone marrow adiposity. 12-week-old *Ctnnb1*$^{lox(2-6)/lox(2-6)}$;*CtsKCre* experimental animals showed a dramatic decrease in cortical and trabecular bone in the distal part of the femur (A) associated with an increase in bone marrow adiposity (B).

On the other hand, consistent with the μCT analysis, the femur cortical midshaft showed no differences between experimental and control mice at all stages analyzed (not shown). It should be noted, that the long bone phenotype was not restricted to the distal femur, as similar findings were observed in the proximal tibia (not shown) and in the humerus as is shown later in the figure 33.

A similar low-bone-mass phenotype is gradually established in the vertebrae of *Ctnnb1*$^{lox(2-6)/lox(2-6)}$;*CtsKCre* mice (Fig. 32A-B). The histological sections of 4-week-old experimental vertebrae show that

bone is still present in the periphery of the vertebra, but at 8 and 12 weeks of age, the peripheral bone is lost with age and few trabeculae are remained (Fig. 32B).

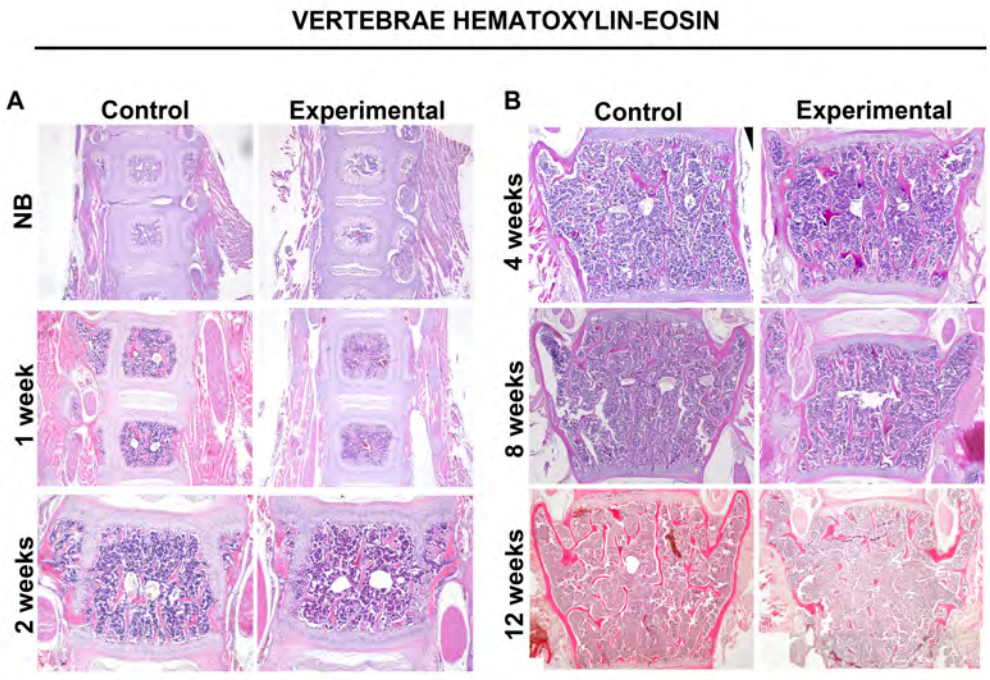

Figure 32. Hematoxylin-eosin stained sections of vertebrae from NB to 12-week-old mutant and control mice. Before 4-week-old, no differences were shown between experimental and control mice (A). From 8 weeks of age, the vertebrae of experimental mice showed a progressive loss of peripheral and trabecular bone (B).

4.3.2 Analysis of bone phenotype in the humerus

Having shown the bone loss phenotype in the femurs and vertebrae of *Ctnnb1*$^{lox(2\text{-}6)/lox(2\text{-}6)}$;*CtsKCre* mice, we wanted to determine whether the

phenotype was restricted to hindlimbs and vertebrae or was generalized. In line with the previous results, the analysis of the humerus at 12 weeks of age in control and experimental mice, also showed a reduction in both cortical and trabecular bone compartments in the area close to the proximal growth plate reminiscent of the phenotype seen in the mutant femurs (Fig. 33 arrows). This indicated that the phenotype seems to affect endochondral formed bones.

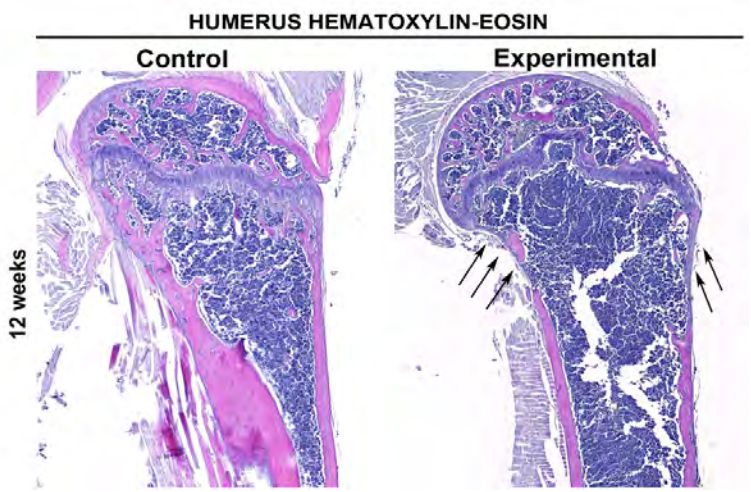

Figure 33. Histological sections of proximal humerus stained with hematoxylin-eosin. The proximal humerus of *Ctnnb1*$^{lox(2-6)/lox(2-6)}$;*CtsKCre* mutants showed a decrease in both cortical and trabecular bone compared to controls.

These results of the histological analysis indicated that Wnt/βcatenin signaling in *CtsK*-expressing cells is not necessary for normal skeletogenesis up to the end of the first month of postnatal life and

suggest that excess bone destruction, starting between 4 and 6 weeks, might be the primary mechanism involved in the bone loss phenotype.

4.4 Analysis of osteoblast cell markers in the Ctnnb1$^{lox(2-6)/lox(2-6)}$;CtsKCre mice

To assess bone development and osteoblastic cells in our experimental mice, we studied by *in situ* hybridization (ISH) the expression of different osteoblast markers such as *Collagen 1* (*Col1*) and *Bone Sialoprotein* (*Bsp*) from newborn to 4-week-old in the distal femur of experimental and control mice (Fig. 34) and in vertebra (data not shown). The expression pattern of *Col1* and *Bsp* in these sections were restricted to the periosteum and in osteoblastic cells of the ossification centers, mostly located around the growth plate. As shown in Fig. 34, no differences were found between *Ctnnb1*$^{lox(2-6)/lox(2-6)}$;*CtsKCre* mice and their controls, indicating that bone forming cells are not altered.

The fact that cortical and trabecular bone was fully developed at 4 weeks of age and bone formation markers expression (*Col 1* and *Bsp*) did not display differences with control mice, suggests that bone resorption might be the main mechanism involved in the loss bone phenotype instead of bone formation impairment.

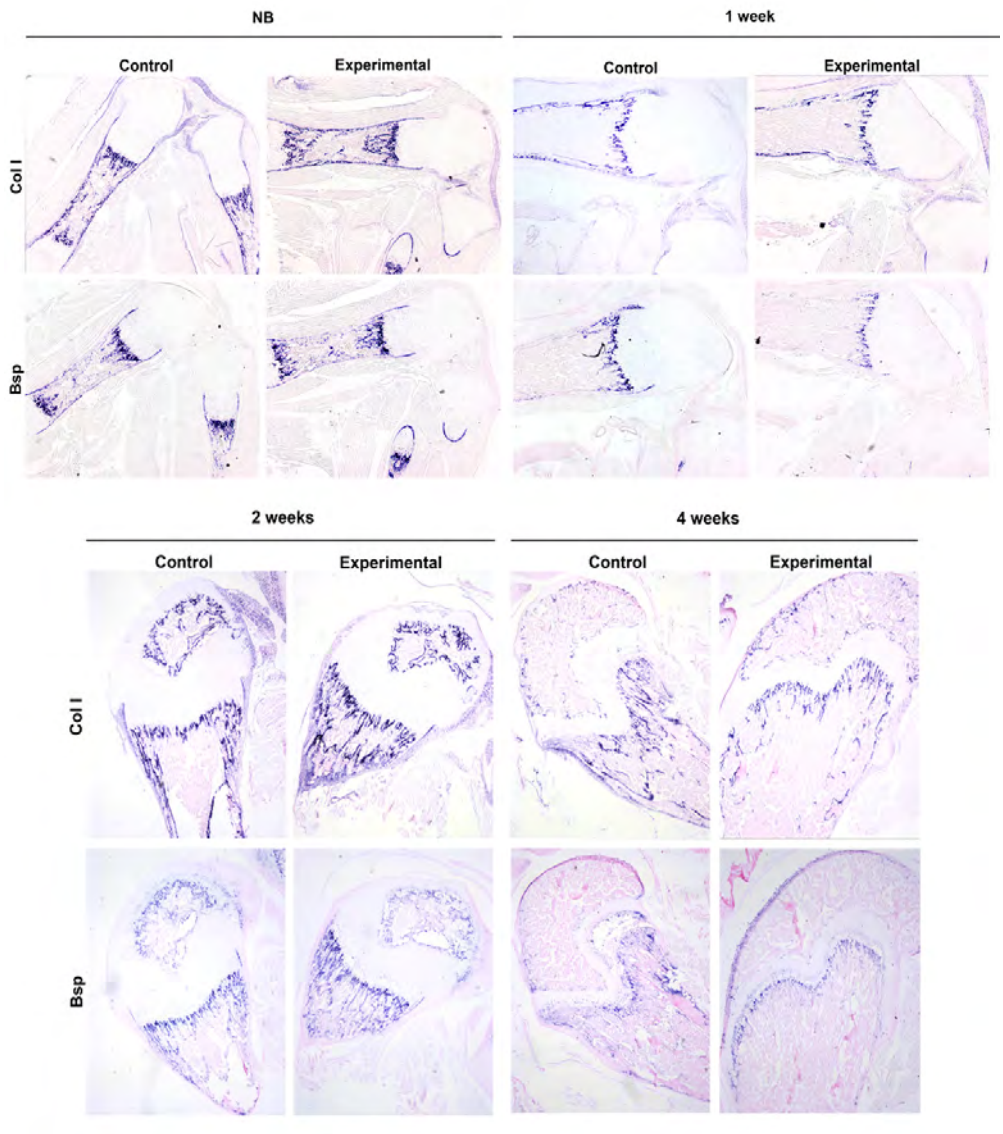

Figure 34. *In situ* hybridization for *Col1* and *Bsp* in sections from NB to 4-week-old of distal femur. No differences were found between the *Ctnnb1*$^{lox(2\text{-}6)/lox(2\text{-}6)}$;*CtsKCre* experimental and *Ctnnb1*$^{lox(2\text{-}6)/lox(2\text{-}6)}$ control mice in the expression pattern of *Col1* and *Bsp* osteoblast markers in femur.

4.5 In vivo and in vitro analysis of osteoclast cells

4.5.1 *In vivo* quantification of osteoclast numbers

To elucidate whether the striking bone loss in the cortical and trabecular bone compartments observed in long bones and vertebrae of our *CtsKCre* experimental model is due to an increase in bone resorption because of an increase in osteoclast numbers, we performed TRAP staining in sections of 12-week-old experimental and control femurs and vertebrae when the phenotype is fully established.

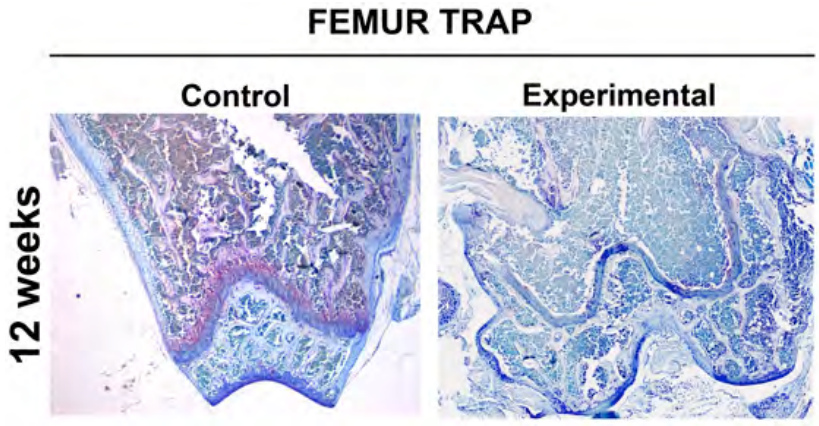

Figure 35. TRAP staining in distal femur of 12-week-old control and experimental mice. Compared with control littermates, in *Ctnnb1*$^{lox(2-6)/lox(2-6)}$;*CtsKCre* mice at this stage, few osteoclasts are found because of the little bone remained in the distal region of the femur.

As it is shown in Fig. 35, few TRAP positive cells, considered as osteoclasts, were found at the distal femur. We consider that this finding is due to the fact that, in line with the above described results,

much of the bone had been already resorbed and little cortical and trabecular bone is remained where osteoclasts could adhere and continue resorbing. So that, we decided to perform TRAP staining at earlier stages from NB to 12 weeks of age (Fig. 36).

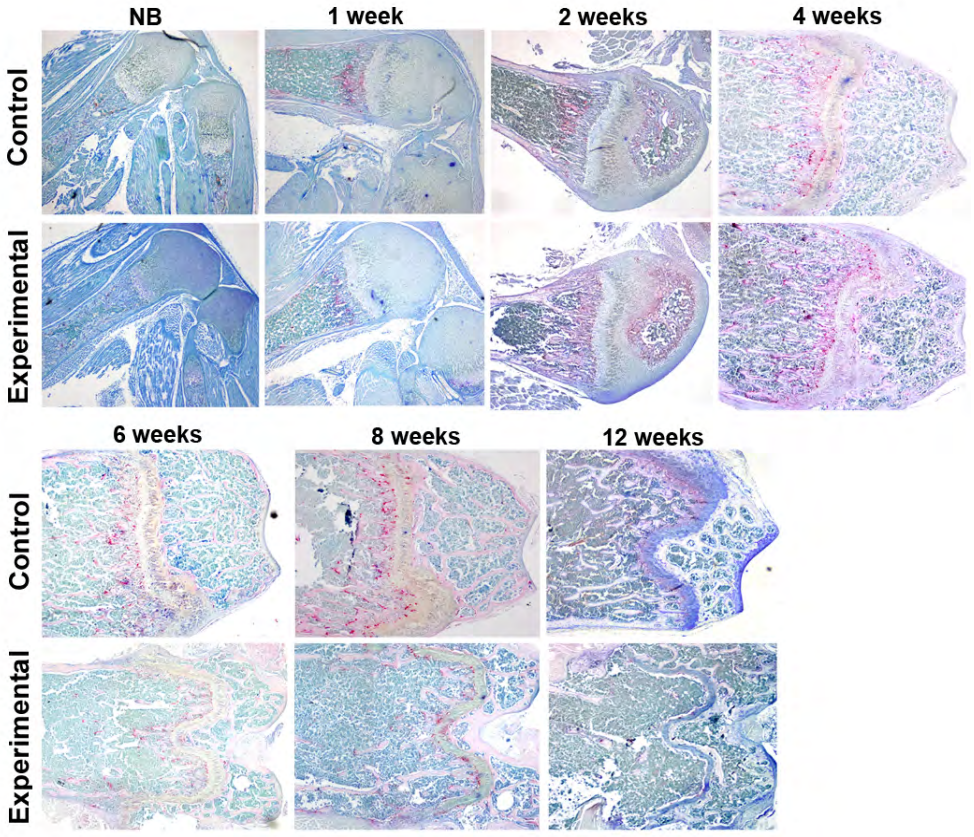

Figure 36. TRAP staining in *Ctnnb1*$^{lox(2-6)/lox(2-6)}$ control and *Ctnnb1*$^{lox(2-6)/lox(2-6)}$*;CtsKCre* experimental distal femurs at several stages from NB to 12-week-old mice. Distal femur sections were stained with TRAP in the stages from NB to 12-week-old femur. No differences in TRAP^{+} cells are noticed until 4-week-old in experimental distal femur.

As shown in Fig. 36 and 37, an elevated number of TRAP positive cells were noticed at 4 weeks of age. This fact is in agreement with the onset of the loss bone phenotype found in our experimental mice.

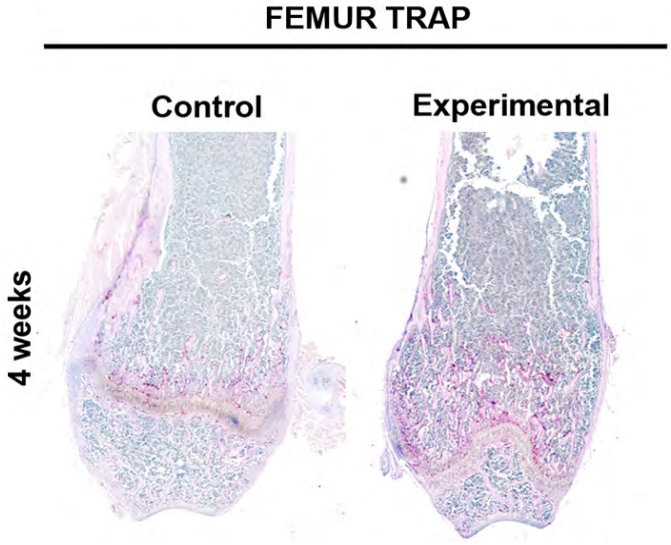

Figure 37. TRAP staining at distal femur of 4-week-old mice. An increase of TRAP^{+} cells was noticed at 4 weeks of age in *Ctnnb1*$^{lox(2-6)/lox(2-6)}$;*CtsKCre* mice, where more number of osteoclasts are detected according to the emergence of the phenotype.

Like in femur, the TRAP positive cells are more numerous in vertebra of 4-week-old experimental mice as compared with their controls, and in line with the previous findings, here the number of TRAP positive cells also decreased as the cortical and trabecular bone is resorbed (Fig. 38).

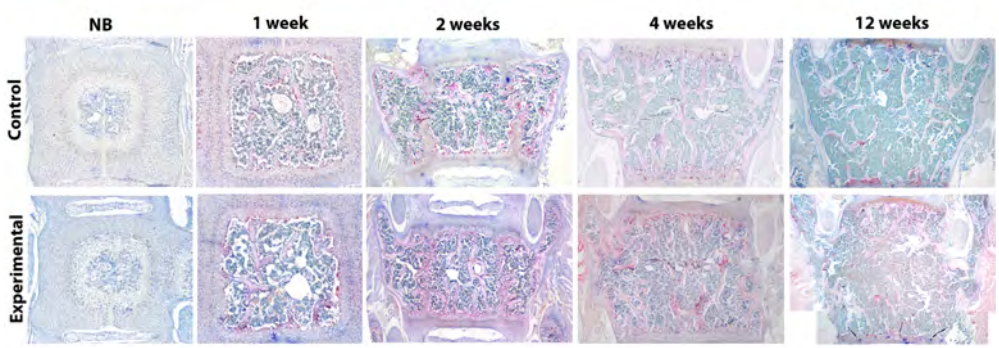

Figure 38. TRAP staining in *Ctnnb1*$^{lox(2-6)/lox(2-6)}$ control and *Ctnnb1*$^{lox(2-6)/lox(2-6)}$;*CtsKCre* experimental vertebrae at several stages from NB to 12-week-old mice. At 4 weeks of age, more number of osteoclasts was detected in experimental than in control mice. Before this stage no differences in TRAP positive cells were noticed.

To determine whether the number of osteoclasts was truly greater *in vivo*, changes in osteoclast numbers were quantified through histomorphometric analysis on the trabecular bone of the three representative lumbar vertebrae (L2-L4) of experimental and control animals to determine if the number of osteoclasts is truly greater *in vivo*. As the major differences in the TRAP stained femurs and vertebrae were noticed at 4 weeks of age just before the phenotype was apparent, a cohort of 6 mice per genotype of 4 weeks of age, were sacrificed. Vertebra samples were stained with TRAP (Fig. 39C). In line with our studies in TRAP staining sections, the results sustained that *Ctnnb1*$^{lox(2-6)/lox(2-6)}$;*CtsKCre* mice presented a significative increase in the number of osteoclasts *in vivo* per area ($p=0.0027$) (Fig. 39A) and perimeter ($p=0.0003$) relative to their control littermates (Fig. 39B). However, in accordance with our

previous results, the bone area per total area (BA/TA) did not show differences at this stage (Fig. 39D), confirming the late onset of the bone loss phenotype.

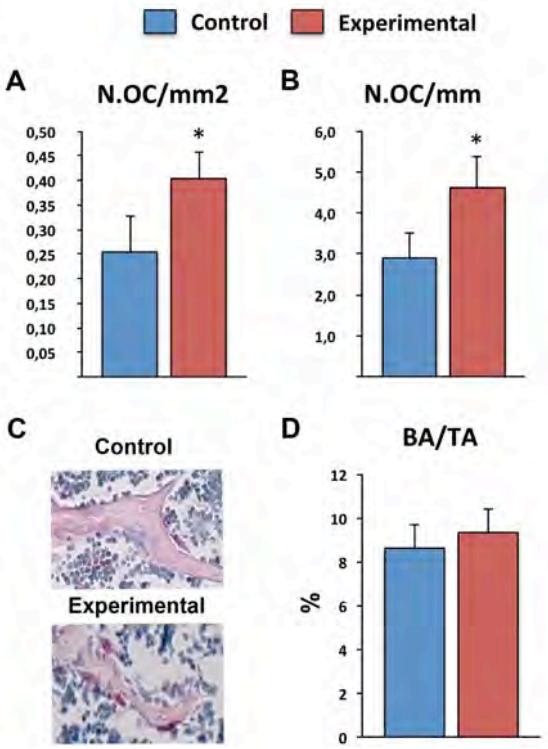

Figure 39. Histomophometric analysis. Determination of the osteclast numbers per area (A) and perimeter (B) of longitudinal decalcified sections of L2-L4 vertebrae from 4-week-old mice. In experimental vertebrae, it was revealed a significative increase of osteoclast numbers *in vivo* as was clearly noticed in the vertebra images (C) but no differences were found in BA/TA (D). (n=6 per genotype). *Bars, Mean*± SD, *= P ≤ 0.05.

Therefore, our histomorphometric results confirm a transient increase in osteoclast numbers that could be the primary cause of the bone defects in *Ctnnb1*$^{lox(2-6)/lox(2-6)}$;*CtsKCre* mice.

4.5.2 Osteoclast development analysis *in vitro*

The increased number of osteoclasts consequence of *βcatenin* deletion could be due to an increase in osteoclastogenesis, thus we compared osteoclast development from the BM cells of experimental and control long bones. Three mice were used per genotype and three technical replicates performed for each animal as described in the Materials and Methods section. On the fifth day of incubation, cells were fixed and stained for TRAP staining. Multinucleated TRAP positive cells were quantified as osteoclasts (more than three nuclei). As shown in Fig. 40, the number of osteoclasts observed from *Ctnnb1*$^{lox(2-6)/lox(2-6)}$;*CtsKCre* mice was significantly higher ($p=0.02$) than from control littermates. Importantly, osteoclasts developed in the absence of *βcatenin* exhibited a normal morphology indicating that βcatenin is dispensable for the intracellular cytoskeleton architecture and cell-cell adhesion of osteoclasts. As suggested in previous studies, plakoglobin may substitute for βcatenin in these functions (Hu et al. 2005; Huelsken et al. 2000).

These results show that the removal of Wnt/βcatenin signaling from late stage osteoclasts results in increased osteoclasts numbers derived from BM cells. Since the genetic manipulation occurs at the late state of osteoclast differentiation, we reasoned that the elevated

number of osteoclasts could not result from increased osteoclast proliferation therefore we looked for alternative explanations.

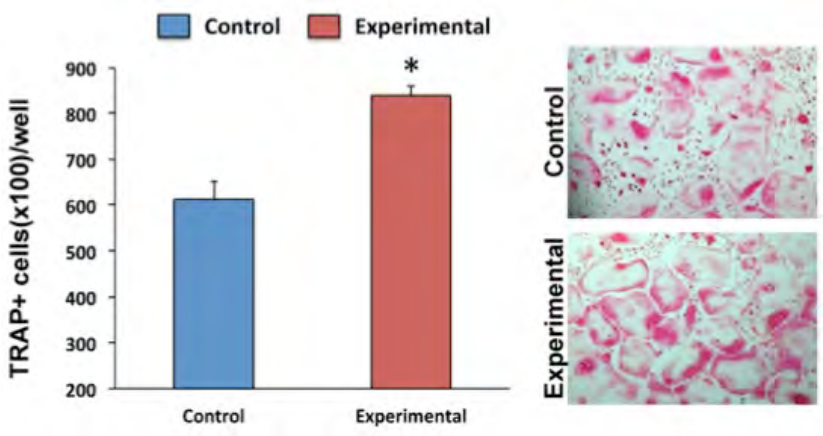

Figure 40. Osteoclast culture assay. Osteoclast cultures were developed from experimental and control BM cells of 4-5-week-old mice to assess changes in osteoclastogenesis. The assay revealed an increase in osteoclast numbers in the experimental osteoclasts compared with controls (n=3 per genotype). *Bars, Mean*± SD, *= P ≤ 0.05.

4.5.3 Analysis of Wnt/βcatenin function in osteoclast survival.

Osteoclasts have a short life span and die by apoptosis, therefore, changes in their life span may alter osteoclast numbers. Since *Ctnnb1*$^{lox(2\text{-}6)/lox(2\text{-}6)}$;*CtsKCre* mice have the *βcatenin* gene deleted in the late stages of osteoclastic differentiation, indeed when these cells are postmitotic, we proceeded to study the effect of Wnt/βcatenin signaling in the control of their life span. Osteoclasts were developed

in *in vivo* cultures from BM cells of experimental and control animals with medium supplemented with M-CSF and RANKL. The fourth day of culture, WNT3A was added to the osteoclast cultures to examine a possible pro-apoptotic effect of the canonical Wnt pathway in osteoclasts. After 24 hours of treatment, cells were fixed and apoptosis was determined by the TUNEL assay. As shown in Fig. 41, WNT3A treated osteoclasts showed a significant increase (p=0.003) in apoptotic cells compared with the untreated controls. In the experimental animals, this WNT3A effect was abrogated, indicating that βcatenin is required for the pro-apoptotic effect of WNT3A.

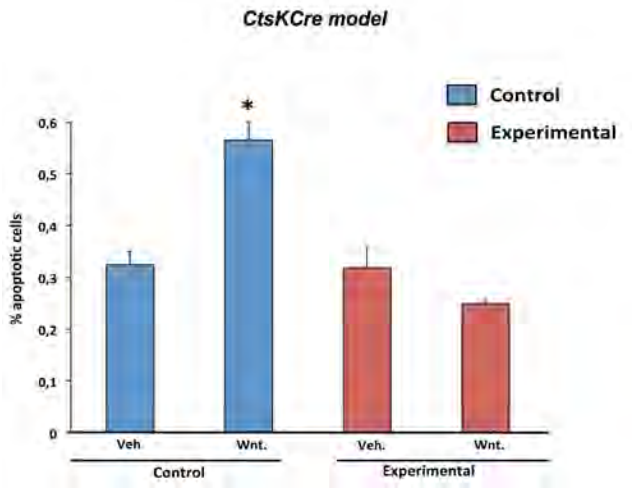

Figure 41. *Ctnnb1*$^{lox(2-6)/lox(2-6)}$;*CtsKCre* TUNEL assay. Wnt signaling effect on apoptosis was assessed through TUNEL analysis in osteoclast cultures from BM cells of *Ctnnb1*$^{lox(2-6)/lox(2-6)}$;*CtsKCre* and their control mice. Control osteoclasts treated with WNT3A showed an increase of apoptotic cells compared with untreated osteoclasts, while experimental treated and untreated osteoclasts did not show differences (n=2 in triplicates, *Bars, Mean*± SD, *= P ≤ 0.05).

These results suggest that removal of *βcatenin* from mature osteoclasts protect them from apoptosis, indicating that Wnt signaling has a pro-apoptotic effect in osteoclasts.

We wanted to know whether this mechanism was also present in osteoclasts developed from mice in which *βcatenin* was deleted from the osteoclast precursors. For this purpose *LysozymeMCre* line was used. Therefore we got experimental mice, so called *Ctnnb1*$^{lox(2-6)/lox(2-6)}$;*LysMCre* and their respective control *Ctnnb1*$^{lox(2-6)/lox(2-6)}$ mice. We performed the same experiment using osteoclasts obtained from both experimental and control mice of the *LysMCre* line, and similar results were obtained (Fig. 42).

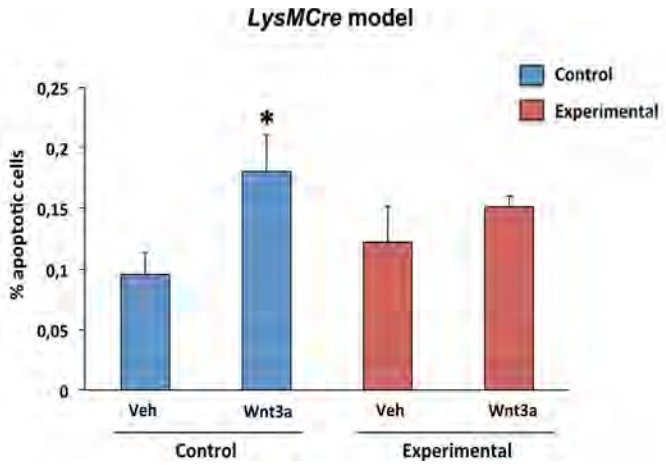

Figure 42. *Ctnnb1*$^{lox(2-6)/lox(2-6)}$;*LysMCre* TUNEL assay. As in *CtsKCre* line apoptosis assay, WNT3A treated *Ctnnb1*$^{lox(2-6)/lox(2-6)}$ control osteoclasts presented an increase of apoptotic cells compared with untreated cells. However, treated *Ctnnb1*$^{lox(2-6)/lox(2-6)}$;*LysMCre* experimental cells did not show differences compared with untreated osteoclasts (n=2 in triplicates, *Bars, Mean*± SD, *= P ≤ 0.05).

Taken together, these results indicate that osteoclastic Wnt/βcatenin signaling promotes osteoclast apoptosis and attenuates osteoclast numbers *in vitro.* Thus, osteoclasts deficient in *βcatenin* could extend their life span and contribute to the bone loss phenotype of *Ctnnb1*$^{lox(2-6)/lox(2-6)}$;*CtsKCre* mice in a cell-autonomous manner.

4.6 CtsK expression analysis in bone cells other than osteoclasts

4.6.1 Discrepancy between osteoclastic *βcatenin* loss-of-function models

Previous studies where *βcatenin* was removed using *LysMCre* line in osteoclast precursors, showed a milder bone loss phenotype than the one obtained in this study with the *CtsKCre* line (Fig. 43A). In those experiments, the experimental mice showed a decrease in bone mass due to an increase in the number of osteoclasts leading to increased resorption and associated with an increase in proliferation and accelerated osteoclastogenesis (Albers et al. 2013; Otero et al. 2012; Wei et al. 2011).

Since the absence of *βcatenin* in mature osteoclasts is common to both *LysMCre* and *CtsKCre* models (Fig. 43B), the discrepancy between the bone phenotype in *Ctnnb1*$^{lox(2-6)/lox(2-6)}$*;LysMCre* and *Ctnnb1*$^{lox(2-6)/lox(2-6)}$*;CtsKCre* mice, suggests the involvement of additional cell targets in one or both models that could be playing a role in the bone loss phenotype.

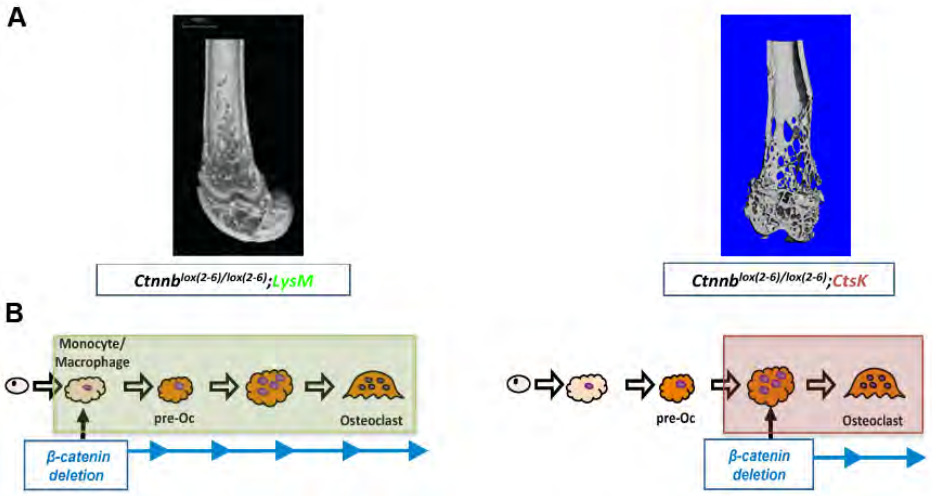

Figure 43. Comparison of *Ctnnb1*$^{lox(2-6)/lox(2-6)}$*;LysMCre* and *Ctnnb1*$^{lox(2-6)/lox(2-6)}$*;CtsKCre* bone phenotypes. Comparative µCT images between both *Cre* lines (Otero et al. 2012 and ours) display discrepancies in the bone phenotypes suggesting an indirect effect (A), thus in spite of lacking *βcatenin* in osteoclasts is common to both models (B), the *Ctnnb1*$^{lox(2-6)/lox(2-6)}$*;CtsKCre* mouse displays a higher marked bone loss .

4.6.2 Analysis of *βcatenin* expression in bone

In support of this hypothesis, *βcatenin* qPCR in whole tibia at 12 weeks of age, revealed that the *βcatenin* was reduced by almost 80%, much more than expected if only osteoclasts, which represent only a scanty 3-5% proportion of total bone cells, were responsible for this decrease (Fig. 44). This suggests that *Ctsk* is also expressed in cells distinct from osteoclasts in bone.

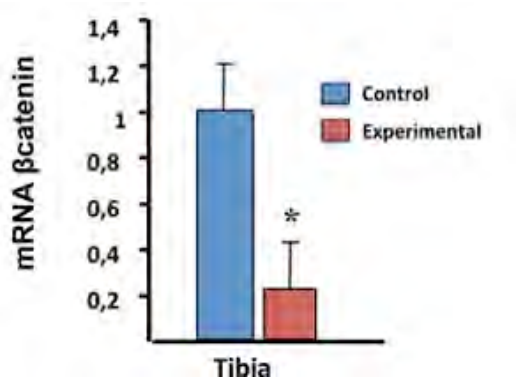

Figure 44. *βcatenin* deletion at 12-week-old tibia. Quantitative PCR was performed to assess *βcatenin* deficiency in whole tibia at 12 weeks of age. *Ctnnb1* gene deletion in *Ctnnb1*$^{lox(2-6)/lox(2-6)}$;*CtsKCre* tibia was nearly 80% compared with their controls. qPCR was normalized with *gapdh* (n=4 per genotype). *Bars, Mean*± SD, *= P ≤ 0.05.

4.6.3 Analysis of *Rankl* and *Opg* expression in bone

In the other bone cells, such as chondrocytes, osteoblasts or osteocytes, it is well known that loss of *βcatenin* is associated with loss of bone mass due in part to an indirect effect in the osteoclasts through changes in the RANKL/OPG ratio, the best known crosstalk between bone cells. To determine whether RANKL/OPG system was deregulated in the *Ctnnb1*$^{lox(2-6)/lox(2-6)}$;*CtsKCre* mice, quantitative PCR was performed in 4-week-old tibia from 4 animals per genotype, when the number of osteoclasts is significative increased and phenotype starts to emerge (Fig. 45). The measures indicated a reduction in *Opg* mRNA levels while *Rankl* expression remained without differences compared with their controls.

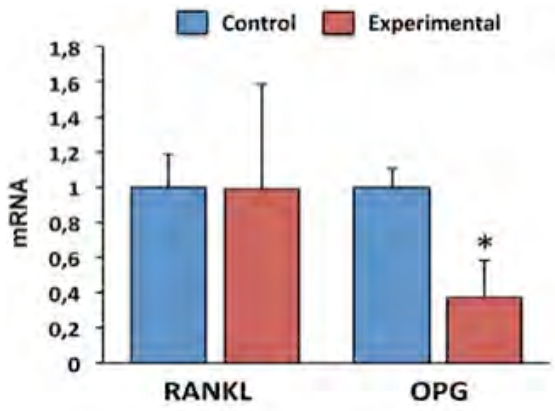

Figure 45. Analysis of the RANKL/OPG system in the *Ctnnb1*$^{lox(2-6)/lox(2-6)}$;*CtsKCre* mice. qPCR in 4-week-old tibia revealed that *Opg* expression was deleted more than 60% compared with their control littermates while *Rankl* levels remained without changes. qPCR was normalized with *tubulin* (n=4 per genotype). *Bars, Mean*± SD, *= P ≤ 0.05.

These results indicated that the low-bone-mass phenotype in our *Ctnnb1*$^{lox(2-6)/lox(2-6)}$;*CtsKCre* mice, mediated by increased osteoclast numbers, is caused by the combinations of two mechanisms. First, *βcatenin* cell-autonomous effect in the osteoclasts modulating its life span, and second by an indirect mechanism mediated by some additional cell type able to modulate the RANKL/OPG ratio.

4.6.4 Study of *CtsK* expression pattern in bone

In order to determine which other cell type could be contributing to the phenotype, the expression pattern of *CtsK* was analyzed by *in situ* hybridization (ISH) in femur sections from mouse embryonic day (E) 13.5 to 4-week-old control mice (Fig. 46 and not shown).

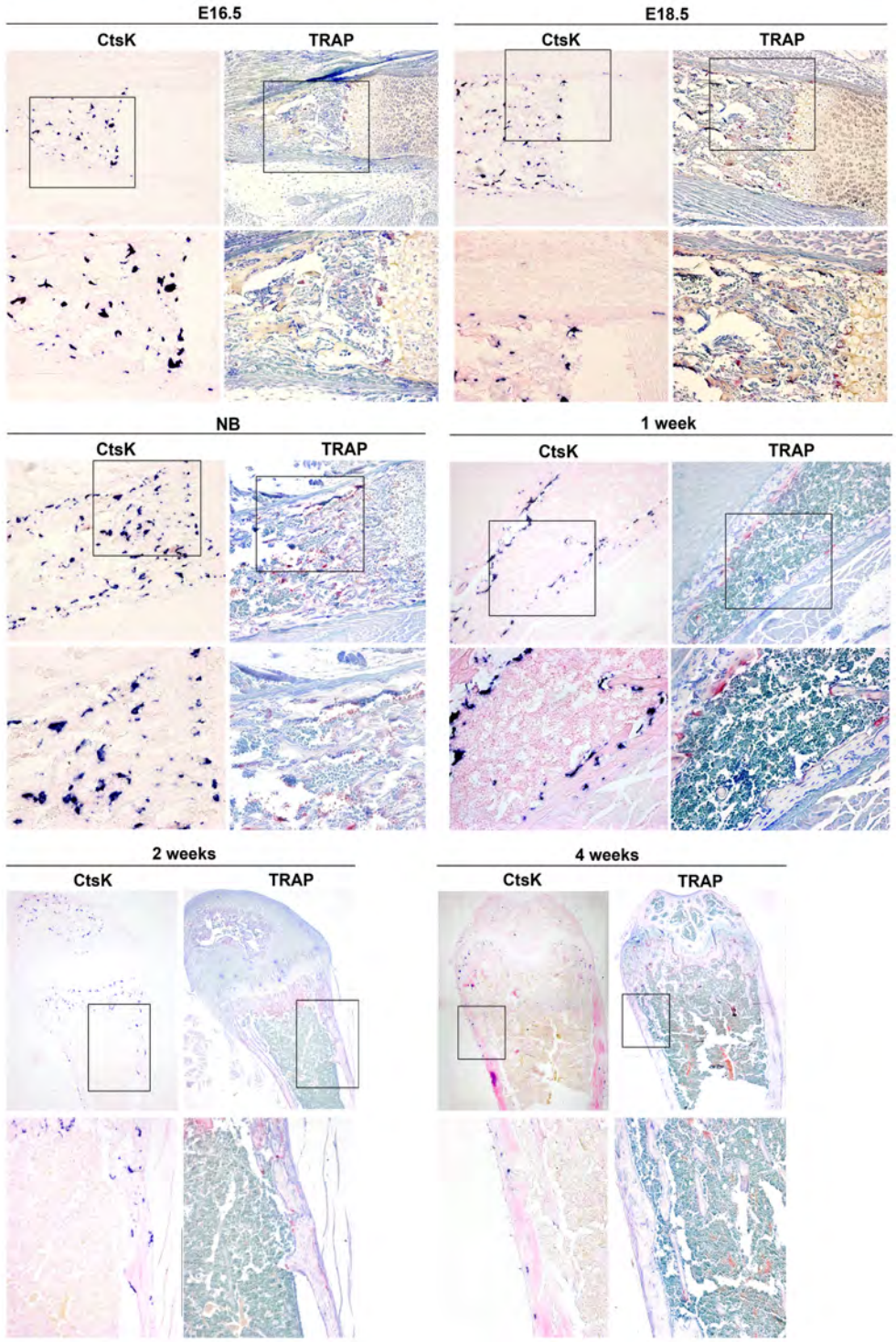
E16.5
CtsK
TRAP
E18.5
CtsK
TRAP
NB
CtsK
TRAP
1 week
CtsK
TRAP
2 weeks
CtsK
TRAP
4 weeks
CtsK
TRAP

Figure 46. TRAP staining and *CtsK in situ* hybridization from E16.5 to 4-week-old femur sections. To determine if other cells were expressing *CtsK* and contributing to the phenotype, we performed *CtsK* expression pattern study through ISH in E13.5 to 4-week-old distal femurs, where *CtsK* expression is unexpected shown in TRAP negative cells from newborn mice as it can be noticed in the magnified images.

CtsK expression was first detected at E16.5, and in this and the following developmental stages, the expression pattern of *CtsK*-expressing cells overlapped with the localization of TRAP stained positive cells, suggesting that those cells corresponded to osteoclasts and confirming that osteoclast are the primary cells expressing *Ctsk* (Fig. 46). However, starting from NB stage the expression of *CtsK* was found in non-TRAP positive cells (discarding that they could be osteoclasts), located in the inner layer of periosteum (Fig. 47, arrows), which is composed by differentiated osteogenic progenitors, adult mesenchymal progenitor cells and osteoblasts (Dwek 2010; Roberts et al. 2015).

These results suggest that osteogenic precursor cells located in the inner layer of the periosteum, can express *CtsK* and contribute to a decrease in bone mass of the *Ctnnb1*$^{lox(2\text{-}6)/lox(2\text{-}6)}$;*CtsKCre* mutant mice.

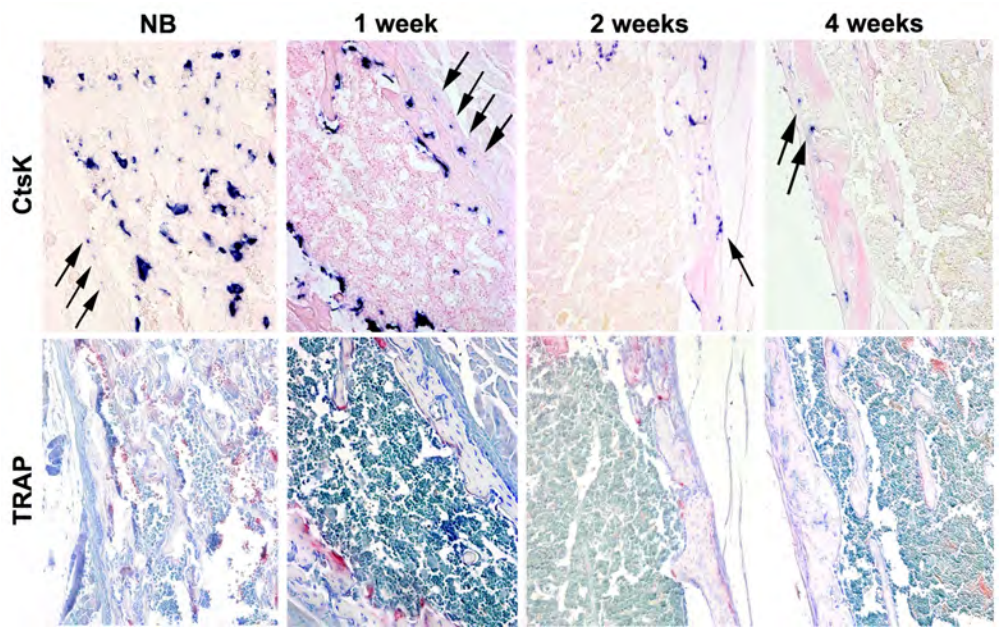

Figure 47. TRAP staining and *CtsK in situ* hybridization from NB to 4-week-old femur sections. *CtsK* expression was unexpected shown in TRAP negative cells (black arrows) from newborn mice as it can be noticed in the images from NB to 4-week-old femur sections.

4.6.5 *CtsK*-expressing cells in the periosteum are osteoblastic lineage cells

The periosteal *CtsK*-expressing cells appeared scattered in the inner layer, not in contact with the bone surface but immediately adjacent to the line of cuboid osteoblasts (Fig. 48).

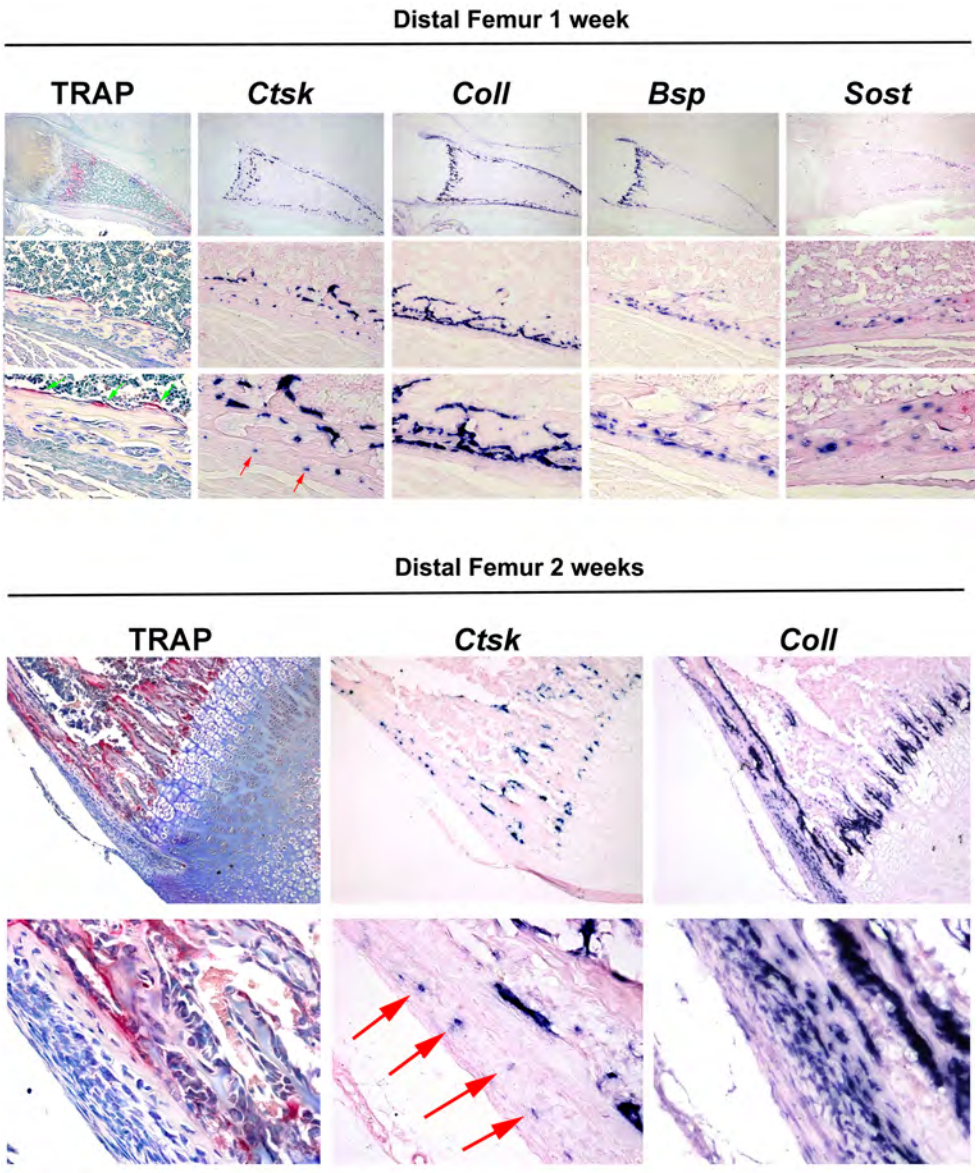

Figure 48. *Ctsk*, *Col1*, *Bsp* and *Sost* mRNA expression. *Ctsk*, *Col1*, *Bsp* and *Sost* ISH and TRAP staining was performed in histological sections of distal femurs of control and experimental mice. From 2-week-old, periosteal *CtsK*-expressing cells matched in expression with *Col1*-expressing cells, but not coincidences were found at 1 week old mice or earlier stages.

As our phenotype of *Ctnnb1*$^{lox(2\text{-}6)/lox(2\text{-}6)}$;*CtsKCre* mice resembles phenotypes in which *βcatenin* was removed of osteogenic cells (Glass et al. 2005; Kramer et al. 2010) and it is known that those cells are able to synthesize OPG, lead us to consider that osteoblast lineage cells can be potential candidates. Therefore, to identify the *CtsK* positive expressing cells in the inner layer of periosteum different to osteoclasts, we analyzed osteoblast lineage markers expression such as *Collagen type 1* (*Col1*), *Bone Sialoprotein* (*Bsp*) and *Sclerostin* (*Sost*). At 1 week of age, these cells were negative for *Col1*, *Bsp*, and *Sost*. From 2-week-old, these cells also expressed *Col1* but no *Bsp* or *Sost*, suggesting they are a subpopulation of undifferentiated osteogenic cells (Fig. 48, arrows).

Together, these results strongly indicate that the *CtsKCre* line targets cells other than osteoclasts in bone and that deletion of *βcatenin* in these cells contributes to the low-bone-mass phenotype of *Ctnnb1*$^{lox(2\text{-}6)/lox(2\text{-}6)}$;*CtsKCre* mutant mice.

5. DISCUSSION

5) DISCUSSION

To improve the understanding of the role of canonical Wnt pathway in mature osteoclasts, we generated mice in which *βcatenin* was inactivated in cells that expressed *Cathepsin K (Ctnnb1$^{lox(2-6)/lox(2-6)}$;CtsKCre*). We decided to use the *CtskCre* deleter line because *Ctsk* was considered the best marker of osteoclasts in their late stages of maturation. The deletion of *βcatenin* in our experimental mice, assessed by qPCR, was specific but partial. This incomplete recombination can be due to cells of other lineages distinct to hematopoietic or to non-fully-developed osteoclasts present in the osteoclast cultures that expressed normal levels of *βcatenin.* This result is in line with previously reported partial recombination described with other deleter lines (Glass et al. 2005; Kramer et al. 2010).

In this work, we have analyzed the skeletal features of mice lacking *βcatenin* in *CtsK*-expressing cells. The experimental *Ctnnb1$^{lox(2-6)/lox(2-6)}$;CtsKCre* mice were born at the expected Mendelian ratio and developed normally up to 4 weeks after birth from which time they showed a progressive low-bone-mass phenotype with a dramatic reduction of both cortical and trabecular bone, mainly in the distal femur, proximal tibia and vertebra as well as similar findings were seen at the proximal end of the humerus. Finally, they prematurely died by the end of the third month of postnatal life with sick appearance. In experimental animals, both cortical and trabecular bone are formed without differences with the control group until 4 weeks of age, as shown in the histological analysis. Interestingly, at 4-week-old, an increase in osteoclast numbers was detected in TRAP

stained bone sections preceding the high bone loss detected at 12 weeks of age, suggesting that some defects must be occurring on osteoclasts. In addition, the normal expression of osteogenic markers such as *Col1* and *Bsp* indicated normal bone formation in the experimental animals. Moreover, we proved that stimulation of Wnt/βcatenin signaling in osteoclasts, attenuated osteoclast development promoting its apoptosis of *in vitro* bone marrow cell cultures. Furthermore, we also demonstrated that the experimental phenotype correlates with a high decrease in expression of *βcatenin* and *Opg* in whole bone, being the latter the major osteoclastogenic inhibitory factor expressed mainly by the osteoblastic lineage cells. These results suggested that other bone cells could be involved and contribute to the bone loss found in the experimental mice. Moreover, *CtsK*-expressing cells were found in the inner layer of periosteum, which indicates that osteogenic cells can be the other cells that were contributing to the low-bone-mass phenotype of the *Ctnnb1*$^{lox(2\text{-}6)/lox(2\text{-}6)}$;*CtsKCre* mice.

Most of the studies on Wnt/βcatenin signaling in bone are focused in the osteoblast lineage. These studies demonstrated that canonical Wnt pathway is considered to be one of the major pathways regulating bone formation through its action on osteoblasts. Activation of Wnt/βcatenin pathway in osteoblastic cells increased bone mass through a dual mechanism. In pre-osteoblastic cells, canonical Wnt signaling acts in a direct manner promoting osteoblastogenesis that increase bone formation (Hu et al. 2005; Day et al. 2005; Hill et al. 2005; Rodda & McMahon 2006). However, in mature osteoblasts and osteocytes, the Wnt pathway acts by an indirect mechanism, via

promoting *Opg* expression and therefore decreasing osteoclastogenesis and bone resorption (Glass et al. 2005; Kramer et al. 2010; Rodda & McMahon 2006; Wang et al. 2014).

However, much less is known about the role of canonical Wnt pathway in the osteoclast biology. Despite the fact that some studies of Wnt/βcatenin pathway in osteoclast lineage were performed through *LysMCre* line, targeting the monocyte-macrophage cells, it is needed to develop more studies to get a more definitive picture of the function of Wnt/βcatenin signaling in the mature osteoclast. Therefore, the current study aimed to analyze the bone phenotype of mice in which *βcatenin* was conditionally deleted in mature osteoclasts.

5.1 βcatenin cell-autonomous function in osteoclasts

It is well established that osteoclasts die by apoptosis, modulating osteoclast survival. Our *in vitro* experiments provide compelling evidence for a role of cell-autonomous Wnt/βcatenin signaling in reducing the life span of osteoclasts. Moreover, several *in vitro* studies have demonstrated that changes in their life span by accelerating or delaying the dying process may alter osteoclast numbers and therefore bone mass. Those studies showed the role of Wnt/βcatenin signaling in reducing the life span of osteoclasts in a cell-autonomous manner (Chen & Long 2013) and demonstrated that modulation of osteoclasts life span leads to changes in bone mass (Manolagas 2000). Indeed, it is well known that estrogens protect the skeleton, at least in part, via pro-apoptotic effects on osteoclasts (Nakamura et al. 2007; Martin-Millan et al. 2010). Deletion of *estrogen*

receptor α (*ERα*) in osteoclast lineage cells, similar to deletion of *βcatenin*, increases osteoclast numbers and decreases bone mass. In contrast to estrogens, glucocorticoids promote the loss of bone mass, leastwise in part, via prolongation of osteoclasts life span. Interestingly, like estrogens and glucocorticoids, Wnt/βcatenin signaling seems to exert an opposite effect on osteoblasts and osteoclasts: survival promotion in osteoblasts and uncommitted osteoblast progenitors (Almeida et al. 2005), and apoptosis promotion in osteoclasts. Although the Wnt/βcatenin pathway is best known by its proliferative effects, such as previously mentioned in osteoblasts and uncommitted progenitors, it can also exert pro-apoptotic actions. For example, it has been reported that cell death induced by hypoxia reoxygenation in cardiomyoblasts of rats is mediated by Wnt/βcatenin through up-regulation of *Wnt3a* and increasing caspase activities (Zhang et al. 2009). Moreover, Wnt/βcatenin signaling decreases melanoma cell invasiveness by a mechanism that enhances the expression of pro-apoptotic proteins such as BIM and PUMA and decrease the levels of anti-apoptotic proteins like MCL (Zimmerman et al. 2013). In line with these studies, our findings showed an increase in apoptosis of WNT3A treated control osteoclasts while experimental osteoclasts remained without changes. This suggests a pro-apoptotic effect of Wnt/βcatenin signaling in osteoclasts that could have an osteoprotective role in bone.

During the development of this thesis, previous studies from our own group and other authors (Otero et al. 2012; Albers et al. 2013; Wei et al. 2011) have studied the role of Wnt/βcatenin signaling in the osteoclast lineage focusing on osteoclast precursors such as

macrophage-neutrophil and monocyte cells, mostly using the *LysMCre* line (Clausen B.E et al. 1999). Lysozyme M is an enzyme characteristic of the immature cells of the monocyte-macrophage lineage and therefore of osteoclast precursors. The *Ctnnb1*$^{lox(2-6)/lox(2-6)}$*;LysMCre* mice presented a mild bone loss phenotype associated with an increase in osteoclast numbers *in vivo*, this observation is in line with our *CtskCre* model that exhibited a high number of osteoclasts. Moreover, our *in vitro* results in *Ctnnb1*$^{lox(2-6)/lox(2-6)}$*;CtskCre* mice are in agreement with the features described in the model in which *βcatenin* was deleted in *LysM*-expressing cells, where the number of osteoclasts developed from bone marrow cultures was also increased. As happens in the *LysMCre* model, we have demonstrated that this increase in osteoclast numbers is due, at least in part, to apoptosis inhibition, as explained before, indicating that an extension of the life span of osteoclasts is a common cell-autonomous mechanism contributing to the bone loss phenotype in both models.

Furthermore, Wei et al. used *CtsKCre* line to study Wnt signaling in pre- and mature osteoclasts. Their results, also displayed an osteoporotic phenotype but with milder differences than ours. This contrast can be explained by the age of the mice at the time of the analysis, since they analyzed 24-week-old mice (Wei et al. 2011).

5.2 Implication of the osteoblast lineage in the low-bone-mass phenotype in Ctnnb1$^{lox(2-6)/lox(2-6)}$;CtskCre model

Surprisingly, the deletion of *βcatenin* in a late stage of osteoclasts development, resulted in a much more severe bone loss phenotype than its removal from an early precursor as occur in the *Ctnnb1*$^{lox(2-}$

6)/lox(2-6);LysMCre mice models. Therefore, considering that in both animal models, the mature osteoclasts are deficient in *βcatenin*, this striking discrepancy between models suggests that the increase osteoclast numbers observed in our mutant animals must have been the result of indirect additional factors in addition to the autonomous osteoclast component.

Several observations point to *Ctnnb1$^{lox(2-6)/lox(2-6)}$;CtsKCre* phenotype is the result of additional indirect effects and suggests that contribution of a non-osteoclastic-cell type must be taking place in the mechanism by which the animals lose bone. These observations are: First, differences in the phenotypes of *CtsKCre* and *LysMCre* models where in both, *βcatenin* is deleted in mature osteoclasts. Second, the striking reduction of the *βcatenin* expression in whole bone, which considering that the proportion of osteoclasts in bone is very low, it suggests that other bone cells apart from osteoclasts are also expressing *Ctsk*. Third, the decrease of the *Opg* expression levels in bone, which indicates that an indirect mechanism must be contributing to the increase in osteoclast numbers. Fourth, the similarity of our *Ctnnb1$^{lox(2-6)/lox(2-6)}$;CtsKCre* mice phenotype with other phenotypes where mesenchymal lineage cells, such as chondrocytes, osteoblasts and osteocytes, are involved. And finally, the increased adiposity of the bone marrow in the experimental mice, which suggests that lack of *βcatenin* in non-osteoclastic cells would have reflected a cell fate shift from the osteo-chondroprogenitors to adipocytes as previously reported (Song et al. 2012) where *Osx-expressing* cells lacking *βcatenin* showed excessive adiposity in the bone marrow.

In order to identify which bone cells, apart from osteoclasts, could express *Ctsk* in our model, expression pattern experiments were performed. Since the phenotype of the *Ctnnb1*$^{lox(2-6)/lox(2-6)}$;*CtskCre* mutant is similar to those mutants in which *βcatenin* deficiency occurs in osteoblastic lineage cells such as osteoblasts and osteocytes (Glass et al. 2005; Kramer et al. 2010) they could be possible candidates for the indirect effect. Moreover, it is established that they are able to synthetized OPG. Therefore, we proceed to analyze the temporal expression pattern of *CtsK* and the osteoblast lineage cell markers such as *Col1*, *Bsp* and *Sost* from E13.5 to 4 weeks of age. Surprisingly, during the study, we found that expression of *CtsK* was not restricted to mature osteoclasts. *CtsK in situ* hybridization revealed *CtsK*-expressing cells in the inner layer of the periosteum that also express *Collagen 1* from 2 weeks of age, while no TRAP staining was detected in this zone. The inner layer of periosteum is highly cellular, mainly composed by osteoblast lineage cells that express *Col1*. Therefore, we assume that they are a subpopulation of osteoblastic cells, indicating that these cells lack *βcatenin* and contribute to the bone phenotype of the *Ctnnb1*$^{lox(2-6)/lox(2-6)}$*;CtsKCre* mice. These osteoblast lineage cells at the inner layer of the periosteum must maintain a crosstalk with osteoclasts by modulating the RANKL/OPG ratio. However, although it has been reported that osteocytes can express *Ctsk* under certain circumstances (Qing et al. 2012), our study failed to detect cells that concomitantly expressed *Sost* and *Ctsk* during the period studied as determined by ISH.

It may be worth taking into account that *CtsK* expression has also been recently described in the perichondrium area surrounding the

metaphysis, being part of an anatomic structure called the groove of Ranvier, which is considered to be involved in bone development and contains osteochondro-progenitors cells (Yang 2013). The authors used ROSA26 reporter mice to describe the *CtsK* positive cells in the groove of Ranvier, which indicates cells that expressed or are expressing *Ctsk* and their descendants. However, despite a careful analysis, we did not detect *CtsK* expression in this area, discarding the participation of this structure in the phenotype of our experimental mice. These differences in expression can be explained because *CtsK* is not expressed at the moment of our analysis but it could be expressed at earlier stages. Nevertheless, though these cells of the groove of Ranvier could contribute to our outcomes and these cells can play a role in determining the phenotype in our model, there is a concern regarding the fact that the groove of Ranvier have been described in long bones, but not in vertebrae and it is unknown if these cells are able to synthesize OPG.

Therefore, the study of the indirect effect in our mutant phenotype, reveals that the *CtskCre* line has activity both in mature osteoclasts and other *CtsK*-expressing cells presumably from the osteoblastic lineage present in the inner layer of periosteum and that the final bone phenotype of *Ctnnb1*$^{lox(2\text{-}6)/lox(2\text{-}6)}$*;CtskCre* mice is a combination of the absence of Wnt/βcatenin signaling in both cell types.

In summary, Wnt/βcatenin signaling in *CtsK*-expressing cells leads to an increase bone mass phenotype reducing osteoclast numbers by decreasing their life span in a cell-autonomous manner whereas osteoblasts, as previously reported, decreased osteoclast numbers

through an indirect effect mediated by the osteoclastogenesis inhibitory factor OPG, that in our model, presumably is expressed from pre-osteoblastic cells localized at the inner layer of the periosteum. Therefore, it is the combination of both mechanisms, the cell-autonomous and the indirect effect, that leads to the elevated osteoclasts numbers and the osteoporotic phenotype in the *Ctnnb1*$^{lox(2\text{-}6)/lox(2\text{-}6)}$;*CtskCre* mice. These findings support the osteoprotective effects of canonical Wnt signaling in bone environment.

Moreover, careful interpretations should be done when *CtsKCre* deleter line is used and underscores the importance of a careful monitorization of *Cre* lines for a correct interpretation of the phenotype causal mechanisms. Thus, this study supports transcendent information to consider regarding the utilization of Wnt neutralizing antibodies that target its antagonists, as promising novel therapeutic approaches to new drugs for bone diseases treatments.

6. CONCLUSIONS

6) CONCLUSIONS

1. The specific deletion of *βcatenin* in *CtsK*-expressing cells leads to a severe low-bone-mass phenotype, detectable from the 4th week of postnatal life.

2. Experimental mice exhibit a normal bone development, and there are no changes in *Col1* and *Bsp* expression in bone during the first month of postnatal life.

3. The low-bone-mass observed in our experimental animals affects both, the appendicular and axial skeleton in both, the cortical and trabecular compartments.

4. The low-bone-mass phenotype observed in experimental mice is associated with increased osteoclast numbers detected by TRAP staining and by histomorphometry quantification. This finding is sufficient to explain the phenotype.

5. The number of osteoclasts derived from bone marrow cultures from experimental mice, is higher than the ones obtained from control littermates.

6. WNT3A induces osteoclast apoptosis *in vitro* and this effect is blunted by absence of *βcatenin* in both *LysozymeMCre* and *CathepsinKCre* mice indicating the cell-autonomous effect of *βcatenin* in these cell type.

7. Experimental bones show a dramatic reduction in *Opg* expression as compared with their controls, while *Rankl* expression is not modified. This increase in the RANKL/OPG ratio indicates an indirect activation of osteoclasts.

8. *CtsK* expressing but not TRAP positive cells were detected in the inner layer of the periosteum. From 2 weeks of age, these cells also express *Collagen 1*. This suggests that a pool of osteoblastic cells localized at the periosteum also express *CathepsinK*.

9. Our results indicate that the phenotype of experimental mice combines the consequence of removing *βcatenin* in two distinct cell types: the mature osteoclasts and a sub-population of osteoblastic cells. The *βcatenin* removal in osteoclasts prolongs their life span in a cell-autonomous manner. The removal in osteoblasts indirectly increases osteoclast numbers by reducing *Opg* expression in osteoblastic cells.

10. Our work stresses the importance of an exhaustive characterization of *Cre* lines for an adequate interpretation of the phenotype.

7. CONCLUSIONES

7) CONCLUSIONES

1. La deleción específica de *βcatenina* en células que expresan *CatepsinaK,* produce un fenotipo caracterizado por una marcada pérdida de masa ósea, detectable a partir de las 4 semanas de vida postnatal.

2. Durante el primer mes de vida postnatal, los ratones experimentales muestran un desarrollo normal de los huesos, incluyendo la expresión de *Colágeno tipo 1* y *Sialoproteina ósea*.

3. La disminución de masa ósea en los ratones experimentales se observa tanto en el esqueleto apendicular como axial y afecta tanto al compartimento cortical como al trabecular.

4. El fenotipo de baja masa ósea observado en ratones experimentales está asociado a un aumento del número de osteoclastos detectado por tinción TRAP y cuantificación histomorfométrica. Este hallazgo sería suficiente para explicar nuestro fenotipo.

5. El número de osteoclastos derivados de los cultivos de médula ósea de ratones experimentales es mayor que el de los ratones control.

6. WNT3A induce apoptosis en los osteoclastos *in vitro* y éste efecto es mitigado por la ausencia de *βcatenina*, tanto en los ratones del modelo de *LisozimaM* como en el de *CathepsinaK*, indicando un efecto autónomo-celular de la vía canónica de Wnt en el osteoclasto.

7. En comparación con los controles, los huesos experimentales muestran un fuerte descenso en la expresión de *Opg*, mientras que la expresión de *Rankl* no muestra diferencias. El aumento del balance RANKL/OPG indica una activación indirecta de los osteoclastos.

8. Células que expresan *CatepsinaK* pero no son TRAP positivas se localizan en la capa interna del periostio. A partir de 2 semanas de edad, estas células también expresan *Colágeno tipo 1*. Esto sugiere que una población de células osteoblásticas situadas en el periostio también expresan *CatepsinaK*.

9. Nuestros resultados indican que el fenotipo de los ratones experimentales es el resultado de la eliminación de *βcatenina* en dos tipos de células distintas: el osteoclasto maduro y una sub-población de células osteoblásticas. La deleción de *βcatenina* en los osteoclastos prolonga su esperanza de vida de una manera autónomo-celular. Y su eliminación en los osteoblastos aumenta indirectamente el número de osteoclastos mediante la reducción de la expresión de *Opg* en células osteoblásticas.

10. Nuestro trabajo pone de manifiesto la importancia de una caracterización exhaustiva de las líneas Cre para una adecuada interpretación del fenotipo.

8. REFERENCES

8) REFERENCES

Akiyama, H. et al., 2004. Interactions between Sox9 and β-catenin control chondrocyte differentiation. *Genes and Development*, 18(9), pp.1072–1087.

Albers, J. et al., 2013. Canonical Wnt signaling inhibits osteoclastogenesis independent of osteoprotegerin. *Journal of Cell Biology*, 200(4), pp.537–549.

Aliprantis, A.O. et al., 2008. NFATc1 in mice represses osteoprotegerin during osteoclastogenesis and dissociates systemic osteopenia from inflammation in cherubism. *Journal of Clinical Investigation*, 118(11), pp.3775–3789.

Almeida, M. et al., 2013. Estrogen receptor-alfa signaling in osteoblast progenitors stimulates cortical bone accrual. *Journal of Clinical Investigation*, 123(1), pp.394–404.

Almeida, M. et al., 2005. Wnt proteins prevent apoptosis of both uncommitted osteoblast progenitors and differentiated osteoblast by β-catenin-dependent and -independent signaling cascades involving Src/ERK and phosphatidylinositol 3-kinase/AKT. *Journal of Biological Chemistry*, 280(50), pp.41342–41351.

Asagiri, M. & Takayanagi, H., 2007. The molecular understanding of osteoclast differentiation. *Bone*, 40(2), pp.251–264.

Axelrod, J.D. et al., 1998. Differential recruitment of dishevelled provides signaling specificity in the planar cell polarity and Wingless signaling pathways. *Genes and Development*, 12(16), pp.2610–2622.

Balemans, W. et al., 2002. Identification of a 52 kb deletion downstream of the SOST gene in patients with van Buchem disease. *Journal of medical genetics*, 39(2), pp.91–97.

Balemans, W. et al., 2001. Increased bone density in sclerosteosis is due to the deficiency of a novel secreted protein (SOST). *Human molecular genetics*, 10(5), pp.537–543.

Bandyopadhyay, A. et al., 2006. Genetic analysis of the roles of BMP2, BMP4, and BMP7 in limb patterning and skeletogenesis. *PLoS genetics*, 2(12), p.e216.

Birchmeier, W., 2011. Orphan receptors find a home Unlocking the secrets. *Nature*, 476, pp.7–8.

Boutros, M. et al., 1998. Dishevelled activates JNK and discriminates between JNK pathways in planar polarity and wingless signaling. *Cell*, 94(1), pp.109–118.

Boyce, B.F. & Xing, L., 2007. Biology of RANK, RANKL, and osteoprotegerin. *Arthritis research & therapy*, 9 Suppl 1, p.S1.

Boyden, L.M. et al., 2002. High Bone Density Due To a Mutation in LDL-Receptor–Related Protein 5. *The new England Journal of Medicine*, 337(20), pp.509–515.

Brault, V. et al., 2001. Inactivation of the beta-catenin gene by Wnt1-Cre-mediated deletion results in dramatic brain malformation and failure of craniofacial development. *Development*, 128(8), pp.1253–1264.

Brunkow, M.E. et al., 2001. Bone Dysplasia Sclerosteosis Results from Loss of the SOST Gene Product , a Novel Cystine Knot – Containing Protein. *American Journal of Human Genetics*, 68, pp.577–589.

Bruzzaniti, A. & Baron, R., 2006. Molecular regulation of osteoclast activity. *Reviews in Endocrine and Metabolic Disorders*, 7(1-2), pp.123–139.

Carmon, K.S. et al., 2012. LGR5 Interacts and Cointernalizes with Wnt Receptors To Modulate Wnt/ -Catenin Signaling. *Molecular and Cellular Biology*, 32(11), pp.2054–2064.

Chaoyang, L. et al., 2004. MMP9 Plays a critical role in bone remodeling in the absence of cathepsin K. *Annual Meeting of the Orthopaedic Research Society*, 0879, p.41210.

Chen, I. & Long, F., 2013. β-catenin Promotes Bone Formation And Suppresses Bone Resorption in Postnatal Growing Mice. *Journal of Bone and Mineral Research*, 28(5)(9), pp.1160–1169.

Chesnut, C.H. et al., 2008. Salmon calcitonin: a review of current and future therapeutic indications. *Osteoporosis international*, 19(4), pp.479–491.

Clausen B.E et al., 1999. Conditional gene targeting in macrophage and granulocytes using LysMcre mice. *Transgenic Research*, 96(October), pp.317–330.

Cohen, Jr, M.M., 2006. The New Bone Biology: Pathologic, Molecular, and Clinical Correlates. *American journal of medical genetics. Part A*, 143A(18), pp.2106–2112.

Cui, Y. et al., 2011. Lrp5 functions in bone to regulate bone mass. *NIH public access*, 17(6), pp.684–691.

Dang, Z.C. et al., 2002. Exposure of KS483 cells to estrogen enhances osteogenesis and inhibits adipogenesis. *Journal of bone and mineral research*, 17(3), pp.394–405.

Dao, D.Y. et al., 2010. Axin2 Regulates Chondrocyte Maturation and Axial Skeletal Development. *Journal of Ortopaedic Research*, 28(1), pp.89–95.

Dao, D.Y. et al., 2012. Cartilage-specific β-catenin signaling regulates chondrocyte maturation, generation of ossification centers, and perichondrial bone formation during skeletal development. *Journal of Bone and Mineral Research*, 27(8), pp.1680–1694.

Day, T.F. et al., 2005. Wnt/β-catenin signaling in mesenchymal progenitors controls osteoblast and chondrocyte differentiation during vertebrate skeletogenesis. *Developmental Cell*, 8(5), pp.739–750.

Day, T.F. & Yang, Y., 2008. Wnt and hedgehog signaling pathways in bone development. *The Journal of bone and joint surgery. American volume*, 90 Suppl 1, pp.19–24.

Dougall, W.C. et al., 1999. RANK is essential for osteoclast and lymph node development. *Genes and Development*, 13, pp.2412–2424.

Ducy, P. et al., 1997. Osf2/Cbfa1: a transcriptional activator of osteoblast differentiation. *Cell*, 89(5), pp.747–754.

Dwek, J.R., 2010. The periosteum: what is it, where is it, and what mimics it in its absence? *Skeletal Radiology*, 39(4), pp.319–323.

Eisman, J.A. et al., 2011. Odanacatib in the treatment of postmenopausal women with low bone mineral density: Three-year continued therapy and resolution of effect. *Journal of Bone and Mineral Research*, 26(2), pp.242–251.

Everts, V. et al., 2003. Cathepsin K Deficiency in Pycnodysostosis Results in Accumulation of Non-Digested Phagocytosed Collagen in Fibroblasts. *Calcified Tissue International*, 73(4), pp.380–386.

Fleischmann, A. et al., 2000. Fra-1 replaces c-Fos-dependent functions in mice. *Genes and Development*, 14(21), pp.2695–2700.

Gallagher, J.C. & Tella, S.H., 2014. Prevention and treatment of postmenopausal osteoporosis. *Journal of Steroid Biochem Mol Biol*, 142, pp.155–170.

Girasole, G. et al., 1992. 17 Beta-Estradiol Inhibits Interleukin-6 Production By Bone Marrow-Derived Stromal Cells and Osteoblasts in Vitro: a Potential Mechanism for the Antiosteoporotic Effect of Estrogens. *The Journal of clinical investigation*, 89(3), pp.883–91.

Glass, D. a. et al., 2005. Canonical Wnt signaling in differentiated osteoblasts controls osteoclast differentiation. *Developmental Cell*, 8(5), pp.751–764.

Gong, Y. et al., 2001. LDL receptor-related protein 5 (LRP5) affects bone accrual and eye development. *Cell*, 107(4), pp.513–523.

Goto, T., Yamaza, T. & Tanaka, T., 2003. Cathepsins in the osteoclast. *Journal of Electron Microscopy*, 52(6), pp.551–558.

Graham, T.A. et al., 2000. Crystal Structure of a β-Catenin/Tcf Complex Deletion analysis of the β-catenin armadillo repeats. *Cell*, 103, pp.885–896.

Guo, X. et al., 2004. Wnt/β-catenin signaling is sufficient and necessary for synovial joint formation. *Genes and Development*, 18(19), pp.2404–2417.

Hadjidakis, D.J. & Androulakis, I.I., 2006. Bone remodeling. *Annals of the New York Academy of Sciences*, 1092, pp.385–396.

Hartikka, H. et al., 2005. Heterozygous mutations in the LDL receptor-related protein 5 (LRP5) gene are associated with primary osteoporosis in children. *Journal of bone and mineral research*, 20(5), pp.783–789.

Hayman, A.R. & Cox, T.M., 2003. Tartrate-resistant acid phosphatase knockout mice. *Journal of bone and mineral research*, 18(10), pp.1905–1907.

Heisenberg, C.P. et al., 2000. Silberblick/Wnt11 mediates convergent extension movements during zebrafish gastrulation. *Nature*, 405(6782), pp.76–81.

Hens, J.R. et al., 2005. TOPGAL mice show that the canonical Wnt signaling pathway is active during bone development and growth and is activated by mechanical loading in vitro. *Journal of bone and mineral research* 20(7), pp.1103–1113.

Hill, T.P. et al., 2005. Canonical Wnt/β-catenin signaling prevents osteoblasts from differentiating into chondrocytes. *Developmental Cell*, 8(5), pp.727–738.

Holmen, S.L. et al., 2005. Essential role of β-catenin in postnatal bone acquisition. *Journal of Biological Chemistry*, 280(22), pp.21162–21168.

Hu, H. et al., 2005. Sequential roles of Hedgehog and Wnt signaling in osteoblast development. *Development (Cambridge, England)*, 132(1), pp.49–60.

Huelsken, J. et al., 2000. Requirement for beta-catenin in anterior-posterior axis formation in mice. *The Journal of cell biology*, 148(3), pp.567–578.

Jilka, R.L. et al., 1998. Loss of estrogen upregulates osteoblastogenesis in the murine bone marrow evidence for autonomy from factors released during bone resorption. *Journal of Clinical Investigation*, 101(9), pp.1942–1950.

Kaifu, T. et al., 2003. Osteopetrosis and thalamic hypomyelinosis with synaptic degeneration in DAP12-deficient mice. *The Journal of clinical investigation*, 111(3), pp.323–32.

Kameda, T. et al., 1997. Estrogen Inhibits Bone Resorption by Directly Inducing Apoptosis of the Bone-resorbing Osteoclasts. *Journal of Experimental Medicine*, 186(4), pp.489–495.

Kamiya, N. et al., 2008. Disruption of BMP signaling in osteoblasts through type IA receptor (BMPRIA) increases bone mass. *Journal of bone and mineral research*, 23(12), pp.2007–2017.

Kapinas, K. & Delany, A.M., 2011. MicroRNA biogenesis and regulation of bone remodeling. *Arthritis Research & Therapy*, 13(3), p.220.

Karsenty, G., Kronenberg, H.M. & Settembre, C., 2009. Genetic control of bone formation. *Annual review of cell and developmental biology*, 25, pp.629–648.

Kato, M. et al., 2002. Cbfa1-independent decrease in osteoblast proliferation, osteopenia, and persistent embryonic eye vascularization in mice deficient in Lrp5, a Wnt coreceptor. *Journal of Cell Biology*, 157(2), pp.303–314.

Ke, J. et al., 2013. Structure and function of Norrin in assembly and activation of a Frizzled 4-Lrp5/6 complex. *Genes and Development*, 27(21), pp.2305–2319.

Keupp, K. et al., 2013. Mutations in WNT1 cause different forms of bone fragility. *American Journal of Human Genetics*, 92(4), pp.565–574.

Kieslinger, M. et al., 2005. EBF2 regulates osteoblast-dependent differentiation of osteoclasts. *Developmental Cell*, 9(6), pp.757–767.

Kim, J.H. & Kim, N., 2014. Regulation of NFATc1 in Osteoclast Differentiation. *Journal of bone metabolism*, 21(4), pp.233–41.

Kim, Y. et al., 2005. Contribution of nuclear factor of activated T cells c1 to the transcriptional control of immunoreceptor osteoclast-associated receptor but not triggering receptor expressed by myeloid cells-2 during osteoclastogenesis. *The Journal of biological chemistry*, 280(38), pp.32905–13.

Koga, T. et al., 2004. Costimulatory signals mediated by the ITAM motif cooperate with RANKL for bone homeostasis. *Nature*, 428(April), pp.758–763.

Kohli, S.S. & Kohli, V.S., 2011. Role of RANKL-RANK/osteoprotegerin molecular complex in bone remodeling and its immunopathologic implications. *Indian journal of endocrinology and metabolism*, 15(3), pp.175–181.

Kornak, U. et al., 2001. Loss of the ClC-7 Chloride Channel Leads to Osteopetrosis in Mice and Man. *cell*, 104(3), pp.210–215.

Kramer, I. et al., 2010. Osteocyte Wnt/beta-catenin signaling is required for normal bone homeostasis. *Molecular and cellular biology*, 30(12), pp.3071–3085.

Kronenberg, H.M., 2003. Developmental regulation of the growth plate. *Nature*, 423(6937), pp.332–6.

Krum, S. a et al., 2008. Estrogen protects bone by inducing Fas ligand in osteoblasts to regulate osteoclast survival. *The EMBO journal*, 27(3), pp.535–545.

Laine, C.M. et al., 2013. WNT1 Mutations in Early-onset Osteoporosis and Osteogenesis Imperfecta. *New England Journal of Medicine*, 368(19), pp.1809–1816.

Lee, N.K., 2010. Molecular Understanding of Osteoclast Differentiation and Physiology. *Endocrinology and Metabolism*, 25(4), p.264.

Levasseur, R., Lacombe, D. & De Vernejoul, M.C., 2005. LRP5 mutations in osteoporosis-pseudoglioma syndrome and high-bone-mass disorders. *Joint Bone Spine*, 72(3), pp.207–214.

Li, L. et al., 1999. Dishevelled proteins lead to two signaling pathways. Regulation of LEF-1 and c-Jun N-terminal kinase in mammalian cells. *The Journal of biological chemistry*, 274(1), pp.129–134.

Li, X., Liu, P., et al., 2005. Dkk2 has a role in terminal osteoblast differentiation and mineralized matrix formation. *Nature genetics*, 37(9), pp.945–952.

Li, X. et al., 2010. Inhibition of sclerostin by monoclonal antibody increases bone formation, bone mass, and bone strength in aged male rats. *Journal of bone and mineral research*, 25(12), pp.2647–2656.

Li, X. et al., 2009. Sclerostin antibody treatment increases bone formation, bone mass, and bone strength in a rat model of postmenopausal osteoporosis. *Journal of bone and mineral research*, 24(4), pp.578–588.

Li, X., Zhang, Y., et al., 2005. Sclerostin binds to LRP5/6 and antagonizes canonical Wnt signaling. *Journal of Biological Chemistry*, 280(20), pp.19883–19887.

Livak, K.J. & Schmittgen, T.D., 2001. Analysis of relative gene expression data using real-time quantitative PCR and the 2(- Δ Δ C(T)) Method. *Methods*, 25(4), pp.402–408.

Lomaga, M.A. et al., 1999. TRAF6 deficiency results in osteopetrosis and defective interleukin-1, CD40, and LPS signaling. *Genes and Development*, 13(8), pp.1015–1024.

Long, F., 2011. Building strong bones: molecular regulation of the osteoblast lineage. *Nature Reviews Molecular Cell Biology*, 13(1), pp.27–38.

Loots, G.G. et al., 2005. Genomic deletion of a long-range bone enhancer misregulates sclerostin in Van Buchem disease. *Genome Research*, 15, pp.928–935.

Luchin, a et al., 2000. The microphthalmia transcription factor regulates expression of the tartrate-resistant acid phosphatase gene during terminal differentiation of osteoclasts. *Journal of bone and mineral research*, 15(3), pp.451–460.

Macdonald, B.T. et al., 2007. Bone mass is inversely proportional to Dkk1 levels in mice. *Bone*, 41(3), pp.331–339.

Maeda, K., Takahashi, N. & Kobayashi, Y., 2013. Roles of Wnt signals in bone resorption during physiological and pathological states. *Journal of Molecular Medicine*, 91(1), pp.15–23.

Manolagas, S.C., 2000. Corticosteroids and fractures: a close encounter of the third cell kind. *Journal of bone and mineral research*, 15(6), pp.1001–1005.

Manolagas, S.C., 1999. Editorial: Cell number versus cell vigor - What really matters to a regenerating skeleton? *Endocrinology*, 140(10), pp.4377–4381.

Mao, B. et al., 2002. Kremen proteins are Dickkopf receptors that regulate Wnt/beta-catenin signalling. *Nature*, 417(6889), pp.664–667.

Martin-Millan, M. et al., 2010. The estrogen receptor-alpha in osteoclasts mediates the protective effects of estrogens on cancellous but not cortical bone. *Molecular endocrinology*, 24(2), pp.323–34.

Mócsai, A. et al., 2004. The immunomodulatory adapter proteins DAP12 and Fc receptor gamma-chain (FcRgamma) regulate development of functional osteoclasts through the Syk tyrosine kinase. *Proceedings of the National Academy of Sciences of the United States of America*, 101(16), pp.6158–63.

Modarresi, R. et al., 2009. WNT/beta-catenin signaling is involved in regulation of osteoclast differentiation by human immunodeficiency virus protease inhibitor ritonavir: relationship to human immunodeficiency virus-linked bone mineral loss. *The American journal of pathology*, 174(1), pp.123–135.

Motyckova, G. et al., 2001. Linking osteopetrosis and pycnodysostosis: regulation of cathepsin K expression by the microphthalmia transcription factor family. *Proceedings of the National Academy of Sciences of the United States of America*, 98(10), pp.5798–5803.

Nakamura, T. et al., 2007. Estrogen Prevents Bone Loss via Estrogen Receptor α and Induction of Fas Ligand in Osteoclasts. *Cell*, 130(5), pp.811–823.

Nakashima, K. et al., 2002. The novel zinc finger-containing transcription factor Osterix is required for osteoblast differentiation and bone formation. *Cell*, 108(1), pp.17–29.

O'Driscoll, S.W. et al., 2001. The chondrogenic potential of periosteum decreases with age. *Journal of Ortopaedic Research*, 19, pp.95–103.

Okazaki, R. et al., 2002. Estrogen promotes early osteoblast differentiation and inhibits adipocyte differentiation in mouse bone marrow stromal cell lines that express estrogen receptor (ER) alpha or beta. *Endocrinology*, 143(6), pp.2349–2356.

Ominsky, M.S. et al., 2010. Two doses of sclerostin antibody in cynomolgus monkeys increases bone formation, bone mineral density, and bone strength. *Journal of Bone and Mineral Research*, 25(5), pp.948–959.

Otero, K. et al., 2012. TREM2 and b-catenin regulate bone homeostasis by controlling the rate of osteoclastogenesis. *J. Immunology*, 29(6), pp.997–1003.

Otto, F. et al., 1997. Cbfa1, a candidate gene for cleidocranial dysplasia syndrome, is essential for osteoblast differentiation and bone development. *Cell*, 89(5), pp.765–771.

Padhi, D. et al., 2011. Single-dose, placebo-controlled, randomized study of AMG 785, a sclerostin monoclonal antibody. *Journal of Bone and Mineral Research*, 26(1), pp.19–26.

Page-McCaw, A., Ewald, A.J. & Werb, Z., 2007. Matrix metalloproteinases and the regulation of tissue remodelling. *Nat Rev Mol Cell Biol*, 8(3), pp.221–233.

Parfitt, a. M., 2002. Targeted and nontargeted bone remodeling: Relationship to basic multicellular unit origination and progression. *Bone*, 30(1), pp.5–7.

Parr, B. a et al., 1993. Mouse Wnt genes exhibit discrete domains of expression in the early embryonic CNS and limb buds. *Development*, 119(1), pp.247–261.

Pettit, A.R. et al., 2001. TRANCE / RANKL Knockout Mice Are Protected from Bone Erosion in a Serum Transfer Model of Arthritis. , 159(5), pp.1689–1699.

Pfeilschifter, J. & Mundy, G.R., 1987. Modulation of type beta transforming growth factor activity in bone cultures by osteotropic hormones. *Proceedings of the National Academy of Sciences of the United States of America*, 84(7), pp.2024–8.

Pyott, S.M. et al., 2013. WNT1 Mutations in Families Affected by Moderately Severe and Progressive Recessive Osteogenesis Imperfecta. *The American Journal of Human Genetics*, 92(4), pp.590–597.

Qiang, Y. et al., 2010. Characterization of Wnt/beta-catenin signalling in osteoclasts in multiple myeloma. *Br J Haematol*, 148(5), pp.726–738.

Qing, H. et al., 2012. Demonstration of Osteocytic Perilacunar/Canalicular Remodeling in Mice during Lactation. *J Bone Mineral Research*, 27(5), pp.1018–1029.

Reddy, S. V. et al., 1999. Cell Biology of Paget ' s Disease. *Journal of bone and mineral research*, 14, pp.3–8.

Reddy, S. V., 2004. Etiology of Paget's disease and osteoclast abnormalities. *Journal of Cellular Biochemistry*, 93(4), pp.688–696.

Riancho, J. a. et al., 2011. Wnt receptors, bone mass, and fractures: Gene-wide association analysis of LRP5 and LRP6 polymorphisms with replication. *European Journal of Endocrinology*, 164(1), pp.123–131.

Riancho, J. a. & Delgado-Calle, J., 2011. Mecanismos de interacción osteoblasto-osteoclasto. *Reumatologia Clinica*, 7(SUPPL.2), pp.1–4.

Roberts, S.J. et al., 2015. Uncovering the periosteum for skeletal regeneration : The stem cell that lies beneath. *Bone*, 70, pp.10–18.

Rodan, G.A., 2000. Therapeutic Approaches to Bone Diseases. *Science*, 289(5484), pp.1508–1514.

Rodan, S.B. & Duong, L.T., 2008. Cathepsin K – A new molecular target for osteoporosis. *IBMS BoneKEy*, 5(1), pp.16–24.

Rodda, S.J. & McMahon, A.P., 2006. Distinct roles for Hedgehog and canonical Wnt signaling in specification, differentiation and maintenance of osteoblast progenitors. *Development*, 133(16), pp.3231–3244.

Roodman, G.D. et al., 1990. Interleukin 6 - A potential autocrine/paracrine factor in Paget's disease of bone. *Journal of Clinical Investigation*, 89(1), pp.46–52.

Ross, F.P., 2006. M-CSF, c-Fms, and signaling in osteoclasts and their precursors. *Annals of the New York Academy of Sciences*, 1068, pp.110–116.

Russell, R.G.G. et al., 2007. Mechanisms of action of bisphosphonates: similarities and differences and their potential influence on clinical efficacy. *Osteoporosis International*, 19(6), pp.733–759.

Salo, J. et al., 1997. Removal of osteoclast bone resorption products by transcytosis. *Science (New York, N.Y.)*, 276(5310), pp.270–273.

Semënov, M., Tamai, K. & He, X., 2005. SOST is a ligand for LRP5/LRP6 and a Wnt signaling inhibitor. *Journal of Biological Chemistry*, 280(29), pp.26770–26775.

Shapiro, L., 2001. Β-Catenin and Its Multiple Partners : *Cell*, 8(6), pp.6–9.

Sharma, S.M. et al., 2007. MITF and PU.1 recruit p38 MAPK and NFATc1 to target genes during osteoclast differentiation. *Journal of Biological Chemistry*, 282(21), pp.15921–15929.

Shevde, N.K. et al., 2000. Estrogens suppress RANK ligand-induced osteoclast differentiation via a stromal cell independent mechanism involving c-Jun repression. *Proceedings of the National Academy of Sciences of the United States of America*, 97(14), pp.7829–7834.

So, H. et al., 2003. Microphthalmia transcription factor and PU.1 Synergistically induce the leukocyte receptor osteoclast-associated receptor gene expression. *Journal of Biological Chemistry*, 278(26), pp.24209–24216.

Song, L. et al., 2012. Loss of Wnt/b-catenin signaling causes cell fate shift of preosteoblasts from osteoblasts to adipocytes. *Changes*, 29(6), pp.997–1003.

Staehling-Hampton, K. et al., 2002. A 52-kb deletion in the SOST-MEOX1 intergenic region on 17q12-q21 is associated with van Buchem disease in the Dutch population. *American Journal of Medical Genetics*, 110(2), pp.144–152.

Stepan, J.J. et al., 2003. Mechanisms of action of antiresorptive therapies of postmenopausal osteoporosis. *Endocrine Regulations*, 37(4), pp.225–238.

Styrkarsdottir, U. et al., 2013. Nonsense mutation in the LGR4 gene is associated with several human diseases and other traits. *Nature*, 497(7450), pp.517–20.

Tada, M. & Smith, J.C., 2000. Xwnt11 is a target of Xenopus Brachyury: regulation of gastrulation movements via Dishevelled, but not through the canonical Wnt pathway. *Development*, 127(10), pp.2227–2238.

Takayanagi, H. et al., 2002. Induction and activation of the transcription factor NFATc1 (NFAT2) integrate RANKL signaling in terminal differentiation of osteoclasts. *Developmental Cell*, 3(6), pp.889–901.

Tondravi, M.M. et al., 1997. Osteopetrosis in mice lacking haematopoietic transcription factor PU.1. *Nature*, 386(6620), pp.81–84.

Topczewski, J. et al., 2001. The Zebrafish Glypican Knypek Controls Cell Polarity during Gastrulation Movements of Convergent Extension. *Developmental Cell*, 1(2), pp.251–264.

Troen, B.R., 2004. The role of cathepsin K in normal bone resorption. *Drug news & perspectives*, 17(1), pp.19–28.

Vaananen, K., 2004. Mechanism of osteoclast mediated bone resorption—rationale for the design of new therapeutics. *Advanced Drug Delivery Reviews*, 57(7), pp.959–971.

Vortkamp, a et al., 1996. Regulation of rate of cartilage differentiation by Indian hedgehog and PTH-related protein. *Science*, 273(5275), pp.613–622.

Wallingford, J.B. & Habas, R., 2005. The developmental biology of Dishevelled: an enigmatic protein governing cell fate and cell polarity. *Development*, 132(20), pp.4421–4436.

Wang, B. et al., 2014. Chondrocyte β-catenin signaling regulates postnatal bone remodeling through modulation of osteoclast formation in a murine model. *Arthritis and Rheumatology*, 66(1), pp.107–120.

Wei, W. et al., 2011. Biphasic and Dosage-Dependent Regulation of Osteoclastogenesis by β-Catenin. *Molecular and Cellular Biology*, 31(23), pp.4706–4719.

Weivoda, M.M. et al., 2016. Wnt Signaling Inhibits Osteoclast Differentiation by Activating Canonical and Noncanonical cAMP/PKA Pathways. , 31(1), pp.65–75.

Winslow, M.M. et al., 2006. Calcineurin/NFAT Signaling in Osteoblasts Regulates Bone Mass. *Developmental Cell*, 10(6), pp.771–782.

Witte, F. et al., 2009. Comprehensive expression analysis of all Wnt genes and their major secreted antagonists during mouse limb development and cartilage differentiation. *Gene Expression Patterns*, 9(4), pp.215–223.

Yadav, V.K. et al., 2008. Lrp5 controls bone formation by inhibiting serotonin synthesis in the duodenum: an entero-bone endocrine axis. *Cell*, 127(5), pp.358–366.

Yamaguchi, A., Komori, T. & Suda, T., 2010. Regulation of osteoblast differentiation mediated by bone morphogenetic proteins, hedgehogs and cba1. *Endocrine review*, 658(1), pp.43–49.

Yang, Y., 2003. Wnts and Wing: Wnt Signaling in Vertebrate Limb Development and Musculoskeletal Morphogenesis. *Birth Defects Research Part C - Embryo Today: Reviews*, 69(4), pp.305–317.

Yoshida, H. et al., 1990. The murine mutation osteopetrosis is in the coding region of the macrophage colony stimulating factor gene. , p.Nature vol.345.

Zaidi, M., Moonga, B.S. & Abe, E., 2002. Calcitonin and bone formation : a knockout full of surprises. *Journal of Clinical Investigation*, 110(12), pp.1769–1771.

Zhang, Z. et al., 2009. Secreted frizzled related protein 2 protects cells from apoptosis by blocking the effect of canonical Wnt3a. *J Mol Cell Cardiol*, 46(3), pp.370–377.

Zheng, H.F. et al., 2012. WNT16 influences bone mineral density, cortical bone thickness, bone strength, and osteoporotic fracture risk. *PLoS Genetics*, 8(7).

Zimmerman, Z.F. et al., 2013. Activation of Wnt/ β -catenin signaling increases apoptosis in melanoma cells treated with trail. *PloS one*, 8(7), p.e69593.

AGRADECIMIENTOS

Agradecimientos

En primer lugar quiero agradecer a Marian, Marta y Jesús su confianza en mi desde el primer momento, sus grandes consejos y todo lo que me han enseñado tanto a nivel laboral como personal durante estos años.

También me gustaría agradecer su compañerismo, su apoyo y su tiempo a todos mis compañeros con los que he compartido tantas horas en el laboratorio: Marisa, MªFélix, Federica, Marian T., Teresa, Mamen, Endika, Carlos, Irene, Sara, Mar, Rocío, Marc y en especial a Patri y Lucía que aparte de compañeras, me llevo a dos grandes amigas. Sin olvidarme del resto de mis compañeros del IBBTEC y de la Facultad de Medicina y de todos los buenos momentos que he pasado junto a ellos. Gracias a todos por vuestra ayuda y amistad.

Agradezco también a todos mis amigos y a mi familia, en particular a mis padres, mi hermana María y mis sobrinos Antonio y Blanca que siempre me apoyaron incondicionalmente y entendieron mis “tiempos” durante estos años. Finalmente a Manuel, por tu comprensión y paciencia infinita, siempre estuviste ahí animándome y confiando en mi.